NIU Journal of Health Sciences

Nexus International University, Uganda.

Published in July, 2026

ISSN: 3136-6457 (Print)

ISSN: 3136-6449 (Online)

Published by:

Nexus International University,
Kampala, Uganda.

NIU Journal of Health Sciences Copyright©2026
Nexus International University ISSN: 3136-6449; 12(1) 3

Editorial

This edition of NIU *Journal of Health Sciences* touches on as Lung Cancer Prevention Awareness, Volumetric Modulated Arc Therapy (VMAT) for Left-Sided Breast Cancer Assessment, *Toxoplasma gondii* Infection and Their Effects on Human Brain Health, among others.

One of the papers, in this issue, calls for more research to be conducted into lung cancer, as a way of improving understanding and hearing from the general public. Develop student-centered education programs that focus on increasing awareness of lung cancer risk factors and prevention. It therefore, recommends introducing Cross-sectional studies on awareness and attitude among adults to prevent lung cancer.

Another paper also reveals that Volumetric Modulated Arc Therapy (VMAT) planning provided consistent and clinically satisfactory dosimetric outcomes for both the target volumes and surrounding normal tissues. The chest wall PTV had an average V95 of 97.2%, while the lymph node PTV reached 98.7%, demonstrating sufficient target coverage with satisfactory conformity and dose uniformity. In terms of organs at risk, cardiac exposure was kept low, with the heart receiving an average dose of 5.0 Gy. The ipsilateral lung experienced mean V5, V20, and V30 values of 56.6%, 25.0%, and 21.0%, respectively. It is revealed that VMAT achieved efficient target coverage, demonstrating good dose conformity and uniformity, all while keeping radiation exposure to nearby organs at risk within acceptable limits. These results endorse the clinical practicality of using VMAT for treating left-sided breast cancer.

On the whole, this edition of *NIU Journal of Health Sciences* features many empirical and theoretical based articles which can be of great benefit to every reader.

Professor Oyetola O. Oniwide

Nexus International University,
P.O. Box 70773,
Kampala, Uganda.
editor@niujournals.ac.ug
June, 2026.

NIU Journal of Health Sciences Copyright©2026
Nexus International University ISSN: 3136-6449; 12(1) 5-14

Comparison between UroLift and Transurethral Resection of the Prostate in the Treatment of Benign Prostatic Hyperplasia

Dr. Sinan Diya Khair, M.B.Ch.B.
Resident Physician (Bachelor of Medicine and Bachelor of Surgery)

Dr. Ali Abdul-Baqi Ismail, F.I.C.M.S., F.A.C.S.
Consultant Urologist — Supervisor
Fellow of the Iraqi Council for Medical Specializations · Fellow of the American College of Surgeons

Affiliation:
Department of Urology, _____ College of Medicine, _____ University,
The Nasiriyah Center for Urology and Nephrology, Dhi Qar Governorate, Republic of Iraq

Abstract

Background: Benign Prostatic Hyperplasia (BPH) is among the most prevalent chronic urological conditions in aging men, producing lower urinary tract symptoms (LUTS) that markedly reduce quality of life. Transurethral Resection of the Prostate (TURP) has long served as the surgical gold standard, yet it carries substantial risks of bleeding, TUR syndrome, prolonged catheterization, and long-term sexual dysfunction. The Prostatic Urethral Lift (UroLift) is a minimally invasive, non-ablative alternative that mechanically retracts obstructing prostatic lobes using permanent implants.
Problem: There is limited comparative, prospective evidence on the relative efficacy and safety of UroLift versus TURP under the specific clinical, economic, and cultural conditions of Iraq.
Methods: A prospective comparative clinical study was conducted at The Nasiriyah Center for Urology and Nephrology from October 2022 to April 2023, enrolling 21 male BPH patients divided into a UroLift group (9 patients) and a TURP group (12 patients). Outcomes assessed at 3 months included IPSS, Quality of Life index, maximum urinary flow rate (Qmax), Post-Void Residual (PVR) volume, serum PSA, and surgical complications. Data were analyzed with SPSS v26 using t-tests, chi-square, and Fisher's Exact test (significance at $p \leq 0.05$).
Results: Both techniques produced significant symptomatic improvement, but UroLift was statistically superior in IPSS (3.44 ± 0.88 vs 5.08 ± 2.49; $p = 0.0018$), Qmax (21.33 ± 5.61 vs 16.17 ± 4.56 mL/s; $p = 0.031$), PVR (23.56 ± 23.77 vs 52.05 ± 32.11 mL; $p = 0.038$), and PSA (0.78 ± 0.61 vs 1.48 ± 0.95; $p = 0.050$). Overall complications were far lower with UroLift (33.33% vs 91.67%; $p = 0.005$), which uniquely preserved sexual function in 100% of patients. Conclusions: UroLift achieved efficacy comparable or superior to TURP in relieving obstruction while offering a substantially safer profile and complete preservation of sexual function, making it a compelling minimally invasive option for suitable BPH patients.

Keywords: Benign Prostatic Hyperplasia; UroLift (Prostatic Urethral Lift); Transurethral Resection of the Prostate (TURP); Lower Urinary Tract Symptoms; Minimally Invasive Surgery.

1. Introduction

Benign Prostatic Hyperplasia (BPH) is one of the most prevalent chronic issues in urology in the modern world, owing to its close relationship with the biological process of aging in men. BPH results from the uncontrolled proliferation of epithelial and stromal cells, producing progressive mechanical compression of the prostatic urethra. This gives rise to several lower urinary tract symptoms (LUTS), classified into:

Voiding difficulties such as a weak urinary stream, hesitancy, difficulty starting the urine flow, and intermittency.
Storage symptoms such as urge incontinence, frequent nighttime urination, and incomplete bladder emptying. [2]
The end result of this symptom profile is significant deterioration in the patient's quality of life, with poor social, psychological, and physiological outcomes.

For more than six decades, urological societies have regarded Transurethral Resection of the Prostate (TURP) as the "Gold Standard" against which new treatments are tested. TURP is well documented in reducing glandular size, improving peak flow rate, and reducing post-void residual urine — but this surgical success carries a considerable clinical cost. [1]

Major problems associated with TURP include:
Risks of excessive intra- or post-operative bleeding, which may require blood transfusion.
TUR (Transurethral Resection) Syndrome, caused by absorption of non-ionic irrigation fluids with monopolar systems.

Longer hospital stays requiring continuous bladder irrigation and urinary catheterization.

Most importantly, TURP has a significant long-term negative influence on sexual function. Retrograde ejaculation occurs in about 65%–80% of patients due to anatomical destruction of the bladder neck, and there is a risk of urinary incontinence and erectile dysfunction owing to thermal damage to the collateral neurovascular bundle. These problems created a strong need for minimally invasive surgical techniques (MIST) that provide efficacy without structural damage.

Against this technological backdrop, the Prostatic Urethral Lift (PUL), known medically as the UroLift system, represents a qualitative step forward and a genuinely new surgical concept. This approach involves no cutting, burning, or ablation of prostatic tissue; instead, it produces a purely mechanical effect by displacing the hypertrophic lobes that block the urethral lumen. Small permanent implants are placed via cystourethroscope under direct visualization, producing an instant and lasting opening of the prostatic urethral lumen while preserving the bladder neck and the vessels and nerves essential for reproductive function. [8]

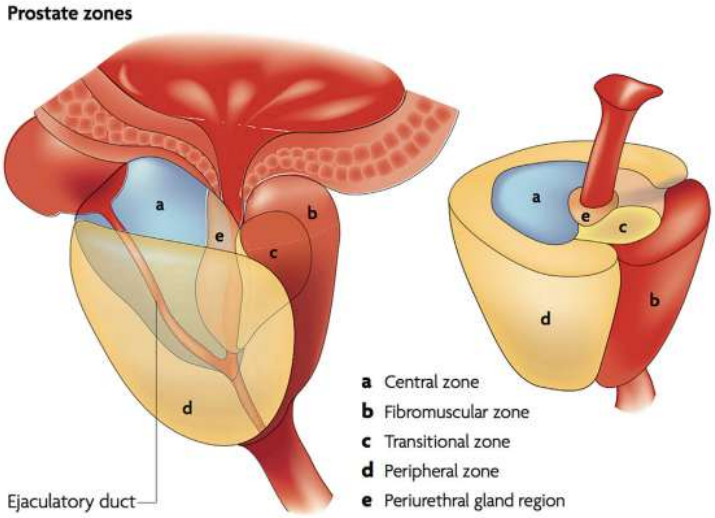

Figure 1: *The Prostatic Urethral Lift (UroLift) mechanism of action.*

1.1 Significance of the Study and Strategic Objectives

The significance of this research lies in its prospective, clinical, comparative assessment under specific geographic and clinical conditions — those of Iraq, and particularly of an advanced specialization center (The Nasiriyah Center for Urology and Nephrology). Under these conditions, economic and logistic factors together with patients' culture influence surgical decisions. The study provides a statistically grounded platform to help urologists make reasonable clinical decisions when weighing the traditional technique against modern, imported alternatives that require substantial investment.

The strategic and operational objectives of this dissertation cover the following critical aspects: [5]
Evaluating the reduction in severity of obstructive and storage symptoms through the standardized International Prostate Symptom Score (IPSS) and its correlated Quality of Life (QoL) index, before operation and at 3 months post-operatively.

Objectively measuring changes in peak urinary flow rate (Qmax, mL/s) and Post-Void Residual (PVR) urine volume via ultrasonographic examination.

Determining serum Prostate-Specific Antigen (PSA) as a biomarker of tissue modification and inflammation in relation to surgical treatment.

Documenting and comparing all early and late surgical complications for both UroLift and TURP, focusing on bleeding, infections, acute urinary retention, and sexual (ejaculatory and erectile) function.

Evaluating operative time, patient-reported pain scores, duration of hospital stay, and the required period of indwelling catheterization. [3]

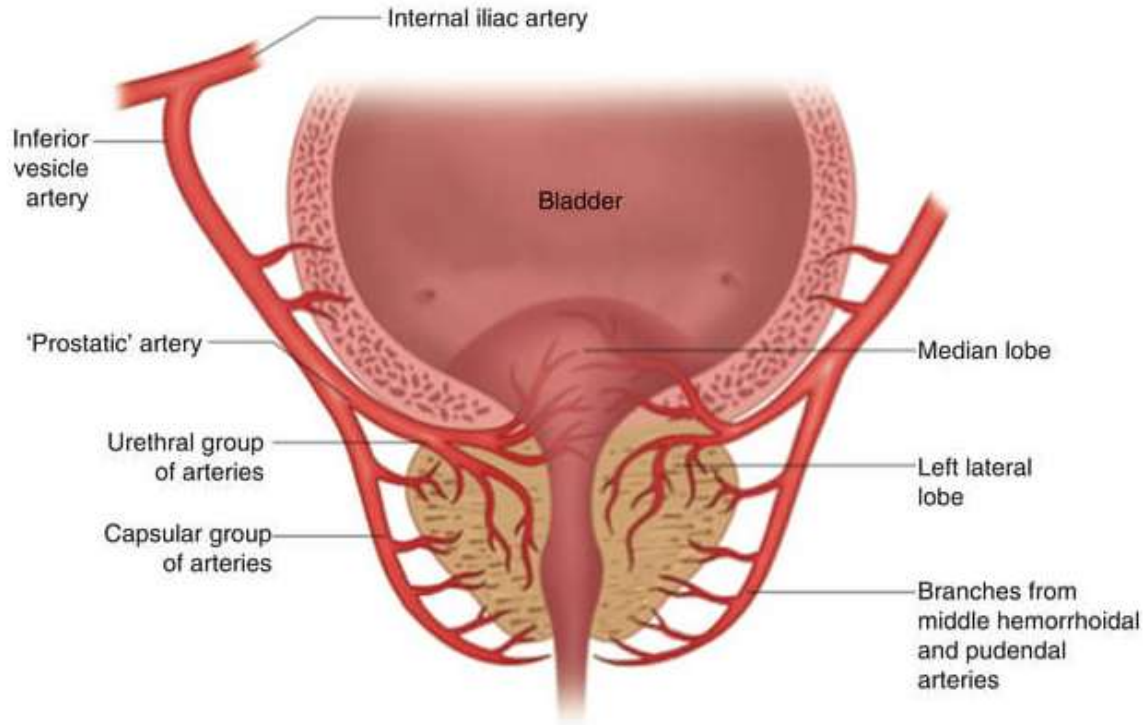

Figure 2: *Comparative overview of the study parameters.*

1.2 Research Hypotheses and Questions

The study was generated from the following scientific hypothesis:
"The Prostatic Urethral Lift (UroLift) procedure provides similar or near-identical clinical and physiological effectiveness in enhancing voiding function and alleviating symptoms compared to the standard Transurethral Resection of the Prostate (TURP), but with fundamental and substantial superiority in safety, avoidance of complications, and full preservation of sexual function and post-operative quality of life."

To test this hypothesis, the study seeks to answer the following questions:

Question 1: How large is the improvement in IPSS and QoL scores 3 months after UroLift compared to TURP, and is this difference statistically significant?

Question 2: Is the mechanical lifting of hypertrophied tissue in UroLift associated with an equal improvement in Qmax and decrease in PVR compared to complete tissue ablation in TURP?

Question 3: What are the exact percentages of irritative, hemorrhagic, and sexual complications in both groups at the Nasiriyah Specialized Center?
Question 4: How does the type of surgical intervention influence serum PSA levels following the designated follow-up period?

2. Background and Literature Review

2.1 Surgical Anatomy and the Four Tissue Zones of the Prostate

The prostate gland is the most important male gland of the genitourinary system. It has the form of an inverted chestnut: its base is directed upward and attached to the bladder neck, while its apex is directed downward, adjacent to the urogenital diaphragm and external urethral sphincter that provide voluntary control of micturition. In a young healthy man, the gland measures about 4 cm transversely, 3 cm vertically, and 2 cm anteroposteriorly, weighing 15–20 g. The prostatic urethra passes vertically through the gland for about 3 cm and then bends forward at the verumontanum — a key anatomical landmark, since resection below it destroys the external sphincter and causes urinary incontinence. [6]

Modern histopathology has moved beyond the outdated lobar anatomy (right, left, middle) and instead uses McNeal's Zonal Anatomy, dividing the gland into four zones:

Peripheral Zone — Accounts for about 70% of the volume of the typical prostate. It surrounds the distal urethra posteriorly and laterally and is the region most easily palpated on Digital Rectal Examination. It is the main site of 75%–80% of prostatic adenocarcinomas and is most susceptible to prostatic inflammation.

Central Zone — The second largest zone (~25% of volume). This wedge-shaped region surrounds the ejaculatory ducts and is highly resistant to cancer and benign proliferation, with fewer than 5% of prostate cancers arising here.

Transition Zone — In healthy young men, no more than 5% of gland volume, formed by two small lobes flanking the proximal prostatic urethra. This is the only site where Benign Prostatic Hyperplasia develops. With aging, constant nodular growth compresses the central urethra into a narrow slit that impedes urination. The transition zone also accounts for about 10%–15% of prostate tumors. [5]

Anterior Fibromuscular Stroma — A purely non-glandular zone forming the anterior wall and about one-third of gland volume, composed of smooth muscle and elastic fibrous tissue. No hyperplastic or malignant lesions develop here, but it is surgically important because UroLift uses this dense stroma to anchor its urethral implants.

2.2 Vascularization and the Neural Network of the Prostate

The prostate is supplied mainly by the inferior vesical artery, a major branch of the internal iliac artery. On reaching the base of the gland, it divides into two branches:

The capsular branch, which traverses the external surface within the fibrous capsule, sending perforating vessels into the peripheral and core zones. These arteries lie adjacent to the neurovascular bundle responsible for penile erection.
The urethral branch, which enters at the bladder-neck–prostate junction and runs along the urethra to supply the transition and periurethral zones. In BPH, these vessels become greatly enlarged, which is why their transection during TURP causes significant hemorrhage. [10]

Venous drainage occurs via the prostatic venous plexus, located between the true fibrous capsule and the outer fascial layer. Its anterior portion communicates with the dorsal venous plexus (Santorini plexus) and drains into the internal iliac veins. Injury to this network during TURP causes extensive, difficult-to-manage bleeding and provides the major route for systemic uptake of non-ionic irrigating fluids, predisposing patients to TUR syndrome with acute dilutional hyponatremia and pulmonary edema.

The prostate has a dual autonomic nerve supply from the inferior hypogastric plexus:

Sympathetic fibers — Originating from T11–L2, these drive contraction of the smooth muscle of the prostatic stroma and bladder neck during ejaculation to propel semen forward.

Parasympathetic fibers — Arising from the pelvic splanchnic nerves, these regulate glandular secretions.

The nerves and vessels responsible for erection travel through a precise, delicate plane posterolaterally along the prostate. This area is highly prone to thermal injury during monopolar or bipolar electroresection in TURP, often

resulting in permanent impotence — a risk absent in the purely mechanical UroLift procedure, which applies no heat or cautery. [12]

2.3 Pathological Mechanisms, Genetic and Environmental Risk Factors

The biology of BPH is complex, involving cell proliferation together with hormonal, environmental, and genetic influences. Its defining feature is true hyperplasia — an actual increase in the number of epithelial and stromal cells. Male sex hormones catalyze the process. Free testosterone within prostatic cells is converted by 5-alpha reductase (Type II), abundant in stromal tissue, into dihydrotestosterone (DHT), a hormone about ten times more potent. DHT binds androgen receptors, enters the nucleus, and activates transcription of growth-factor genes (FGF and TGF-beta). With age, the balance between cell growth and apoptosis is disrupted. Persistent hormonal stimulation prolongs cell life and delays apoptosis, increasing cell mass and producing hyperplastic nodules. Chronic silent abacterial prostatitis contributes as well: lymphocyte and mast-cell infiltration produces inflammatory cytokines that drive fibrosis and raise smooth-muscle tone through adrenergic receptors. [2]

Regarding risk factors, current research shows clear correlations between lifestyle, genetics, and disease progression: Age — the strongest independent risk factor. About 50% of men show histologic BPH by age 60, rising to over 85%–90% beyond age 80.

Genetics — familial BPH tends to occur earlier (before age 60), with larger glands and greater need for surgery; risk rises about fourfold when a first-degree relative is affected.

Obesity and metabolic syndrome — waist circumference correlates positively with prostate size and LUTS severity; insulin resistance and hyperglycemia increase sympathetic activity and IGF-1, accelerating proliferation.

Diet and lifestyle — high saturated fat and red meat intake and physical inactivity aggravate symptoms, while a fiber- and antioxidant-rich diet is somewhat protective. [11]

3. Methods and Materials

3.1 Study Design and Sample

A prospective comparative clinical research methodology was adopted to ensure scientific validity. Field procedures were carried out in the departments of The Nasiriyah Center for Urology and Nephrology, Republic of Iraq, from October 2022 to April 2023. The sample comprised 21 male patients with Benign Prostatic Hyperplasia and moderate-to-severe LUTS who were unresponsive to conventional medical therapy (alpha-blockers and 5-alpha reductase inhibitors) or refused it because of severe side effects. [7]

The study population was divided by strict clinical and anatomical criteria into two cohorts:

Group 1 (UroLift Group): 9 patients who underwent the mechanical Prostatic Urethral Lift technique.
Group 2 (TURP Group): 12 patients who underwent classic conventional transurethral resection.

3.2 Inclusion and Exclusion Criteria

Inclusion criteria:
Adult male participants over 50 years old.
IPSS scores ≥ 13 points.
Prostate size 30–80 cm^3 measured by TRUS.
Maximum urine flow rate below 12 mL/s.
Post-Void Residual volume below 250 mL, to exclude bladder detrusor failure.

Exclusion criteria:

Significant enlargement of the prostate median lobe with intravesical displacement, since PUL cannot be used in such cases.
Prostate cancer (unexplained elevated PSA or abnormal Digital Rectal Exam with positive biopsy).
Pre-existing urethral strictures.
Bladder calculi.
Neurogenic bladder or neurological disorders affecting voiding dynamics, such as Parkinson's disease or Multiple Sclerosis.

3.3 Preoperative Evaluation and Surgical Protocols

All patients underwent a standardized preoperative evaluation: medical history, general physical examination, Digital Rectal Examination, complete laboratory investigations (renal function, urinalysis, urine culture, serum PSA), IPSS questionnaires, and digital uroflowmetry. Postoperative follow-up was performed systematically at the 3-month mark. [9]

UroLift protocol: Patients were placed in the lithotomy position under advanced local anesthesia (intraurethral 2% lidocaine gel with a perineal nerve block or conscious sedation, per patient preference). A 20 F rigid cystourethroscope with a 0° lens integrated in the UroLift Delivery System was used. After ruling out a median lobe, the scope was retracted to the prostatic urethra and the areas of maximum obstruction identified. The delivery system was oriented at the 2 o'clock and 10 o'clock positions and firm pressure compressed the hypertrophic lobe toward the outer capsule. A fine 19-gauge needle pierced the tissue and capsule, the nitinol capsular tab was deployed, the needle retracted while tensioning the monofilament PET tether, and the stainless-steel urethral end-piece was clipped to the inner urethral wall. On average, 4 implants (range 3–5) were placed per patient to achieve a continuous open, U-shaped lumen. Most patients did not require postoperative catheterization and voided freely, going home within hours. [8]

TURP protocol: Performed under spinal or general anesthesia in the lithotomy position using a 26 F continuous-flow resectoscope with a tungsten wire loop, monopolar current, and 1.5% glycine irrigation. The electrosurgical unit was set to 120 W (cutting) and 80 W (coagulation). Resection began with the median lobe (when present), then the lateral lobes of the transition zone, shaving tissue from the bladder neck to the verumontanum, with electrocoagulation of bleeding vessels. Resected chips were evacuated with an Ellik evacuator and sent for histopathology to exclude occult malignancy. A 22–24 F three-way Foley catheter (balloon 30–50 mL) was inserted under tension with continuous bladder irrigation using normal saline. Hospitalization of 2–4 days was required for monitoring of hematuria and irrigation until clearance, followed by a Trial Without Catheter (TWOC). [10]

3.4 Statistical Analysis

Data were analyzed using the Statistical Package for the Social Sciences (SPSS), version 26. Continuous variables were presented as Mean ± Standard Deviation, and categorical variables as frequency tables with percentages. Continuous variables were compared with Student's t-test; complication rates were compared with the chi-square and Fisher's Exact tests. Results were considered statistically significant at $p \leq 0.05$ and highly significant at $p < 0.01$.

4. Results

Values obtained from patients' charts at the 3-month follow-up revealed the principal differences in the physiological and clinical efficacy of both methods, which were analyzed for statistical significance.

4.1 Clinical and Laboratory Parameters (3-Month Follow-Up)

IPSS: Both groups began in the severe category (>22 points). At 3 months, both showed remarkable improvement, but with a highly significant advantage for UroLift, whose mean IPSS fell to 3.44 ± 0.88 (very mild symptoms) versus

5.08 ± 2.49 for TURP (p = 0.0018). Mechanical lifting provided faster, more effective relief, likely because it avoids the pain and irritation of tissue sloughing and thermal cautery that prolong healing after TURP. [7]
Qmax: The UroLift group reached 21.33 ± 5.61 mL/s — an excellent physiological flow well above the smooth-voiding threshold — versus 16.17 ± 4.56 mL/s for TURP (p = 0.031). UroLift alters urethral geometry without scar tissue or bladder-neck contractures that hinder flow.
PVR: Both groups improved, but UroLift achieved near-complete bladder emptying with a mean PVR of 23.56 ± 23.77 mL versus 52.05 ± 32.11 mL for TURP (p = 0.038), confirming the efficiency of the mechanical lift in relieving urethral resistance.
PSA: Mean PSA at 3 months was 0.78 ± 0.61 for UroLift versus 1.48 ± 0.95 for TURP (p = 0.050). Electroresection creates a large field for tissue regeneration and inflammation, raising PSA in the early months, whereas UroLift keeps tissue intact and provokes no glandular inflammatory response. [9]

4.2 Surgical Complications and Sexual Function

Any complication or side effect occurred in only 33.33% of UroLift patients (3 of 9) versus 91.67% of TURP patients (11 of 12). This difference was highly significant on Fisher's Exact test (p = 0.005).

Qualitative analysis of complications:

Irritative symptoms (dysuria, frequency, minor pelvic pain): 1 UroLift patient (11.11%), mild and self-resolving within two weeks with analgesics; 2 TURP patients (16.67%), more severe and prolonged due to the raw resected cavity and thermal injury.
Urinary incontinence: none in the UroLift group (0%), as the technique spares the external sphincter and bladder-neck dynamics; 3 TURP patients (25%) had temporary incontinence requiring pads and Kegel exercises.
Hematuria / Acute Urinary Retention: no acute hematuria or retention in UroLift patients, all discharged the same day without continuous catheterization; all TURP patients had expected gross hematuria, one developed AUR from clot obstruction requiring re-catheterization and longer stay, and two developed UTI (16.67%) from prolonged catheterization.
Epididymitis: 1 UroLift case (11.11%) at two weeks, from minor urinary reflux through the ejaculatory ducts, fully resolved with oral antibiotics without sequelae.

Sexual function — the most clinically decisive outcome: UroLift preserved erectile function and normal ejaculation in 100% of patients, owing to its purely mechanical action that spares the bladder neck and neurovascular bundles. By contrast, 3 TURP patients (25%) developed severe sexual dysfunction as retrograde ejaculation ("dry orgasm") from removal of bladder-neck smooth muscle, along with reduced erectile function from thermal spread to the cavernous nerves.

5. Discussion

The findings of this prospective comparative study directly address the research hypothesis and questions. Both UroLift and TURP produced genuine, significant improvements in obstructive and storage symptoms relative to baseline, confirming that each is an effective treatment for BPH. However, across every primary outcome measured at 3 months — IPSS, Qmax, PVR, and PSA — UroLift demonstrated a statistically significant advantage.

The superior symptomatic relief seen with UroLift (IPSS 3.44 ± 0.88 vs 5.08 ± 2.49; p = 0.0018) can be attributed to the absence of a raw resected surface and thermal injury, which in TURP require a prolonged healing period accompanied by irritative symptoms. The better Qmax and PVR results reflect the geometric reopening of the urethral lumen without the scar tissue and bladder-neck contractures that can follow electroresection. The lower post-operative PSA after UroLift is consistent with tissue preservation and the absence of an inflammatory regenerative field.

The most striking difference lies in the safety profile. The overall complication rate was almost three times higher after TURP (91.67% vs 33.33%; p = 0.005), and only TURP produced urinary incontinence, acute retention, catheter-related UTI, and — most importantly — sexual dysfunction. UroLift preserved sexual function in 100% of patients,

directly answering the study's central question regarding the preservation of ejaculatory and erectile function. These observations are consistent with the mechanistic rationale of the technique, which avoids manipulation of the bladder neck and the posterolateral neurovascular bundles.

Taken together, the results support the study hypothesis: UroLift offers efficacy comparable — and in several parameters superior — to TURP, while providing a fundamentally safer profile. The main limitations are the relatively small sample size (21 patients) and the short 3-month follow-up, which does not capture the long-term durability of the mechanical implants. Larger, longer-term studies are warranted to confirm these findings and to evaluate cost-effectiveness under local conditions.

6. Conclusions

This research examined, through accurate clinical study and observation, one of the most important and fastest-growing topics in current urological surgery. Conducted at The Nasiriyah Center for Urology and Nephrology, the prospective comparative study provided evidence-based answers distinguishing two treatment methods from two different surgical eras in the management of BPH.

The study demonstrated that technological development in medical engineering has broken the long-standing monopoly of TURP as the sole gold standard through the Prostatic Urethral Lift (UroLift). Moving away from a philosophy of tissue cutting and destruction toward mechanical lifting and displacement proved well suited to the needs of the modern patient. UroLift achieved excellent efficacy in opening the urinary passage — in several parameters better than conventional resection — while ensuring the safety and preservation of sexual and vital functions that were considered impossible in conventional endoscopic procedures.

Based on statistical inference from the 3-month follow-up, the study reached the following conclusions:

Both modalities produced significant improvement in obstructive and storage symptoms, but UroLift showed statistical superiority in reducing IPSS (3.44 ± 0.88 vs 5.08 ± 2.49; $p < 0.0018$).

UroLift produced a steady physiological increase in Qmax (21.33 ± 5.61 mL/s), statistically better than TURP (16.17 ± 4.56 mL/s; $p = 0.031$).

Ultrasound confirmed UroLift's superiority in reducing PVR (23.56 ± 23.77 mL vs 52.05 ± 32.11 mL; $p = 0.038$).
Serum PSA stabilized better after UroLift (0.78 ± 0.61 vs 1.48 ± 0.95; $p = 0.050$), reflecting reduced post-repair inflammation.

UroLift showed a markedly safer profile, with post-operative complications in only 33.33% of patients versus 91.67% for TURP ($p = 0.005$).

Recommendation: UroLift should be considered a first-line minimally invasive option for suitable BPH patients — particularly those for whom preservation of sexual function is a priority — provided that anatomical selection criteria (absence of an obstructing median lobe) are met. Larger, longer-term studies are recommended to confirm durability and cost-effectiveness under local conditions.

7. Acknowledgment

The authors sincerely thank the medical and nursing staff of The Nasiriyah Center for Urology and Nephrology for their support throughout the data-collection and follow-up phases of this study, and gratefully acknowledge the patients who consented to participate. The authors received no specific financial grant for this research.

8. Conflict of Interest

The authors declare that the study was conducted in accordance with the applicable ethical standards and with the informed consent of all participating patients. The authors declare that they have no conflict of interest, financial or otherwise, related to the equipment, techniques, or manufacturers referenced in this study.

9. References

[1] Reeves F, Everaerts W, Murphy DG. The Surgical Anatomy of the Prostate. Prostate Cancer, 2nd ed., 2016, pp. 253–263.
[2] Ittmann M. Anatomy and Histology of the Human and Murine Prostate. Cold Spring Harb Perspect Med. 2018 May 1;8(5): a030346.
[3] Bhavsar A, Verma S. Anatomic imaging of the prostate. Biomed Res Int. 2014; 2014:728539.
[4] McNeal JE. Cancer volume and site of origin of adenocarcinoma in the prostate: relationship to local and distant spread. Hum Pathol. 1992;23(3):258–66.
[5] Kiyoshima K. Anatomical features of periprostatic tissue and its surroundings: a histological analysis of 79 radical retropubic prostatectomy specimens. Jpn J Clin Oncol. 2004; 34:463–8.
[6] Yoham AL, Bordoni B. Anatomy, Abdomen and Pelvis: Inferior Hypogastric Plexus. StatPearls Publishing, 2023.
[7] Barry MJ, Fowler FJ Jr, Bin L, et al. The natural history of patients with benign prostatic hyperplasia as diagnosed by North American urologists. J Urol. 1997; 157:10–4.
[8] Parsons JK. Modifiable risk factors for benign prostatic hyperplasia and lower urinary tract symptoms: new approaches to old problems. J Urol. 2007; 178:395–401.
[9] Rassweiler J, Teber D, Kuntz R, et al. Complications of transurethral resection of the prostate (TURP): incidence, management, and prevention. Eur Urol. 2006;50(5):969–79.
[10] Roehrborn CG, Gange SN, Shore ND, et al. The prostatic urethral lift for the treatment of lower urinary tract symptoms associated with prostate enlargement due to benign prostatic hyperplasia: the L.I.F.T. Study. J Urol. 2013; 190:2161–2167.
[11] Gratzke C, Barber N, Speakman MJ, et al. Prostatic urethral lift vs transurethral resection of the prostate: 2-year results of the BPH6 prospective, multicentre, randomized study. BJU Int. 2017; 119:767–775.
[12] Sønksen J, Barber NJ, Speakman MJ, et al. Prospective, randomized, multinational study of prostatic urethral lift versus transurethral resection of the prostate: 12-month results from the BPH6 study. Eur Urol. 2015;68(4):643–652.

NIU Journal of Health Sciences Copyright©2026
Nexus International University ISSN: 3136-6449; 12(1) 15-20

Immunoregulatory Effects of IL-37 and IL-38 on Intestinal Inflammation in Celiac Disease

ASEEL ADEEB AHMED[1] and RAYA ZAID ALI[2]
[1]*The Open Educational College, Diyala Study Center, Diyala, Iraq.*
[2]*Departement of Biology, College of Education for Pure Science, University of Diyala, Diyala, Iraq.*
Corresponding author: Raya Zaid Ali (raya.zaid@uodiyala.edu.iq)

Abstract. In people who are genetically predisposed, gluten consumption causes celiac disease, a chronic immune-mediated condition that results in ongoing inflammation and damage to the mucosa of the small intestine. In addition to measuring important inflammatory markers (IL-6, TNF-α, and CRP) and their correlation with anti-inflammatory cytokines, this study sought to explore the immunoregulatory roles of IL-37 and IL-38 in intestinal inflammation in individuals with celiac disease. Forty healthy controls and fifty celiac disease patients participated in the study. Standard laboratory techniques were used to measure the levels of serum cytokines. The findings showed that patients had considerably higher levels of CRP, TNF-α, and IL-6 than controls, indicating an active inflammatory condition. Additionally, patients' levels of IL-37 and IL-38 were markedly elevated, indicating a compensatory immunoregulatory response to persistent intestinal inflammation. Regression analysis showed that IL-6 and TNF-α were positive predictors of disease activity, while IL-37 and IL-38 were negative regulatory factors. Correlation analysis showed positive relationships between pro-inflammatory and anti-inflammatory cytokines. The results indicate that IL-37 and IL-38 may have significant immunoregulatory functions in controlling intestinal inflammation in celiac disease. A complex immunological network that aids in the onset and progression of disease is reflected in the imbalance between pro-inflammatory and anti-inflammatory cytokines.

Keywords: IL-37, IL-38, Celiac Disease, Intestinal Inflammation.

1. Introduction

In genetically vulnerable people, especially those with the HLA-DQ2 and HLA-DQ8 haplotypes, dietary gluten consumption causes celiac disease, a chronic immune-mediated enteropathy. Malabsorption, crypt hyperplasia, villous atrophy, and ongoing inflammation of the small intestine mucosa are its hallmarks. According to available data, celiac disease is a systemic immune-mediated syndrome caused by a complex interplay of genetic, environmental, and immunological variables rather than only a gastrointestinal disorder [1][2].

A Th1-skewed immune response is the main mechanism behind the immunopathogenesis of celiac disease. Following deamidation by tissue transglutaminase, gluten-derived peptides activate CD4+ T cells, which then release pro-inflammatory cytokines. Important inflammatory mediators that increase mucosal inflammation, compromise the integrity of the epithelial barrier, and cause villous atrophy include TNF-α, IL-6, IFN-γ, and IL-17. Intestinal damage and disease activity have been repeatedly linked to elevated levels of these cytokines [3][4].

A well-known systemic biomarker of inflammation, CRP is an acute-phase protein that is mainly generated by IL-6. It has been demonstrated to correlate with the inflammatory load in autoimmune and gastrointestinal illnesses,

including celiac disease. Its rise is indicative of a systemic inflammatory response and continuous immune activation outside of the intestinal mucosa [5][6].

Anti-inflammatory cytokines that control immunological homeostasis have received more attention in recent years. Members of the IL-1 cytokine family, IL-37 and IL-38, are new immunoregulatory mediators that have strong anti-inflammatory effects. While IL-38 modifies IL-1 receptor signaling and attenuates inflammatory pathways, IL-37 lowers innate and adaptive immune responses by downregulating pro-inflammatory cytokine production. These cytokines are thought to be essential parts of the natural systems that prevent over-activation of the immune system [7][8].

According to recent studies, the immune response in celiac disease involves a dynamic equilibrium between pro-inflammatory and anti-inflammatory mediators rather than being unidirectional. Exposure to gluten causes T lymphocytes and dendritic cells to become activated, which triggers cytokine cascades that exacerbate gut inflammation. In order to prevent tissue damage and restore immunological balance, regulatory cytokines may be increased concurrently [9][10].

There are relatively few immunological investigations examining cytokine profiles in patients with celiac disease in Iraq, despite the condition's growing recognition in clinical practice. Knowing how inflammatory and regulatory cytokines are balanced in Iraqi patients may help develop prospective immunological biomarkers that are pertinent to local populations and offer important insights into the behavior of the disease.

Therefore, the objective of this study was to measure serum levels of TNF-α, CRP, and IL-6, as well as to examine the immunoregulatory functions of IL-37 and IL-38 in intestinal inflammation in Iraqi patients with celiac disease in comparison to healthy controls, as well as to evaluate their correlations and predictive value in disease activity.

1.2 Materials and Methods

1.2.1 Sample Collection

This study was conducted in Diyala Governorate, Iraq, during the period from January 2025 to March 2026. A total of 90 blood samples were included in this study, comprising 50 samples obtained from patients diagnosed with celiac disease and 40 samples from apparently healthy individuals who served as a control group for comparison.

The patients were clinically diagnosed with celiac disease based on established diagnostic criteria, while the healthy controls had no history of autoimmune or inflammatory disorders. Blood samples were collected from participants attending Baqubah Teaching Hospital and specialized laboratories across Diyala Governorate. Informed consent was obtained from all participants prior to sample collection, in accordance with ethical research standards.

Approximately 6 mL of venous blood was drawn from each participant and transferred into gel tubes. The samples were allowed to clot at room temperature for 10–30 minutes, followed by centrifugation at 3000 rpm for 5 minutes to obtain serum. The separated serum was then carefully collected and stored under appropriate conditions until further analysis.

1.2.2 Sample Measurements

Serum levels of C-reactive protein (CRP), tumor necrosis factor-alpha (TNF-α), interleukin-6 (IL-6), interleukin-37 (IL-37), and interleukin-38 (IL-38) were quantitatively measured in both celiac disease patients and healthy controls. The measurements were performed using the sandwich Enzyme-Linked Immunosorbent Assay (ELISA) technique, following the manufacturer’s instructions provided with the commercially available kits (Biotech Company). All assays were conducted according to standardized laboratory protocols to ensure accuracy and reproducibility of the results.

1.2.3 Statistical Analysis

The Statistical Package for the Social Sciences (SPSS), version 2023, was used to analyze the data. While categorical data were shown as frequencies and percentages, continuous variables were reported as mean ± standard deviation (SD) or mean ± standard error (SE). The independent samples t-test was used to evaluate differences between the patient and control groups. Cohen's d was used to assess the effect size, and when necessary, 95% confidence intervals (CI) were computed.

The correlations between the variables under study were evaluated using Pearson's correlation coefficient (r). The predictive value of independent variables was assessed using multiple linear regression analysis, and the results were presented as beta coefficients (β) with standard errors. Statistical significance was defined as a p-value of less than 0.05.

1.4 Results

Table 1 shows no significant difference in age between the patient and control groups, where the mean ± standard error was 37.2 ± 7.1 years in patients compared to 36 ± 6.9 years in controls (NS). There was also no notable difference in sex distribution, with males accounting for 36% vs 35% and females 64% vs 65% in patients and controls, respectively.

Table 1: Demographic characteristics of study groups

Variable		Patients (n=50)	Controls (n=40)	Probability
Age mean ± SE (Years)		37.2±7.1	36±6.9	NS
Sex frequency (%)	♂	18(36%)	14(35%)	-
	♀	32(64%)	26(65%)	
	Total	50(100%)	40(100%)	

NS: Non-Significant.

Additionally, Table 2 demonstrates a significant difference in IL-6 levels between patients and controls, with a mean ± standard deviation of 18.5 ± 9.2 pg/mL for patients and 4.8 ± 2.1 pg/mL for controls (P > 0.001, d = 2.10). TNF-α likewise showed a significant difference, with values of 22.4 ± 11.6 pg/mL in patients and 6.1 ± 2.7 pg/mL in controls (P > 0.001, d = 1.95). CRP levels also differed significantly, with patients having 8.6 ± 4.3 mg/L and controls having 1.9 ± 0.8 mg/L (P > 0.001, d = 2.30).

Table 2: Pro-inflammatory markers and effect size analysis

Parameter	Mean ± SD		95% CI (patients)	Cohen's d	P-value
	Patients	Control			
IL-6 (Pg/mL)	18.5±9.2	4.8±2.1	2.10	15.9-21.1	>0.001
TNF-α (Pg/mL)	22.4±11.6	6.1±2.7	1.95	19.1-25.7	>0.001
CRP (mg/L)	8.6±4.3	1.9±0.8	2.30	7.4-9.8	>0.001

Table 3 demonstrates a significant difference in IL-37 levels between patients and controls, with mean ± standard deviation of 268 ± 185 pg/mL in patients versus 82 ± 36 pg/mL in controls (P > 0.001, d = 1.20). A significant difference was also found in IL-38, where levels were 185 ± 95 pg/mL in patients compared to 92 ± 28 pg/mL in controls (P > 0.01, d = 0.95).

Table 3: Immuno-regulatory cytokines and effect size

Cytokine	Patients (Mean ± SD)	Controls (Mean ± SD)	95% CI	Effect size (d)	P-value
IL-37 (pg/mL)	268±185	82±36	217-319	1.20	>0.001
IL-38 (pg/mL)	185±95	92±28	158-212	0.95	>0.01

IL-37 and IL-6 (r = 0.62, P > 0.001) and IL-38 and TNF-α (r = 0.58, P > 0.001) are significantly positively correlated, according to Table 4. Furthermore, IL-37 and CRP (r = 0.55, P > 0.001) and IL-37 and IL-38 (r = 0.71, P > 0.001) were found to have a strong positive connection.

Table 4: Correlatien Analysis (spearman/pearson r)

Relationship	Correlatien (r)	Interpretation	P-value
IL-37 with IL-6	+0.62	Moderat positive	>0.001
IL-38 with TNF-α	+0.58	Moderat positive	>0.001
IL-37with CRP	+0.55	Moderat positive	>0.001
IL-37 with IL-38	+0.71	Strong postive	>0.001

According to Table 5, the regression coefficient for IL-6 is β = +0.42 with a standard error of 0.08 (P > 0.001), whereas the regression coefficient for TNF-α is β = +0.39 with a standard error of 0.07 (P > 0.001). On the other hand, IL-38 has β = -0.22 with a standard error of 0.08 (P = 0.01) while IL-37 has a coefficient of β = -0.28 with a standard error of 0.09 (P = 0.004).

Table 5: Mutivuriate regression analysis (dependent variable:CRP)

Predictor	B coefficient	Standard error	p-value	Interpretation
IL-6	+0.42	0.08	>0.001	Proinflammatory driver
TNF-α	+0.39	0.07	>0.001	Proinflammatory driver
IL-37	-0.28	0.09	0.004	Anti-inflammatory effect
IL-38	-0.22	0.08	0.01	Anti-inflammatory effect

1.5 Discussion

Pro-inflammatory cytokines (IL-6, TNF-α, and CRP) were found to be considerably higher in celiac disease patients than in healthy controls. These results are in line with the existing view of celiac disease as an immunological-mediated condition that is mainly caused by the production of various inflammatory mediators and Th1-mediated immune activation. According to recent research, TNF-α and IL-6 are key players in intestinal inflammation because they activate immune cells, increase epithelial permeability, and cause mucosal damage in the small intestine [11][12]. Furthermore, as CRP is a well-known acute-phase protein that is mostly generated by IL-6 signaling, elevated CRP indicates systemic inflammatory activity [13].

Recent studies showing that gluten exposure causes mucosal immune cells to quickly release inflammatory cytokines, resulting in both local and systemic inflammation, supports these conclusions. According to a recent analysis, even in asymptomatic forms of celiac disease, IL-21, IFN-γ, and TNF-α work together to enhance inflammatory responses and cause ongoing mucosal damage [14].

However, the current investigation showed that patients had far higher levels of anti-inflammatory cytokines (IL-37 and IL-38) than controls. This might be seen as a compensating regulatory system designed to reduce excessive inflammation. It is known that IL-37 is a powerful suppressor of both innate and adaptive immune responses, preventing the activation of immune cells and lowering the production of pro-inflammatory cytokines like TNF-α and IL-6. In a similar vein, IL-38 reduces tissue inflammation by modifying inflammatory pathways, especially those associated with the IL-1 family [15][16].

According to recent studies, IL-38 is elevated in a number of autoimmune diseases, including inflammatory bowel disorders, where it supports its immunoregulatory function by reducing tissue damage and suppressing the production of TNF-α and IL-1β [16]. This is in line with recent research, which indicates that elevated IL-38 might be an immune system attempt to offset persistent inflammation.

Significant positive correlations between inflammatory and anti-inflammatory cytokines, such as IL-37 with IL-6, IL-38 with TNF-α, and a substantial link between IL-37 and IL-38, were found by correlation analysis in the current study. These results suggest that immune responses in celiac disease entail a complicated dynamic interaction between pro-inflammatory and regulatory mechanisms rather than being unidirectional. Anti-inflammatory cytokine overexpression most likely results from a negative feedback mechanism triggered by persistent inflammation [17].

Regression analysis also showed that TNF-α and IL-6 are positive predictors while IL-37 and IL-38 are negative predictors, emphasizing their conflicting biological roles. This lends credence to the idea that the balance between

inflammatory and regulatory cytokines determines the severity of celiac disease, and that disruption of this balance leads to long-term mucosal damage [18][19][20][21].

Celiac disease is caused mechanistically when gluten-derived peptides pass through the intestinal epithelium and are altered by tissue transglutaminase, which increases their ability to bind to HLA-DQ2/DQ8 molecules. This causes villous atrophy and persistent inflammation by activating CD4+ T cells and releasing pro-inflammatory cytokines such IL-6, TNF-α, and IFN-γ. On the other hand, as a compensatory reaction to reduce tissue damage, regulatory cytokines including IL-37 and IL-38 are produced [11][22][23][24].

There are several limitations on this study. The results may not be as broadly applicable as they could be due to the tiny sample size. Additionally, the cross-sectional design merely allows connections to be established rather than causal correlations. Furthermore, adherence to a gluten-free diet was not rigorously measured, which could have affected cytokine levels. Additionally, there was no histological association with intestinal biopsy results in the study, which could have improved the interpretation of immune markers. Lastly, there was insufficient control over potential confounders such the length of the illness, genetic background, and related autoimmune disorders. It is advised that larger, longer-term studies be conducted in the future to validate these results.

1.6 Conclusion

The current study shows that pro-inflammatory markers, such as IL-6, TNF-α, and CRP, are much higher in celiac disease patients than in healthy controls, indicating an active state of systemic inflammation. Anti-inflammatory cytokines IL-37 and IL-38 were also markedly elevated concurrently, indicating a compensatory immunoregulatory response to persistent inflammation. A dynamic immunological interplay is shown in the found considerable positive correlations between pro-inflammatory and anti-inflammatory cytokines; regression analysis identifies IL-6 and TNF-α as important positive predictors of disease activity and IL-37 and IL-38 as negative modulators. Overall, our results point to a cytokine imbalance between inflammatory and regulatory pathways as a characteristic of celiac disease, which may play a role in the development and course of the illness.

References

[1] Lebwohl B, Sanders DS, Green PHR. Celiac disease. The Lancet. 2018;391(10115):70–81. DOI: 10.1016/S0140-6736(18)31534-7.
[2] Abadie V, Sollid LM, Barreiro LB, Jabri B. Integration of genetic and immunological insights into celiac disease. Annual Review of Immunology. 2020;38:459–491. DOI: 10.1146/annurev-immunol-042718-041550.
[3] Goel G, King T, Daveson AJ, et al. Cytokine responses in celiac disease following gluten exposure. Clinical and Experimental Immunology. 2020;202(1):58–66. DOI: 10.1111/cei.13369.
[4] Schuppan D, Junker Y, Barisani D. Celiac disease: from pathogenesis to novel therapies. Gastroenterology. 2022;162(3):749–763. DOI: 10.1053/j.gastro.2022.03.021.
[5] Shalimar S, et al. Immune activation and cytokine profile in celiac disease. Alimentary Pharmacology & Therapeutics. 2021;53(4):423–432. DOI: 10.1111/apt.16452.
[6] Fasano A, Catassi C. Celiac disease: clinical features and diagnosis. New England Journal of Medicine. 2021;384(12):1155–1165. DOI: 10.1056/NEJMra1900863.
[7] Dinarello CA, et al. Interleukin-37 and interleukin-38 in inflammation. Nature Reviews Immunology. 2016;16(12):731–743. DOI: 10.1038/nri.2016.6.
[8] van de Veerdonk FL, et al. IL-38 as a regulator of inflammation. Journal of Immunology. 2020;205(8):2115–2122. DOI: 10.4049/jimmunol.2000354.
[9] Jabri B, Sollid LM. T cells in celiac disease. Nature Reviews Immunology. 2017;17(9):553–565. DOI: 10.1038/nri.2017.13.
[10] Zanoni G, et al. Immune regulation in celiac disease. Frontiers in Immunology. 2022;13:880123. DOI: 10.3389/fimmu.2022.880123.
[11] Barone, Maria Vittoria; Auricchio, Renata; Nanayakkara, Merlin; Greco, Luigi; Troncone, Riccardo; Auricchio, Salvatore. Pivotal Role of Inflammation in Celiac Disease. International Journal of Molecular Sciences, (2022); 23(13), Article 7177. DOI: 10.3390/ijms23137177.

[12] Shneor Patt, Yonatan; Lahat, Adi; David, Paula; Patt, Chen; Eyade, Rowand; Sharif, Kassem. Unraveling the Immunopathological Landscape of Celiac Disease: A Comprehensive Review. International Journal of Molecular Sciences, (2023); 24(20), Article 15482. DOI: 10.3390/ijms242015482.
[13] Lebwohl, Benjamin; Sanders, David S.; Green, Peter H. R. Coeliac disease. The Lancet, (2018); 391(10115), 70–81. DOI: 10.1016/S0140-6736(17)31796-8.
[14] Camarca, Antonio; et al. Regulatory immune responses in celiac disease. International Journal of Molecular Sciences, (2023); 24(19), Article 14434. DOI: 10.3390/ijms241914434.
[15] Dinarello, Charles A.; Nold-Petry, Caroline A.; Nold, Mario F. IL-37 and IL-38 in inflammation. Nature Reviews Immunology, (2016); 16(6), 357–368. DOI: 10.1038/nri.2016.6
[16] Han, et al. IL-38 in autoimmune diseases. Cytokine, (2023); 170, Article 156117. DOI: 10.1016/j.cyto.2023.156117.
[17] Galipeau, Heather J.; Verdu, Elena F. Microbiota and celiac disease. Mucosal Immunology, (2022); 15, 235–243.DOI: 10.1038/s41385-021-00479-3.
[18] Jabri, Bana; Sollid, Ludvig M. T cells in celiac disease. Nature Reviews Immunology, (2017); 17(8), 467–478. DOI: 10.1038/nri.2017.13
[19] Treppiccione, Lorella; et al. Immune regulation in celiac disease. International Reviews of Immunology, (2022); 41(4–5), 436–453. DOI: 10.1080/08830185.2022.2044807.
[20] Przemioslo RT, Kontakou M, Nobili V, Ciclitira PJ. Raised pro-inflammatory cytokines interleukin 6 and tumour necrosis factor alpha in coeliac disease mucosa detected by immunohistochemistry. Gut. 1994 Oct;35(10):1398-403. doi: 10.1136/gut.35.10.1398.
[21] Su Z, Tao X. Current Understanding of IL-37 in Human Health and Disease. Front Immunol. 2021 Jun 25;12:696605. doi: 10.3389/fimmu.2021.696605.
[22] Parzanese I, Qehajaj D, Patrinicola F, Aralica M, Chiriva-Internati M, Stifter S, Elli L, Grizzi F. Celiac disease: From pathophysiology to treatment. World J Gastrointest Pathophysiol. 2017 May 15;8(2):27-38. doi: 10.4291/wjgp.v8.i2.27.
[23] Zhu J, Mulder CJJ, Dieleman LA. Celiac Disease: Against the Grain in Gastroenterology. J Can Assoc Gastroenterol. 2019 Dec;2(4):161-169. doi: 10.1093/jcag/gwy042.
[24] Al Rasbi Z, Orsud H, Zoughbor SH, Hajar M, Mahboob A and Sadek B (2025) The role of interleukin-37 and interleukin-38 in the development and remission of autism spectrum disorder: A comprehensive review of neuroinflammatory mechanisms and potential therapeutic implications. Front. Immunol. 16:1716197. doi: 10.3389/fimmu.2025.1716197.

NIU Journal of Health Sciences Copyright©2026
Nexus International University ISSN: 3136-6449; 12(1) 21-28

A Cross-Sectional Survey of Lung Cancer Prevention Awareness among Undergraduate Students

AMER J. KADUSH *, EBTIHAL SATTAR QASIM,**
* Adult Health Nursing Department, College of Nursing, Al-Muthanna University, Iraq. amer.kadoosh@mu.edu.iq, https://orcid.org/0000-0003-4690-4446
** Department of Nursing Techniques, Al-Nasiriyah Technical Institute, Southern Technical University, Nasiriyah, 64001, Iraq, Ebtihal.qassim@stu.edu.iq, https://orcid.org/

Abstract.
Aim: This study was aimed to assess the perception of undergraduate students about lung cancer prevention.
Methodology: The study used a cross-sectional approach, the participants were students of Al-Muthanna University in AL-Samawa city. Starts on: Nov 25, 2024 Ends on: Apr 24, 2025 By Taking a random sample from the pool of students (n=100). Data was collected out of a tool that functions like questionnaires with some falsifiable and non-falsifiable statements. Eight specialists establish validity, which is then verified by a committee of professionals. Pilot research was done on 10% (n=10) of the students to analyze reliability of this questionnaire.
Results: The students showed a good level of awareness about lung cancer, with no significant correlation between awareness and different characteristics (age, sex, residence, social class or economic conditions), however there was significant relationship found in all the related variables to college.
Conclusion: The researchers call for more research to be conducted into lung cancer, as a way of improving understanding and hearing from the general public. Develop student-centered education programs that focus on increasing awareness of lung cancer risk factors and prevention.
Recommendations: Introduction Cross-sectional studies on awareness and attitude among adults to prevent lung cancer.

Keywords: Prevention Lung Cancer, Health Awareness, Cross Sectional Research.

1. Introduction

NCDs, also known as chronic diseases are long duration or generally slow progression disease that usually results from a combination of genetic and physiological factors environmental and behavioral for example non communicable disease NCDs are grouped into four main types: cardiovascular diseases (for example, heart attacks and stroke; cancers; chronic respiratory illnesses such as Chronic obstructive pulmonary disease and asthma. So, bases on world health organization (World health organization, 2023).

Most of the previous definitions of cancer are around similar content as that in a recent National Cancer Institute definition 'Cancer is an uncontrolled growth and spread of abnormal cells where some normal control mechanisms cease to operate'. Exactly these definitions often shift the burden to cancer's clinical manifestations, or side effects — not what it is under its skin, through some sort of definition unburdened by ontology. Even though they reflect historical understandings, these do not take into account the more recent insight that cancer cells are transformed organisms under continuous evolution (Brown et al., 2023).

The cell cycle is a series of different events that happens in the life-span of a cell to duplicate and divide. There are two main phases in this time period, interphase and mitosis. Interphase represents the longest phase and is broken down into three sub-stages: G1, S, and G2. The G1 stage is where the cell grows and prepares for DNA replication. S Phase: DNA synthesis, genetic material duplication and long replication time. G2: the cell grows and approaches mitosis. Cytokinesis, also called the cytoplasmic division phase which is after mitosis and where

cell divides into two daughter cells. Then, the cycle moves on to interphase where it starts all over again. One of the main hallmark features that makes cancer malignant is disturbance in cell cycle which results into so many effects (Almalki, 2023).
The story of lung cancer (LC) epidemiology is intimately associated with the rise and birth of contemporary studies on chronic disease epidemiology. Although an elevated incidence of lung cancer was reported for miners and some other occupational groups in the nineteenth century, a large increase has been observed since the early twentieth century. Although lung cancer was the most commonly diagnosed, and frequently lethality caused by it in men at that time (Tao 2019).

Lung cancer is the second most frequently diagnosed cancer in the United States and leading cause of death from related to cancers. Although smoking is the leading risk factor—accounting for 80% to 90% of lung cancer cases—many other factors have also been identified as possible contributors in the development of this disease. But, few of the known risk factors for lung cancer are clearly causal in never-smokers (i.e., others than radon), which would be the world's 11th commonest cancer and 7th most important cause of a preventive death from all cancers. Despite the fact that lung cancer survival rates have only improved marginally in recent decades, early diagnoses via low-dose CT screening combined with new treatment options including targeted therapies and immunotherapy may decrease mortality and improve prognosis soon (Schabath & Cote, 2019).

On the other hand, there are risk factors which cannot be changed and those that can, non– modifiable: age, brith sex (male female) race or ethnic group; family history of coronary heart disease early death (1st-degree relative such as parents brother sister); hypertension. Age for lung cancer diagnosis (men and women): 70 years old in the US. Roughly 53% are found in people between the ages of 55 and 74, while a further third (37%) occur within even older individuals aged over the age of seventy-five. In the country, it is the number one killer on men above 40 and women over 59. In comparison with women, men are diagnosed and die of lung cancer globally more than twice as often. The main reason behind the existence of this sex gap is that men are more likely to smoke tobacco (Thandra et al., 2021).

Several registry-based studies have identified a positive family history of lung cancer as an important risk factor, suggesting higher familial predisposition to develop young-onset lung cancers. Higher relative risks were observed even when smoking behaviors adjusted for. Tobacco use, passive smoking, exposure to radon gas (in homes and business), air contamination from biomass fuel combustion or diesel exhausts also belong in this aggregate of alterable risk factors with chronic obstructive pulmonary illness susceptibility. The main risk factor for all major histological types of lung carcinoma is cigarette smoking (Malhotra et al., 2016).

Smoking is the major risk factor for all common histological types of lung carcinoma. Since the mid-1960s, epidemiological studies have confirmed that smoking has a harmful impact on lung carcinogenesis and this relationship is recognized by health and regulatory organizations (Huang et al., 2022).

The best and most effective way to reduce the risk of lung cancer is by preventing smoking initiation or supporting quitting. The USPSTF has issued recommendations on approaches to preventing tobacco use in children and adolescents as well as recommending pharmacotherapy and counseling for smoking cessation. Decisions regarding lung cancer screening are often made collaboratively between patients and healthcare providers. Screening benefits depend on risk, with those at higher risk most likely to benefit. However, screening does not prevent most deaths from lung cancer, making it essential to quit smoking. Lung cancer screening can also carry risks, such as false-positive results or incidental findings that could lead to unnecessary tests and procedures, as well the anxiety associated with having a suspicious lung lesion (potentially related malignancy) (Krist et al., 2021).

Aim of the Research:

- Assessing the awareness regarding preventive strategies related to pulmonary cancer among students
- Examine the relationship between awareness and demographic characteristics (age, sex, area of residence or social status).

Methodology:

Study Design
You are aimed your study objective out by using a quantitative descriptive design for cross sectional survey to determine the lung cancer prevention awareness among undergraduate students enrolled at Al-Muthanna University. The study occurred between 28 November 2025 and 19 April, with data collection occurring thereafter.

Organizational Provisions
Approval from Al-Muthanna University was obtained prior to data collection.

Moral Implications
This aspect of the research is important, because it meets ethical standards for scientific evaluation at this first step in sampling (described below):
A side note about confidentiality: the students are not identified.
Students are contacted on an individual basis as per the plan to provide details of the research and its objectives.
For the purpose of this research, all students will by definition have full information on their assignment.
All students are informed that the results of this questionnaire may only be used for educational purposes.
For all students, everyone is informed that any individual has the right to refuse participation in the study.

Context of the Research
This study carried out at (Al-Muthanna University / Al-Samawa City).

Study Sample
Sample Size used Raosoft calculator with data to ensure the final sample size of 105 person is adequate for research furthers, so valid and reliable results will be achieved.

Using a digital tool that helps to calculate the required minimum number of samples needed for validation (available here: http://www.raosoft.com/samplesize.html), the investigator used this link and found five participants refused to participate in study leaving 100 pupils.

Standards for Sample Selection

This study used the following inclusion criteria for selection of subjects:

The students who agreed to participate in the research, received formal consent after being informed of its purpose prior to data collection.
Al-Muthanna University students.

Stages of the Research

1. Development of the Instrument Framework:
The researchers designed a questionnaire supervised by the supervisor as part of achieving the aims of this study project on lung cancer prevention awareness at AL-Muthanna University.

2. Authenticity of the Instrument
A panel of fifteen specialists was shown the instrument to measure its authenticity. The specialists have an average of more than five years in their domain, with a mean tenure of 14.21 years out on the field. The specialists evaluated the survey, and some of the items were modified in this regard.

The Preliminary Investigation

In this preliminary research, however, a reduplication is completed to test reliability and length of time between researchers for specific costs & adverse occurrences then ultimately tweaks the design prior to entire study stages. Besides assessing the optimal response time, a pilot study (covering 10% of the sample comprising at least 10 students) was carried out to determine usability of instruments and understandability of constructed questionnaire.

Reliability of the Instrument

Reliability test was different for both parts of the questionnaire, and in order to know accuracy by major statistic parameter were calculated according Pearson's Correlation Coefficient reliability test indicated awareness. This is calculated without question that the questionnaire was successful and it result designed questionnaire to be reliable.

Data Gathering for Implementation
Data collection procedure Data were collected between March 4, and March 28, of the year 2025.

Techniques for Data Acquisition
The data were collected through a questionnaire on constructive awareness, which was filled with self-reported closed-ended structured questions. Score of (2) for the right response, score of (1) for wrong. The researcher set a threshold of (>0.74) for deficient awareness and (<0.75) proficient awareness determined from evidence-based practice regarding clinical skills in changing care with data collection up to October 2023.

Examination of Data
The analysis was performed using version 26 of the Statistical Package for the Social Sciences (SPSS).

1. Assessment of Normality: Kolmogorov-Smirnov Examination
The Kolmogorov-Smirnov (K-S) test was used to assess normal distribution.
Table (3-2) Testing of Hypothesis for Cognitive Sample:
2. Explanatory Statistical Averages
3. Deductive Examination

It is used to evaluate and quantify the reliability of estimates about a population from data drawn from that group.
Constraints of the Research:

Some students were also uncooperative responding to the questionnaire leading a longer time.
The sample of the study could always be limited to an narrow cohort of university students from one specific, and not a reflection on other type or type characteristics/groups in terms toward greater representation among all within those groups/context).

The study may focus only on some aspects of lung cancer (for example, etiology and clinical signs or prevention) leaving aside others (e.g., management options or psychological problems), limiting the completeness of findings.

Outcomes of the Research:

Table (1): Socio-Demographic Characteristics Data

Socio-demographic characteristic		Frequency	Percentage %
Age	18-20	36	36
	21-23	41	41
	24-26	21	21
	27=>	2	2
	Mean =21.61 St. deviation = 2.269		
Sex	Male	53	53
	Female	47	47
Residence	City	68	68
	Rural	32	32
Social Status	Single	94	94
	Married	6	6
	Divorced	0	0
	Widower	0	0
Economic Status	Sufficient	74	74
	Somewhat Sufficient	22	22
	Not Sufficient	4	4

F: Frequency, %: Percentage, Mean: Arithmetic Mean, SD: Standard Deviation.
The table shows that the 21-23 year old range was the worst affected (41% of ages sample) As shown in Table 1, the majority of students (53%) were male and had experienced more impact than females (47%). Most students lived in the city (68%),

while others lived in rural locations (32%). Students were came from a lower social class (94% unmarried, 6% married). The main part of economic circumstance is to get debatable; country score higher than everything else at 74%.

Table 2: Distribution of Study Variables

Awareness on Lung Cancer prevention		No		Yes		Mean	St. deviation	Assessment
		F	%	F	%			
1	Preventive measures against smoking reduces the risk of getting a lung cancer.	7	7	93	93	1.93	0.526	Good
2	Another benefit of avoiding secondhand smoking is that it may also reduce your risk for lung cancer.	10	10	90	90	1.90	0.302	Good
3	Understanding family medical history and taking precautionary actions can reduce the chances of lung cancer.	25	25	75	75	1.75	0.435	Good
4	Avoiding alcohol consumption may reduce the risk of lung cancer.	13	13	87	87	1.87	0.338	Good
5	Minimize air pollution through contaminated, feeling low or have lung cancer prevented.	11	11	89	89	1.89	0.314	Good
6	Healthy food and regular exercise can reduce the risk of lung cancer.	11	11	89	89	1.89	0.314	Good
7	Adopting safety planning at your workplace may reduce the risk of lung cancer.	10	10	90	90	1.90	0.302	Good
8	Lung cancer management hinges upon screening and early detection.	11	11	89	89	1.89	0.314	Good
9	Hormonal homeostasis, particularly sex hormones, may reduce the incidence of lung cancer.	43	43	57	57	1.57	0.498	Good
10	Avoid exposure to chemicals and gases in workstations, laboratories or palaces of manufacturing	8	8	92	92	1.92	0.273	Good

F.=frequency, % = percentage, Assessment: Adequate <2, an adequate less than or equal 2.
The results presented in this table suggest that the majority of participants have appropriate awareness regarding lung cancer prevention.

Table (3): Recognition of the Research Sample

Variables	Classification	F	%
Preventive awareness of lung cancer among students of University	Good	95	95
	Poor	5	5
	Total	100	100

F.=frequency, %=percentage
The data presented in this table illustrates that the majority of participants are aware of lung cancer prevention.

Table (4): Correlation of Sample Socio-Demographic Attributes and Awareness:

Socio-Demographical Characteristics	Significance
Age	Chi-square=3.776[a] df=3 P. value=0.287 Non-significant
Sex	Chi-square=1.540a df=1 P. value=0.215 Non-significant
Residence	Chi-square=0.155[a] df=1 P. value=0.694 Non-significant
Social status	Chi-square=0.336[a] df=1 P. value=0.562 Non-significant
Economic status	Chi-square=1.849[a] df=2 P. value=0.397 Non-significant

NS: Non-Significant at P>0.05, df: degree of freedom

Student awareness does not differ with age, sex or domicile social class nor economic factors. These variables all showed chi-square values above 0.05, the conventional level of statistical significance

Discussion

Analysis of Results Related To Demographic Characteristics

Student Age

The research showed that most participants were aged between 18 and 27 years, the largest segment of sample (41%) was in a age group ranging from 21 to 23 so considered as majority.
Consistent with the age results validated by (Bakry et al., 2021), that showed mean age of participants is (22.2 ± 1.33) years.
Now for part of the reason students are at a university age, so it's likely their ages reflect this time in life.
Sex
Results showed males (53%) had higher participation than females (47%).
In this survey study performed by Zafar (2022), over two-thirds of the participants were men, with 77.7% identified as male.
Slight majority of respondents were male probably as males prefer to do the completing this survey compared with females.

Societal Standing

The results showed that most Students were single (94%) and few of them had been married (6%).
Social standing manifested by Abo Al-Shiekh et al. (2021) reported that a majority of respondents are single.
Most of the participants were single, being it a developmental stage they had to prioritize their studies rather than matrimony.

Discussion Results on Student Awareness Findings

The study was descriptive in nature, consisting of 100 students from al-Muthanna University and the data showed a good level of awareness preventive. Awareness level peaks at 95%.
The results of research sponsored by (Qadhi, O. A., 2023) reported that pupils with good awareness accounted for (45.5%), moderate awareness was (24.3%) while low aware is the least which reached to be (26).
The results from this study contrast with those of Barros, A., etal. 2025) showed students have less awareness of lung cancer.

Luckman et al.'s source sentence the research conducted by Luckman et al. Most participants (62.6%) had acknowledgment to a strong awareness of the link between lifestyle factors and cancer per Lambert et al (2017)
Results of the study (Krukowska & Olejniczak, 2013) point to increased awareness on risk factors and lung cancer prevention among students.

The research outcomes vary from positive to negative awareness that many aspects can alter the awareness of students such as: demographic variables, area wise variations level (programme and educational material), personal attention during study period and variation in researcher methods for education.

Analyzing the Relationship of a Composite Measure of Awareness with Demographic Characteristics:

The study shows no significant relationship between students' awareness and the variables of age, sex, residence, social status and economical level. The chi-square statistics for these variables are greater than 0.05, the conventional criterion for significance testing.

Summary:

Summary Pertaining to Demographic Attributes

The majority of students ages (21-23 years old) made up 41% while male. The majority of the study participants belonged to college of science (24%), and most were single, 94%.

Summary Relevant to the Initial Objective:
The students' awareness of the risk factors and prevention of lung cancer

Summary Relevant to Objective
The sample of the study is not significantly correlated with age demographic variable, as evidenced by a p-value = 0.287 which exceeds 05 A comparison of the assessment for the study sample indicated no significant association with sex (p = 0.215>0.05).

Suggestions

The investigators recommended the following actions:
A similar study could be conducted on a larger population for greater generalizability.
Develop a well-structured questionnaire to cover various topics regarding the risk factors of lung cancer, preventive measures and awareness towards early detection.
Ask questions that address common misconceptions about lung cancer, such as the idea only smokers can get it.
Ask students about their awareness of lung cancer, as well as their smoking habits and views on health screening in addition to prevention measures.
Suggest incorporating the so-called engaging resources, workshops, seminars or online modules.
Start student-led movements or peer education where students educate their fellow peers on lung cancer.
Support smoking cessation programs and make tools readily available to students wishing to quit.

References

World Health Organization. (2019). Lung cancer (Fact Sheet). World Health Organization. https://www.who.int/news-room/fact-sheets/detail/lung-cancer
Brown, J. S., Amend, S. R., Austin, R. H., Gatenby, R. A., Hammarlund, E. U., & Pienta, K. J. (2023). Updating the definition of cancer. Molecular Cancer Research, 21(11), 1142-1147. https://aacrjournals.org/mcr/article/21/11/1142/729785
Almalki, S. G. (2023). The pathophysiology of the cell cycle in cancer and treatment strategies using various cell cycle checkpoint inhibitors. Pathology-Research and Practice, 154854. https://www.sciencedirect.com/science/article/abs/pii/S0344033823005551
Tao, M. H. (2019). Epidemiology of lung cancer. Lung Cancer and Imaging, 4-1. https://iopscience.iop.org/book/edit/978-0-7503-2540-0/chapter/bk978-0-7503-2540-0ch4
Schabath, M. B., & Cote, M. L. (2019). Cancer progress and priorities: lung cancer. Cancer epidemiology, biomarkers & prevention, 28(10), 1563-1579. https://aacrjournals.org/cebp/article/28/10/1563/71761/Cancer-Progress-and-Priorities-Lung-CancerCancer
Thandra, K. C., Barsouk, A., Saginala, K., Aluru, J. S., & Barsouk, A. (2021). Epidemiology of lung cancer. Contemporary Oncology/Współczesna Onkologia, 25(1), 45-52. Torre, L. A., Siegel, R. L., & Jemal, A. (2016). Lung cancer statistics. Lung cancer and personalized medicine: current Awareness and therapies, 1-19. WHO 2023. https://scholar.google.com/scholar?as_ylo=2021&q=risk+factors+of+lung+cancer&hl=ar&as_sdt=0,5
Malhotra, J., Malvezzi, M., Negri, E., La Vecchia, C., & Boffetta, P. (2016). Risk factors for lung cancer worldwide. European Respiratory Journal, 48(3), 889-902. https://scholar.google.com/scholar?hl=ar&as_sdt=0%2C5&q=risk+factors+of+lung+cancer&oq=risk
Huang, J., Deng, Y., Tin, M. S., Lok, V., Ngai, C. H., Zhang, L., ... & Wong, M. C. (2022). Distribution, risk factors, and temporal trends for lung cancer incidence and mortality: a global analysis. Chest, 161(4), 1101-1111. https://scholar.google.com/scholar?as_ylo=2021&q=risk+factors+of+lung+cancer&hl=ar&as_sdt=0,5
Krist, A. H., Davidson, K. W., Mangione, C. M., Barry, M. J., Cabana, M., Caughey, A. B., ... & US Preventive Services Task Force. (2021). Screening for lung cancer: US Preventive Services Task Force recommendation statement. Jama, 325(10), 962-970. https://jamanetwork.com/journals/jama/fullarticle/2777244
Bakry, S., Alshinkity, M. I., Abeeri, N. A., Albagami, S., Sami, A., Felemban, S. B., & Jastania, R. (2021). The awareness of lung cancer risk factors among health-related students at Umm Al Qura University in Makkah, Saudi Arabia. Medical Science, 25(117), 2998-3006. https://search.app/VxzRq2yKEBBtWndQA

Abo Al-Shiekh, S. S., Ibrahim, M. A., & Alajerami, Y. S. (2021). Breast cancer Awareness and practice of breast self-examination among female university students, Gaza. The Scientific World Journal, 2021(1),6640324. https://onlinelibrary.wiley.com/doi/full/10.1155/2021/6640324

Zainuddin, N., & Thabit, H. (2018). Awareness and perception on lung cancer and its screening: A study among undergraduate students of the International Islamic University Malaysia, Kuantan Campus. Journal of Biomedical and Clinical Sciences (JBCS), 2(2), 61-67. https://typeset.io/pdf/Awareness -and-perception-on-lung-cancer-and-its-screening-a-2prk9g40pw.pdf

Qadhi, O. A., Alghamdi, A., Alshael, D., Alanazi, M. F., Syed, W., Alsulaihim, I. N., & Al-Rawi, M. B. A. (2023). Awareness and awareness of warning signs about Lung cancer among Pharmacy and Nursing undergraduates in Riyadh, Saudi Arabia-an observational study. Journal of Cancer, 14(18), 3378. https://pmc.ncbi.nlm.nih.gov/articles/PMC10647201/

Sherman, S. M., & Lane, E. L. (2015). Awareness of risk factors for breast, lung and cervical cancer in a UK student population Journal of Cancer Education, 30, 660-663. https://link.springer.com/article/10.1007/s13187-014-0770-3

Luckman, S., Xiao, C., McLennan, E., Anderson, A. S., Mutrie, N., & Moug, S. J. (2017). An investigation into UK medical students' Awareness of lifestyle factors on cancer. Scottish Medical Journal, 62(3), 110-114. https://journals.sagepub.com/doi/abs/10.1177/0036933017706896

Krukowska, M., & Olejniczak, D. (2013). Assessment of students' Awareness about risk factors and prevention of lung cancer. Medycyna Rodzinna. https://www.czytelniamedyczna.pl/4677,ocena-wiedzy-studentow-na-temat-czynnikow-ryzyka-i-profilaktyki-nowotworow-pluc.html

Hameed HR, Kadush AJ, Jrood DF, Alabada R. Assessment of Nurses' Knowledge Concerning Gestational Hypertension at Maternity and Pediatric Teaching Hospital in Al-Samawa City. Bahrain Medical Bulletin. 2023 Dec 1;45(4). https://www.bahrainmedicalbulletin.com/December_2023/BMB-23-511.pdf

Kadush AJ, Hameed HR, Jrood DF. Nurses' knowledge of electrocardiogram interpretation at al-hussein teaching hospital in al-samawa city. Health Education and Health Promotion. 2023 Apr 10;11(2):203-7. https://hehp.modares.ac.ir/browse.php?a_id=68165&slc_lang=en&sid=5

Chen, C., & Zeng, H. (2022). Curcumin attenuates myocardial ischemia and reperfusion-induced proinflammatory response through activation of the Nrf-2/HO-1 signaling pathway. *Muthanna Medical Journal*, *9*(1), 41-56. https://muthmj.mu.edu.iq/journal/vol9/iss1/5?utm_source

TS, V., & SN, A. (2026). Knowledge, Attitude and Practice Towards Sarcopenia Among Diabetic Patients Attending Outpatient Department of a Tertiary Care Centre in Kerala, India. *Muthanna Medical Journal*, *13*(1), 65-71. https://muthmj.mu.edu.iq/journal?utm_source

NIU Journal of Health Sciences Copyright©2026
Nexus International University ISSN: 3136-6449; 12(1) 29-34

Dosimetric Evaluation of Volumetric Modulated Arc Therapy (VMAT) for Left-Sided Breast Cancer Assessment of Plan Quality Using Conformity and Homogeneity Indices Using Monaco Treatment

AYA KHALIED EIDAN[1], JENAN HUSSIEN TAHA[2], AHMED MOHAMMED JASIM[3]
[1]Department of Physiology/ Medical Physics, College of Medicine, University of Al-Nahrain, Baghdad, Iraq
ayakhalied585@gmail.com
[2] Department of Physiology/ Medical Physics, College of Medicine, University of Al- Nahrain, Baghdad, Iraq
asjenan@gmail.com, https://orcid.org/ 0000-0003-1966-7166
[3] MD MbCHB FIBMS –RT Board Certified Clinical Radiation Oncologist Iraqi Board Of Medical Specialities.
ahmedmohamed92@gmail.com

Abstract
Introduction: Radiotherapy serves as the main treatment approach for breast cancer on the left side. The challenge lies in ensuring sufficient coverage of the target while reducing radiation exposure to nearby organs at risk. Volumetric modulated arc therapy (VMAT) has been introduced to enhance dose conformity and better protect normal tissues.
Objective: This research aimed to assess the dosimetric properties of VMAT plans for patients with left-sided breast cancer by examining dose–volume histogram (DVH) parameters.
Methods: A retrospective analysis was conducted on fifty VMAT treatment plans. The dosimetric assessment focused on target coverage metrics (V95%, conformity index, and homogeneity index) and the radiation doses received by organs at risk, such as the heart, ipsilateral lung, contralateral lung, contralateral breast, esophagus, and spinal cord.
Results: VMAT planning provided consistent and clinically satisfactory dosimetric outcomes for both the target volumes and surrounding normal tissues. The chest wall PTV had an average V95 of 97.2%, while the lymph node PTV reached 98.7%, demonstrating sufficient target coverage with satisfactory conformity and dose uniformity. In terms of organs at risk, cardiac exposure was kept low, with the heart receiving an average dose of 5.0 Gy. The ipsilateral lung experienced mean V5, V20, and V30 values of 56.6%, 25.0%, and 21.0%, respectively. In contrast, the contralateral lung was subjected to minimal high-dose exposure, as indicated by mean V20 and V30 values of 0.3% and 0.06%. The contralateral breast received an average dose of 3.5 Gy, and the esophagus had a mean dose of 13.1 Gy, with a mean maximum dose of 33.6 Gy. Additionally, the spinal cord's mean maximum dose was 13.6 Gy. These dosimetric results suggest that VMAT effectively targeted irradiation while keeping radiation exposure to nearby critical structures within acceptable clinical thresholds.
Conclusion: VMAT achieved efficient target coverage, demonstrating good dose conformity and uniformity, all while keeping radiation exposure to nearby organs at risk within acceptable limits. These results endorse the clinical practicality of using VMAT for treating left-sided breast cancer.

1. Introduction

Radiation therapy (RT) is a central part of the management of breast cancer with Post-Mastectomy Radiotherapy (PMRT) being a standard adjuvant treatment after breast-conserving surgery, especially in early stage disease. Because of the complex breast anatomy, and the fact that the lungs and heart are organs at risk (OAR), a strict dosimetric control is warranted by hypofractionated regimens that are increasingly being adopted. One of the main challenges in postmastectomy radiotherapy (PMRT) [1], To ensure the best possible target coverage with minimal radiation exposure to healthy tissues in the vicinity. Patients with left sided breast cancer are at increased risk for radiation induced cardiac toxicity because the radiation is close to the heart. Also, over-radiation of the lung may lead to radiation pneumonitis and chronic disease of the lung [2]. Thus, careful treatment planning is essential to

achieve optimal tumour control and to minimise the radiation dose to surrounding normal tissues. Volumetric Modulated Arc Therapy (VMAT) is an advanced form of external beam radiotherapy, which delivers radiation using continuously rotating, adjusting arcs in the machine's gantry, as well as changing the location of the multileaf collimator (MLC), the beam delivery rate and the gantry rotation speed. In suitable patients, this method results in very uniform dose distribution, a high degree of target coverage and sparing of organs at risk, which are better outcomes than those of conventional radiotherapy. Dosimetric analysis is often used in the evaluation of VMAT treatment plans, especially for the use of dose–volume histogram (DVH) parameters and quality indices such as the Conformity Index (CI) and Homogeneity Index (HI) [3]. These metrics provide quantitative information on the degree of target dose coverage, and the amount of exposure to organs at risk, which can be used to optimize treatment plans and to assess the clinical efficacy of radiation therapy [4].

2. Patient and methods

2.1 Patient selection

This prospective dosimetry study will be conducted in the Wasit Oncology Center between November 2025 and May 2026. The study was approved by the Institutional Review Board (IRB) of the College of Medicine at Al-Nahrain University as a research requirement for a Master of Science degree in medical physics. The study included fifty female patients diagnosed with left-sided breast cancer who underwent surgical removal of the tumor from the breast, which was being treated with adjuvant radiotherapy in our study.

2. 2 Computed Tomography (CT) Simulator

The CT simulator was equipped with a dedicated breast board used for patient positioning and immobilization during CT simulation for breast radiotherapy planning, as shown in Figure (1). For those with breast cancer on the left side, the head was turned to the right during CT simulation to aid in positioning and enhance the consistency of the treatment setup. CT images were captured with a 2.5 mm slice thickness, as this thickness allows for more precise visualization of the target volume and adjacent organs at risk. These CT images were then transferred to the MONACO Treatment Planning System (TPS) for contouring and planning the treatment. The delineation of target volumes and organs at risk (OARs) followed the guidelines set by the Radiation Therapy Oncology Group (RTOG) and the European Society for Radiotherapy and Oncology (ESTRO). The Clinical Target Volume (CTV) encompassed the chest wall for all patients, as well as the regional lymph nodes. To ensure consistency in treatment planning comparison, a uniform 5 mm margin was added around the CTV to generate the Planning Target Volume (PTV).

Figure (1): CT Simulation Scanner with Breast Immobilization Board for Breast Cancer Radiotherapy.

2.3 Treatment Planning Techniques

Fifty female patients diagnosed with left breast cancer based on clinical examination by imaging US, MRI, and biopsy to have left breast Cancer, patients underwent surgery, whether partial (lumpectomy) or total resection (mastectomy), with regional lymph nodes, and all patients received adjuvant radiotherapy treatment in our study. The patients were prepared for the GE CT (GE revolution EVO, GE health care, JAPAN Corporation) was used with a slice thickness of 2.5 mm.Linear Accelerator (Synergy Agilty), Elekta 2015.Monaco Elekta HP, vesion

6.2.1. They were treated with an X-ray photon beam 10 MV for VMAT The prescribed dose to the PTV is 40.05 Gy delivered in 15 fractions energy using ELEKTA's Agility linear accelerator.

2.4 VMAT

PTV total was contoured (PTVCW+ PTVLN) and the isocenter where placed at the isocenter, where placed at the center of (PTV total). Two beam (with 2 arc per beam) were used in the planning, the two beams were counter clock wise started from 190º and with arc length (225º and 205º). The grid spacing was (0.3) which is recommended for VMAT. The segment width was 0.5 cm and beamlet width was 0.5 cm auto flash 2 cm that, as illustrated in figure (2).

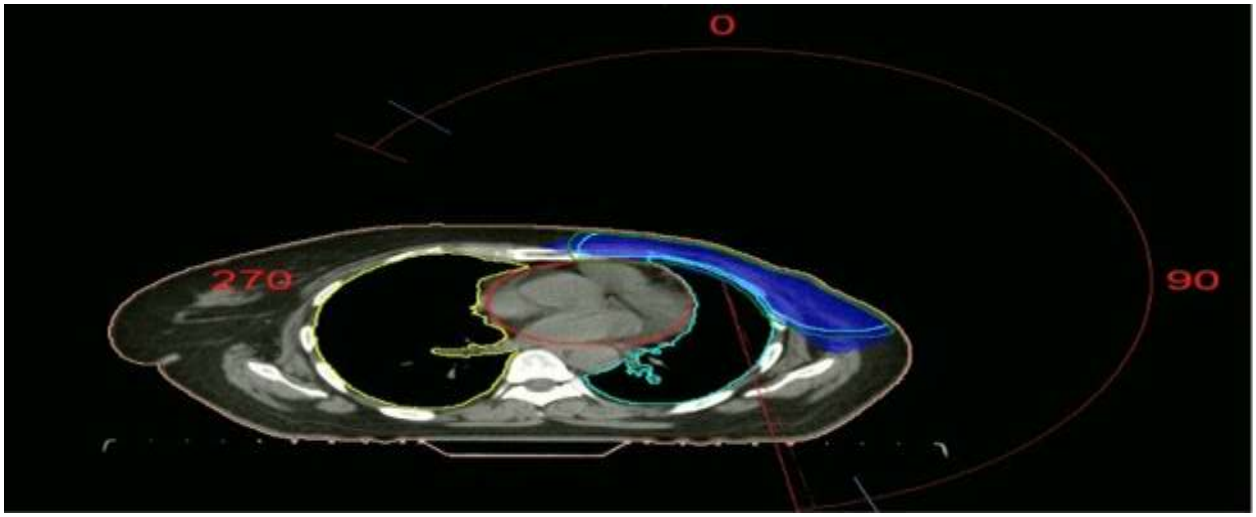

Figure (2): Left breast radiotherapy planning using VMAT technique.

2.6 Plan Evaluation

As per the planning objectives, the Dose Volume Histogram (DVH) parameters were analyzed to find the dose received by PTV and OARs. The dose-volume histogram is a valuable tool to explain and evaluate a treatment plan statistically, so we can find how much (numerically) dosage is received for targets and organs, the dose-volume histogram is a useful tool for describing and evaluating a treatment plan statistically. However, DVH was unable to provide us with a comprehensive picture of the dose distribution, the homogeneity of the dosage, and how the radiation dose is (geometrically) dispersed around the target. The dose conformation on the target and the surrounding tissue volume covered by the reference dose are measured by the conformance index (CI). Several equations have been proposed to describe the Conformity Index (CI) and, homogeneity Index however, in this study, the following equation was used [5], Lomax and Scheib had another definition of conformity index, which took into account the tissue covered with reference radiation dose. They called it the healthy tissue conformity index and could be expressed as follows equation (1):

Healthy tissue conformity index= TV_{RI}/ V_{RI} --------(1

Where:

TV_{RI} is the target volume that is covered with reference radiation dose.

V_{RI} is the volume of reference radiation dose [6].

$HI=D_{5\%}/D_{95\%}$

Where:

$D_{5\%}$ is the maximum In general, the dose homogeneity is a characterization of the absorbed- dose distribution within the target volume. A perfectly homogeneous dose to the PTV would be characterized by a spike in the differential DVH or a vertical drop of the cumulative DVH line for the PTV at that absorbed dose, as proposed by the RTOG target volume, shadowed; volume of reference isodose, enclosed in black dashes, as demonstrated in figure (3) [7] .

$D_{95\%}$ is the minimum dose in 95% of the target volume [11].

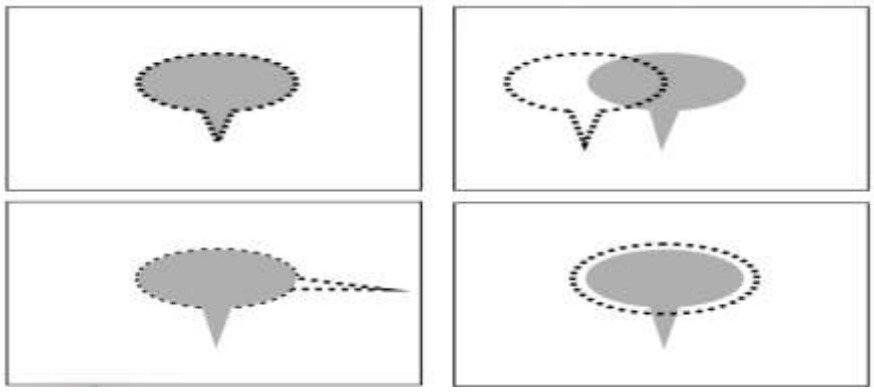

Figure 3: Four possibilities for which the VRI /TV ratio is equal to 1(index proposed by the RTOG) (1) (target volume, shaded; volumeof reference isodose, enclosed in black dashes) [39].

also, the defined homogeneity index was used in the following equation

dose for 5% of the target volume.

$D_{95\%}$ is the minimum dose in 95% of the target volume [8].

3. Statistical analysis

The statistical analysis achieved using SPSS v24 (IBM Inc., Chicago, IL, USA). Descriptive statistical analysis was used to summarize the dosimetric parameters of the VMAT treatment plans. The results were presented as mean ± standard deviation (SD).

4. Results

The results obtained from the Volumetric Modulated Arc Therapy (VMAT) treatment plans. The evaluated dosimetric parameters included the planning target volume (PTV) and organs at risk (OARs) for minimum and maximum doses, as illustrated in table (1).

Table (1): Dose received by organs and target using VMAT planning technique.

Endpoints		min	max	mean	SD	median
Contralateral lung	V5 Gy (%)	13.00	44.00	23.30	6.30	23.40
	V20 Gy (%)	0.00	1.40	0.30	0.10	0.00
	V30 Gy (%)	0.00	0.25	0.06	0.10	0.00
	Mean dose (Gy)	2.90	6.10	3.80	0.60	3.80
Ipsilateral lung	V5 Gy (%)	42.30	68.00	56.60	5.10	56.00
	V20 Gy (%)	19.00	31.00	25.00	2.50	25.40
	V30 Gy (%)	10.10	27.90	21.00	3.50	21.30
	mean dose (Gy)	3.20	10.10	3.50	2.30	3.60
Heart	V5 Gy (%)	10.00	25.70	19.70	3.60	20.20
	V10 Gy (%)	5.20	13.90	8.90	2.40	8.50
	V25 Gy (%)	0.20	4.10	1.08	1.04	1.60
	mean dose (Gy)	3.60	5.90	5.00	0.50	5.10
Contralateral breast	mean dose (Gy)	2.50	4.30	3.50	0.40	3.60
Esophagus	max dose (Gy)	29.20	38.90	33.60	2.20	33.40
	mean dose (Gy)	3.80	15.60	13.10	1.30	12.70
Spinal cord	max dose (Gy)	4.80	28.40	13.60	3.50	13.30
PTV (chest wall)	V95 (%)	94.00	99.90	97.20	1.50	97.40
	CI	0.65	0.90	0.79	0.05	0.80
	HI	1.02	1.11	1.07	0.02	1.07
PTV (lymph nodes)	V95 (%)	96.10	99.90	98.70	1.40	98.40
	CI	0.68	0.90	0.84	0.03	0.85
	HI	1.03	1.09	1.06	0.03	1.06

5. Discussion

Table (1) presents the radiation doses delivered to the organs at risk (OARs) and target volumes using the VMAT planning technique, both lungs showed the dose-volume analysis showed that the VMAT technique effectively spared both the ipsilateral and contralateral lungs. As expected, the ipsilateral lung received higher radiation doses

because of its proximity to the target volume, whereas the contralateral lung received minimal exposure, particularly for V20 and V30. These results show that the VMAT technique yields good target coverage with minimal radiation dose to healthy lung tissue, which can help limit the risk of radiation-induced lung toxicity [9] and demonstrates relatively low radiation doses for the heart. The mean values of V5, V10, and V25 were 19.70%, 8.90%, and 1.08%, respectively, with a mean heart dose of 5.00 Gy. These findings illustrated that VMAT effectively reduced the radiation dose to the heart while maintaining adequate target coverage, which may help decrease the risk of radiation-induced cardiac toxicity. The contralateral breast showed low radiation doses with the VMAT technique, recording a mean does of 3.50±0.40 Gy. These Findings demonstrated effective sparing of the contralateral breast, with only a small volume receiving higher radiation doses. This may help reduce unnecessary radiation exposure and the risk of radiation-induced secondary breast cancer. The esophagus received low radiation doses with the VMAT technique. The maximum and mean doses delivered to the esophagus were 33.60 ± 2.20 Gy and 13.10 ± 1.30 Gy, respectively. These findings indicate effective sparing of the esophagus. These findings indicate effective sparing of the esophagus, with only a small volume receiving moderate and high radiation doses, which may reduce the risk of radiation-induced esophageal toxicity [10], the maximum dose delivered to the spinal cord was 13.60 ± 3.50 Gy. This relatively low maximum dose indicates effective protection of the spinal cord during VMAT treatment while maintaining adequate target coverage. Keeping the maximum dose low is important to minimize the risk of radiation-induced spinal cord injury. The results demonstrated excellent target coverage for both the chest wall and lymph node PTVs. The mean V95 values were 97.20 ± 1.50% and 98.70 ± 1.40%, respectively, which were satisfactory. The mean CI was 0.79 ± 0.05 for chest wall and 0.84 ± 0.03 for the lymph nodes, indicating good dose conformity. Furthermore, the mean HI values were 1.07 ± 0.02 and 1.06 ± 0.03, which means a homogeneous distribution of the dose in both target volumes[11].

The results in Table (1) show that the VMAT technique was able to cover the target with a high precision while avoiding the organs at risk. Chest wall and lymph node target doses were accurately delivered and homogenous, as evidenced by high V95s and acceptable conformity and homogeneity indices. In addition, low doses of radiation are given to the heart, contralateral breast, esophagus, spinal cord and contralateral lung are indications of VMAT's ability to reduce unnecessary radiation exposure to healthy tissues. The doses for the ipsilateral lung were relatively higher due to its close proximity to the target volume, but all the dose parameters were within the clinically acceptable limits. All these results indicate that VMAT delivers the best trade-off between target coverage and organ-at-risk sparing and, therefore, may offer a better treatment quality while minimizing radiation-induced toxicities.

The similarity between the mean and median values in our finding implies that there were no extreme values that significantly affected the data and that the data were not strongly skewed. This indicates that the dosimetric values obtained are likely to be believable and representative of the population studied. Based on their clinical importance and their connection with radiation-induced toxicity, the dosimetric parameters were chosen. The parameter V20 was selected as the most important parameter for the ipsilateral lung since it is highly correlated with the risk of radiation pneumonitis. From a clinical point of view, a V20 of less than 30% is a protective factor to minimize the risk of radiation pneumonitis and a risk factor for the development of radiation pneumonitis-related symptoms like cough and dyspnea. V25 and mean dose were highlighted for the heart, where keeping V25 less than 10% will reduce the incidence of late cardiac side-effects. Moreover, the mean dose to the heart is associated with a relative risk increase of ~7% per 1 Gy. Unnecessary radiation exposure was estimated for the contralateral breast by using the mean dose, as doses exceeding 5 Gy can lead to an increased risk of secondary breast cancer in the future. Lastly, V95%, CI and HI were chosen to assess the target coverage, dose conformity and dose homogeneity for a thorough representation of the treatment plan quality.

6. Conclusion

The dosimetric measures have shown that VMAT can deliver a good dose distribution for left-sided breast cancer patients. The treatment plans included good coverage of the target areas with high V95 values, and satisfactory conformity and homogeneity indices, which indicated excellent coverage of the target areas including the chest wall and regional lymph nodes. It implies that the doses prescribed was accurately and regularly applied in the targeted areas. VMAT significantly reduced radiation dose to the heart, opposite lung, opposite breast, esophagus and spinal cord, while maintaining clinically acceptable dose levels for these organs at risk. The higher doses were received by the ipsilateral lung, but all of the dosimetric parameters evaluated remained within acceptable limits. This study's findings suggest that VMAT is an effective approach to treating left breast cancer patients, with good

target coverage and protection of the surrounding healthy tissues. These dosimetric characteristics may reduce the risk of radiation induced side effects, but remain accurate and high-quality radiotherapy treatment.

Ethical Permissions: The College of Medicine/ Al-Nahrain University has approved the ethical permission for this research (IRB-).

Conflicts of Interest: The authors declared no conflicts of interest.

Authors' Contribution: Aya Khalied (First Author), Introduction Writer/Methodologist/Main Researcher/Discussion Writer (60%); Jenan Hussien Taha (Second Author), Introduction Writer/Statistical Analyst (20%); Ahmed Jasim (Third Author), Discussion Writer (20%)

Funding/ Support: The research article did not receive any funding from any source (my university or any other institute).

References

[1] P. Confidential, A. Society, and R. Oncology, 'Public Comment Draft Postmastectomy Radiation Therapy: An ASTRO / ASCO / SSO Clinical Practice Guideline', pp. 1–36.
[2] 'Breast cancer'. Accessed: Jan. 10, 2026. [Online]. Available: https://www.who.int/news-room/fact-sheets/detail/breast-cancer
[3] C. Tamburella, G. Guibert, O. Santa Cruz, P. Weber, and P. Tsoutsou, 'A volumetric Modulated Arc Therapy (VMAT) combined with deep inspiration breath hold (DIBH) technique for adjuvant irradiation for left sided breast cancer.', arXiv, pp. 1–12, 2017.
[4] E. B. Podgorsak, 'Radiation Oncology Physics: A Handbook for Teachers and Students'.
[5] V. Hernandez et al., 'What is plan quality in radiotherapy? The importance of evaluating dose metrics, complexity, and robustness of treatment plans', *Radiother. Oncol.*, vol. 153, pp. 26–33, 2020, doi: 10.1016/j.radonc.2020.09.038.
[6] T. Kataria, K. Sharma, V. Subramani, K. P. Karrthick, and S. S. Bisht, 'Homogeneity Index: An objective tool for assessment of conformal radiation treatments', vol. 37, no. 4, pp. 207–213, 2012, doi: 10.4103/0971-6203.103606.
[7] C. Voyant, M. Pinpin, D. Leschi, S. Prapant, F. Savigny, and M. A. Acquaviva, 'Hybrid VMAT-3DCRT as breast cancer treatment improvement tool', Sci. Rep., vol. 13, no. 1, pp. 1–23, 2023, doi: 10.1038/s41598-023-50538-x.
[8] R. K. Adair, 'Vibrational resonances in biological systems at microwave frequencies', *Biophys. J.*, vol. 82, no. 3, pp. 1147–1152, 2002, doi: 10.1016/S0006-3495(02)75473-8.
[9] C. Shambhavi et al., 'Dosimetric comparison of volumetric modulated arc therapy, and h-VMAT in left breast radiotherapy under free-breathing and breath-hold conditions', pp. 1–10, 2025.
[10] S. K. Das Majumdar et al., 'A Dosimetric Study Comparing 3D-CRT vs. IMRT vs. VMAT in Left-Sided Breast Cancer Patients After Mastectomy at a Tertiary Care Centre in Eastern India', Cureus, vol. 14, no. 3, 2022, doi: 10.7759/cureus.23568.
[11] M. Mankinen, T. Virén, J. Seppälä, and T. Koivumäki, 'Interfractional variation in whole - breast VMAT irradiation: a dosimetric study with complementary SGRT and CBCT patient setup', *Radiat. Oncol.*, pp. 1–11, 2024, doi: 10.1186/s13014-024-02418-5.

NIU Journal of Health Sciences Copyright©2026
Nexus International University ISSN: 3136-6449; 12(1) 35-46

Biochemical, Physiological, and Immunological Changes Associated with *Toxoplasma gondii* Infection and Their Effects on Human Brain Health

DIANA KHALED KARIM
Department of Chemistry, College of Science, University of Wasit, Wasit, Iraq
diana.khalid@uowasit.edu.iq

Abstract
Toxoplasma gondii is an intracellular protozoan parasite infecting a large percentage of the world's population and potentially staying a long time in human tissues, especially in the central nervous system. The long-term consequences of chronic infection have been linked to neuroinflammation, immune dysfunction, oxidative damage and neurological issues. This study proposed to examine the physiological and immunological changes resulting from infection with Toxoplasma gondii and to assess changes in brain health in humans.
In this cross-sectional study, the age range was 20-60 years and the subjects were divided into four groups: healthy control, acute toxoplasmosis, chronic toxoplasmosis and treated patients with anti-parasitic drugs. The parameters were assessed for physiological, hematological, immunological, oxidative stress and neuroimaging parameters. Neurological examination, cognitive assessment and magnetic resonance imaging (MRI) were used to assess brain involvement, and serum levels of pro-inflammatory cytokines, anti-Toxoplasma antibodies, and oxidative stress biomarkers were determined by standard laboratory techniques.
Particularly, the participants with infection showed substantial changes, as compared to healthy controls ($P < 0.05$). Increased levels of TNF-α, IL-6, IFN-γ, and anti-Toxoplasma antibodies were also observed in acute and chronic toxoplasmosis, along with increased levels of oxidative stress markers and decreased levels of antioxidant capacity. Hematological changes (increase in WBC and changes in immune cell populations) were also observed. MRIs showed different extents of brain involvement, especially in the patients with chronic toxoplasmosis. The levels of inflammatory cytokines correlated positively with neurological abnormalities.
The *Toxoplasma gondii* infection causes a number of physiological, immunological and neurological changes in humans. During chronic infection, the brain may be involved due to the persisting inflammation and oxidative stress. The knowledge of these mechanisms can help to better diagnose, monitor and treat toxoplasmosis and its neurological effects.

Keywords: *Toxoplasma gondii*; Human toxoplasmosis; Neuroinflammation; Immune response; Oxidative stress; Brain involvement; Magnetic resonance imaging (MRI); Neurological manifestations

1. Introduction

Toxoplasmosis is a common zoonosis that results from infection with an obligate intracellular protozoan parasite named *Toxoplasma gondii*, which can infect nearly all warm-blooded animals, including humans. It is regarded as one of the most successful human parasites worldwide as it has the capacity to establish acute and chronic infection and maintain itself in host tissues for prolonged periods. In immunocompetent people, infection is generally either asymptomatic or with mild symptoms, but can result in severe complications in immunocompromised people and pregnant women and in congenitally infected infants (Montoya and Liesenfeld, 2004; Elsheikha et al., 2020).

Humans can catch infection from eating oocysts in food or water that have been shed by infected cats or from eating undercooked meat that contains tissue cysts, or via congenital transmission from the mother to the fetus. Rapidly multiplying tachyzoites spread throughout the body and later transform into bradyzoites which form long-

term tissue cysts in various organs, including the brain, skeletal muscles and retina (Pan et al., 2022; Hakimi et al., 2021).

The infection of *Toxoplasma gondii* is a significant worldwide public health problem. Around one-third of the world's population is estimated to have been exposed to the parasite, though prevalence is very variable from region to region, depending on climate, dietary practices, socioeconomic status, hygiene and exposure to cats and contaminated soil (Wang et al., 2020). Infections are much more common in developing countries because sanitation is poor and people are exposed to contaminated environments (Rostami et al., 2020).

One of the key organs infected by chronic infection with *Toxoplasma gondii* is the CNS. Once the blood–brain barrier is crossed, the parasite may remain in the brain, leading to chronic neuroinflammation and changes in brain function. Persistent infection has been linked with cognitive impairment, memory loss, changes in neurotransmitter signaling and risk for multiple neuropsychiatric disorders (Zhao et al., 2022; Andreou et al., 2024; Mares et al., 2024).

A host immune response is very important in the control of parasite replication. Several pro-inflammatory cytokines such as interferon gamma (IFN-γ), tumour necrosis factor alpha (TNF-α) and interleukin-6 (IL-6) are secreted by innate and adaptive immune responses. These cytokines are crucial to control the proliferation of parasites, but chronic immune activation can lead to oxidative stress, damage to neurons and tissue, especially in the brain (Nasuhidehnavi et al., 2021).

Furthermore, the infection by *Toxoplasma gondii* could affect the physiological homeostasis through modulation of haematological parameters, antioxidant defence mechanisms and metabolic functions (Szewczyk-Golec et al., 2021). High levels of reactive oxygen species (ROS) may overwhelm the body's own antioxidant systems, causing lipid peroxidation, dysfunction of cells and neurological problems (Savadelis et al., 2023; Estato et al., 2023; Yang et al., 2024; Li et al., 2024; Paraboni et al., 2022).

Although extensive research has been conducted on toxoplasmosis, there is still a lack of research that has studied simultaneously the relationships among physiological changes, immune responses, oxidative stress biomarkers, and brain involvement in human patients. Previous studies were mostly conducted on the single manifestation of the disease and did not investigate the systemic and neurological function as a whole (Savadelis et al., 2023; Estato et al., 2023; Yang et al., 2024; Li et al., 2024; Paraboni et al., 2022; Yao et al., 2024).

The current study aimed to explore the physiology and immunology of *Toxoplasma gondii* infection in humans and the effects on the brain. Additionally, this study sought to establish the association between inflammatory response, oxidative stress markers, and neuroimaging aspects in patients with acute, chronic and treated toxoplasmosis (Zhao et al., 2022; Savadelis et al., 2023; Li et al., 2024).

2. Materials and Methods

2.1 Study Design

This cross-sectional clinical study aimed to explore the physiological and immunological alterations, which may occur due to *Toxoplasma gondii* infection, and how it might affect brain function in human beings over 6 months (Pleyer et al., 2020; Robert-Gangneux and Dardé, 2012).

2.2 Study Population

Sixty participants, aged 20 to 60 years were enrolled and assigned to four groups (n = 15 per group) (Rostami et al., 2020).
Group I: Healthy controls (n = 15)
Group II: Acute toxoplasmosis patients (IgM positive) (n = 15)
Group III: Chronic toxoplasmosis patients (IgG positive) (n = 15)
Group IV: Treated toxoplasmosis patients receiving anti-parasitic therapy (n = 15)

2.3 Inclusion and Exclusion Criteria

Inclusion criteria (Robert-Gangneux and Dardé, 2012)
Adults aged 20–60 years.
Laboratory-confirmed toxoplasmosis.
Capacity to give informed consent.
Exclusion criteria (Rostami et al., 2020)
Pregnancy.
HIV infection.
Autoimmune diseases.
Malignancy.
Immunosuppressive treatment.

2.4 Physiological Measurements

During standard clinical examination, physiological parameters such as body mass index (BMI), body temperature, blood pressure, and neurological symptom scores were measured according to standard procedures.

Body weight: The body weight was taken on a calibrated digital weighing scale with an accuracy of 0.1 kg with the participants wearing light clothes and without shoes.

Body temperature: During clinical evaluation, the body temperature was taken with a calibrated digital infrared thermometer or an oral digital thermometer.

2.5 Hematological Analysis

All participants had venous blood samples (5 ml) drawn with aseptics for hematological evaluation. The hematological parameters were analyzed by an automated hematology analyzer according to its manufacturer's instructions. The parameters chosen for evaluation of the systemic effects of *Toxoplasma gondii* infection on blood cell populations and the host immune response.

The following haematological indices were determined:

The levels of white blood cells (WBC): These are used to assess immune activation and inflammatory response as a result of infection.
The red blood cell count (RBC): was measured to determine the effect of the infection on erythropoiesis and oxygen transport.
Hemoglobin concentration (Hb): Test to ensure that there is not anemia or change in carrying capacity of oxygen in the system with systemic inflammation.
Platelet count (PLT): To evaluate changes in hemostasis and inflammation, if an infection occurs.
Neutrophil percentage: This represents a measure of the innate immune response, and is thought to represent the first line of defense against invading pathogens.
Breathing resistance cells: measure to evaluate adaptive immune responses; specifically to evaluate the activation of T lymphocytes regulating intracellular parasites.
Duplicate sampling was done for all laboratory analyses to ensure quality control. The values obtained were noted and expressed as (Mean ± SD) to carry out statistical analysis.

2.6 Immunological Assays (ELISA)

The samples in the serum were centrifuged at 3000 rpm for 15 minutes and then kept at −20°C for analysis. The concentrations of cytokines and antibody were determined by commercial ELISA kits in accordance with the manufacturer's instructions.
All of the above are:
Pro-inflammatory Cytokines: Tumor necrosis factor alpha (TNF-α), Interleukin-6 (IL-6) and Interferon gamma (IFN-γ).
Antibody that is anti-inflammatory: Interleukin-10 (IL-10)
Previously, anti-Toxoplasma antibodies, which included Immunoglobulin G (IgG) and Immunoglobulin M (IgM), were used.
The absorbance values were measured using an ELISA microplate reader at 450 nm.

2.7 Oxidative Stress Biomarkers

Previously described procedures were used to determine oxidative stress biomarkers. The following parameters were measured:
Malondialdehyde (MDA): Lipid peroxidation was assessed by measuring the MDA level.
The activity of the antioxidant defense enzyme superoxide dismutase (SOD) was measured.
Catalase (CAT): CAT activity was determined by the breakdown of hydrogen peroxide.

To assess the intracellular antioxidant status, reduced glutathione (GSH) level was determined.
The overall antioxidant defense system was evaluated as the total antioxidant capacity (TAC) (Szewczyk-Golec et al., 2021; Paraboni et al., 2022).

2.8 Brain Assessment

Neurological examinations, cognitive assessment tests and magnetic resonance imaging (MRI) were used to evaluate brain involvement when available. Brain abnormalities were assessed semi-quantitatively based on their degree of involvement, with 0 for no abnormalities (normal); 1 for mild abnormalities; 2 for moderate abnormalities; and 3 for severe abnormalities. Each participant's severity scores were collected to evaluate the relationship between neuroimaging, neurological symptoms, inflammatory cytokines and oxidative stress biomarkers.

2.9 Statistical Analysis

Data obtained were statistically analyzed using SPSS (Version 26) software. The data were shown as Mean ± Standard Deviation. One-way Analysis of Variance (One-way ANOVA) followed by Tukey's Post Hoc Test for Multiple Comparisons was used to compare among groups. Difference was considered to be statistically significant at $P< 0.05$.

3. Results and Discussion

Significant physiological changes were observed between infected and control participants when the participants were infected with *Toxoplasma gondii* ($P < 0.05$). In acute and chronic toxoplasmosis, body temperature was elevated, neurological symptoms were more frequent and overall physical functioning was impaired. Chronic toxoplasmosis patients showed more pronounced clinical manifestations than patients with acute infection.

The changes can be explained by systemic inflammation, higher metabolic needs, and chronic immune activation as a consequence of *Toxoplasma gondii* infection (Savadelis et al., 2023; Estato et al., 2023). Infected participants reported being tired, having a headache, not concentrating, memory loss and poor cognitive function, especially in those with chronic infection (Savadelis et al., 2023; Yang et al., 2024).

The results indicate that *Toxoplasma gondii* alters the normal physiological homeostasis and adversely affects human health. Previous studies have shown that chronic toxoplasmosis can cause changes in neurotransmitter pathways, neuroinflammation and neurobehavioral abnormalities such as fatigue, decreased cognitive function, and diminished quality of life (Andreou et al., 2024; Savadelis et al., 2023; Li et al., 2024).

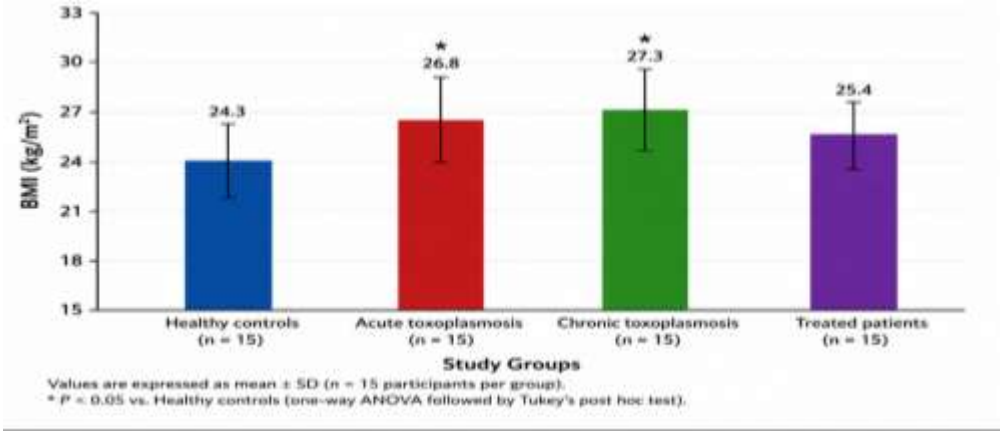

Demographic and clinical data of the patients in each study group are shown in Table 1. The changes in physiological parameters and neurological symptom scores of the study groups are shown in Figures 1 and 2 respectively.

Table 1: Demographic and Clinical Characteristics of Study Participants

Group	Description	Number of Participants (n)
I	Healthy controls	15
II	Acute toxoplasmosis	15
III	Chronic toxoplasmosis	15
IV	Treated patients	15

Figure 1. Comparison of Body Mass Index (BMI) Among Healthy Controls, Acute, Chronic, and Treated Toxoplasmosis Patients

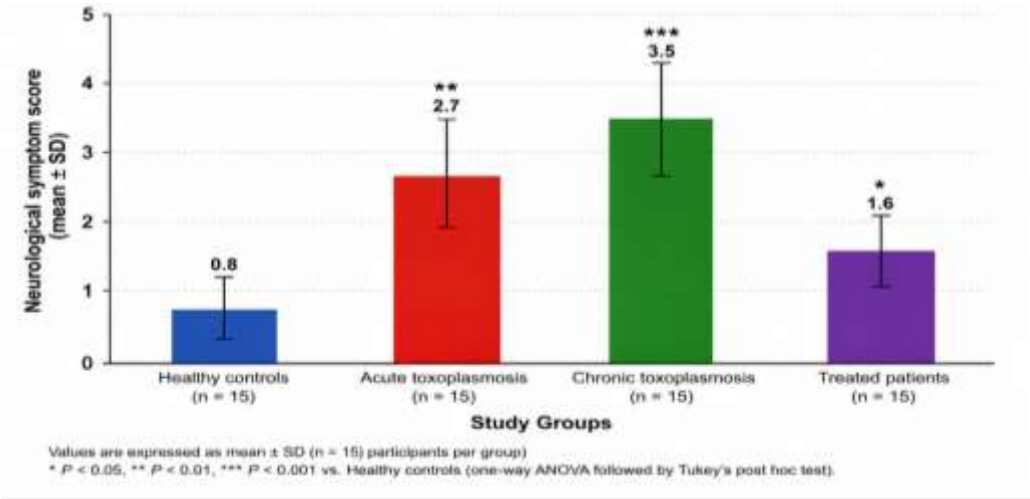

Figure 2. Neurological Symptom Severity Scores across the Study Groups

3.1 Hematological Alterations during Infection

Meanwhile, there were significant hematological changes found between the patients with *Toxoplasma gondii* infection and healthy controls ($P<0.05$). The infected participants had higher levels of white blood cells (WBC) which is an indicator of activation of the immune system in response to a parasitic infection. In acute toxoplasmosis there was a significant association with elevated percentage of neutrophils (innate immune system), while in chronic toxoplasmosis it was with increased percentage of lymphocytes (adaptive immune system) (Torres et al., 2021; Cowan et al., 2022).

There was also moderate decrease in red blood cell (RBC) count, hemoglobin (Hb) levels and platelet counts, especially in the patients with chronic toxoplasmosis. Such changes might be due to chronic systemic inflammation, chronic immune activation and disruption of normal hematopoiesis (Yang et al., 2024).

Previous work has shown that *Toxoplasma gondii* infection influences immune regulation and blood cell populations, and leads to inflammatory responses and systemic physiological disturbances (Cowan et al., 2022; Yang et al., 2024; Li et al., 2024).

The hematological abnormalities seen in the present study suggests that the disease of toxoplasmosis can significantly affect both innate and adaptive immunity, and may play a role in disease progression and neurological disease in patients with toxoplasmosis infection. The changes in hematological parameters are summarized in Table 3 and are shown in Figure 3.

Table 2: Comparison of Physiological Parameters among Healthy Controls, Acute, Chronic, and Treated Toxoplasmosis Patients

Parameter	Control	Acute	Chronic	Treated
BMI (kg/m²)	24.1 ± 2.4	26.8 ± 3.2	27.5 ± 3.5	25.6 ± 2.9
Body temperature (°C)	36.9 ± 0.3	37.9 ± 0.4	37.6 ± 0.3	37.1 ± 0.2
Systolic BP (mmHg)	118 ± 9	126 ± 10	128 ± 11	121 ± 8
Neurological symptom score	0.8 ± 0.4	2.8 ± 0.6	3.5 ± 0.7	1.6 ± 0.5

Table 3: Hematological Profiles of Participants Across the Study Groups

Parameter	Control	Acute	Chronic	Treated
WBC (×10³/µL)	7.2 ± 0.8	10.8 ± 1.2	10.2 ± 1.1	8.3 ± 0.9
RBC (×10⁶/µL)	5.1 ± 0.4	4.6 ± 0.3	4.4 ± 0.3	4.9 ± 0.4
Hb (g/dL)	14.5 ± 0.8	13.1 ± 0.7	12.6 ± 0.8	13.8 ± 0.7
Platelets (×10³/µL)	275 ± 32	235 ± 28	220 ± 25	255 ± 30
Neutrophils (%)	56 ± 5	72 ± 6	60 ± 5	58 ± 4
Lymphocytes (%)	34 ± 4	22 ± 3	42 ± 4	36 ± 4

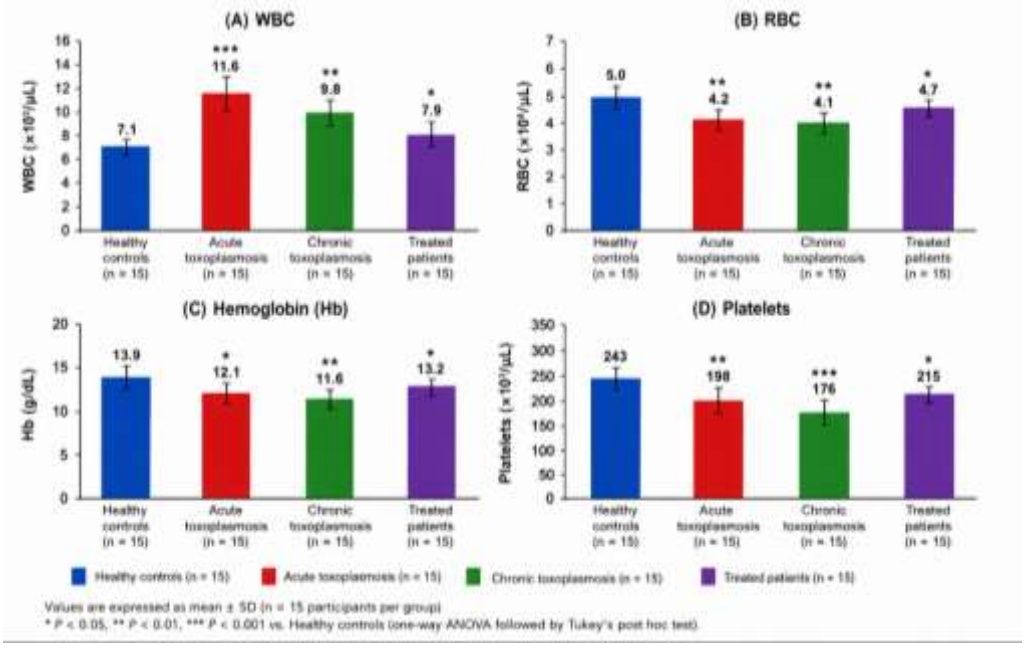

Figure 3. Comparative Analysis of Hematological Parameters Among the Study Groups

3.2 Immunological Responses and Cytokine Alterations

Both acute and chronic toxoplasmosis patients showed significantly higher serum levels of TNF$a, IL-6 and IFNa compared to healthy controls (P<0.05). The greatest rise was observed with IFN-γ, which is an important player in the activation of macrophages and the regulation of proliferation of intracellular parasites (Torres et al., 2021).

The increased levels of TNF-α and IL-6 were indicative of stronger inflammatory responses and recruitment of immune cells to the infected tissues. These cytokines are necessary in the control of proliferation of parasites, but continued production of these cytokines can lead to excessive inflammation and tissue damage, especially when there are chronic infections (Torres et al., 2021; Savadelis et al., 2023).

There was also a moderate rise in levels of IL-10, which is thought to have an anti-inflammatory effect and to help regulate immune activation and immune homeostasis when it is excessive (Torres et al., 2021).
Concerning serological markers, the level of anti-Toxoplasma IgM was significantly elevated in patients with acute toxoplasmosis while the anti-Toxoplasma IgG was significantly higher in patients with chronic toxoplasmosis, which correlated with the development of long-term immunological memory (Szewczyk-Golec et al., 2021).

In line with previous studies, which have found that chronic toxoplasmosis was accompanied by a sustained inflammatory response and immune activation (Savadelis et al., 2023; Li et al., 2024), these findings indicate a long-term inflammatory response and immune activation during chronic toxoplasmosis.

The levels of cytokines and antibodies are summarized in Table 4 and shown in Figures 4 and 5.

Table 4: Serum Inflammatory Cytokine and Anti-Toxoplasma Antibody Levels in the Different Study Groups

Parameter	Control	Acute	Chronic	Treated
TNF-α (pg/mL)	18 ± 3	56 ± 5	61 ± 6	32 ± 4
IL-6 (pg/mL)	12 ± 2	48 ± 4	53 ± 5	25 ± 3
IFN-γ (pg/mL)	20 ± 3	70 ± 6	78 ± 7	40 ± 5
IL-10 (pg/mL)	10 ± 2	18 ± 2	22 ± 3	15 ± 2
IgM (AU/mL)	0.5 ± 0.1	3.2 ± 0.3	1.8 ± 0.2	1.2 ± 0.2
IgG (AU/mL)	0.6 ± 0.1	4.8 ± 0.4	8.6 ± 0.6	5.2 ± 0.5

Values are expressed as mean ± SD. Statistical significance was considered at $P < 0.05$.

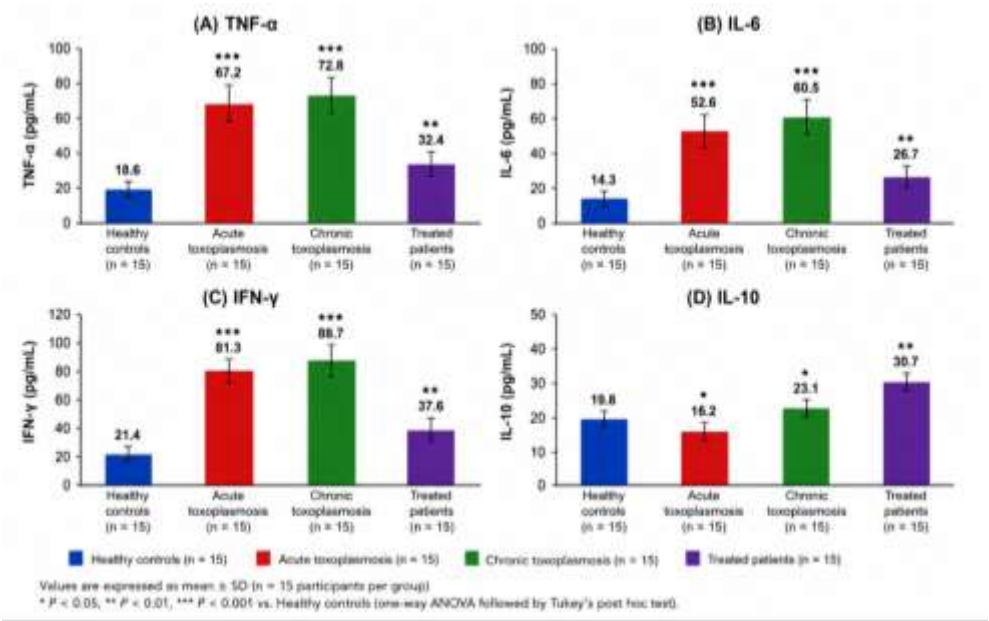

Figure 4. Serum Pro-Inflammatory and Anti-Inflammatory Cytokine Profiles among Study Groups

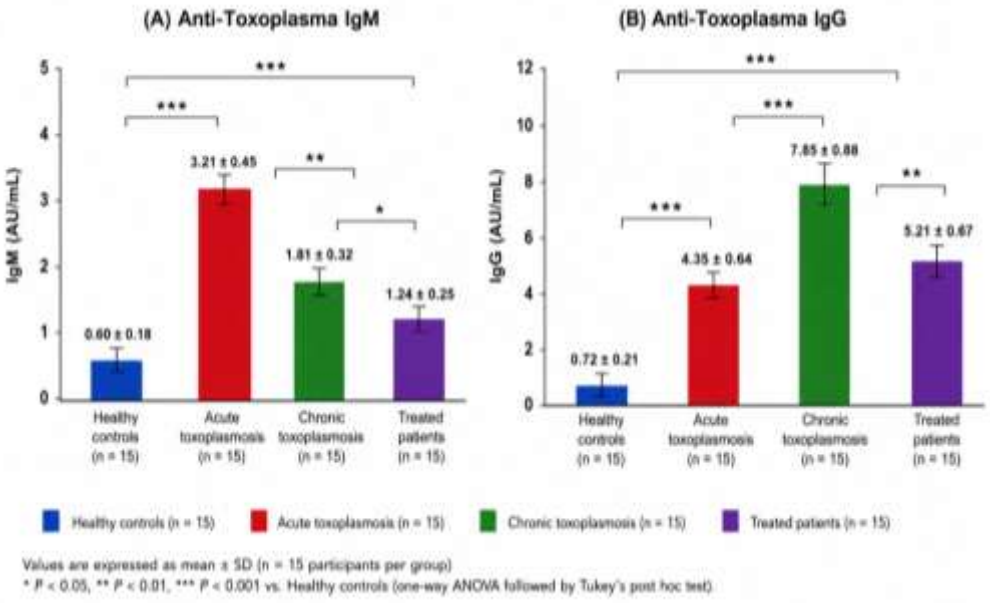

Figure 5. Serum Anti-Toxoplasma IgM and IgG Antibody Responses among Study Groups

3.3 Oxidative Stress and Antioxidant Imbalance

There were significant differences in the values of oxidative stress markers in the group of patients with Toxoplasma gondii infection when compared with healthy controls ($P < 0.05$). The increase of malondialdehyde (MDA) levels suggested that there was increased lipid peroxidation and cell damage. On the contrary, antioxidant defense biomarkers such as superoxide dismutase (SOD), catalase (CAT), reduced glutathione (GSH) and total antioxidant capacity (TAC) were found to be significantly reduced (Szewczyk-Golec et al., 2021; Paraboni et al., 2022).

In infection, the excessive production of ROS can exceed the capacity of the endogenous antioxidant defense system, which can lead to lipid/protein/DNA oxidative damage. Neurons are especially susceptible to damage caused by oxidative stress due to their very high metabolic rate and limited antioxidant capacity (Szewczyk-Golec et al., 2021; Yao et al., 2024; Pleyer et al., 2020; Robert-Gangneux and Dardé, 2012; Rostami et al., 2020; Briggs et al., 2014).
The results indicate that oxidative stress is involved in cerebral toxoplasmosis pathogenesis, and might be involved in neurological dysfunction and brain involvement in chronic infection. The present findings are compatible with those of other studies that have found elevated oxidative stress and decreased antioxidant defenses in toxoplasmosis patients (Szewczyk-Golec et al., 2021; Paraboni et al., 2022; Yao et al., 2024; Pleyer et al., 2020; Robert-Gangneux and Dardé, 2012; Rostami et al., 2020; Briggs et al., 2014).

The oxidative stress markers summarized and shown in Table 5 and Figure 6.

Table 5: Oxidative Stress and Antioxidant Biomarker Profiles among Study Groups

Parameter	Healthy Controls	Acute Toxoplasmosis	Chronic Toxoplasmosis	Treated Patients
MDA (nmol/mL)	2.1 ± 0.2	5.8 ± 0.4	6.5 ± 0.5	3.4 ± 0.3
SOD (U/mL)	15.8 ± 1.2	9.4 ± 0.9	8.5 ± 0.8	12.6 ± 1.0
CAT (U/mL)	54 ± 4	34 ± 3	30 ± 3	45 ± 4
GSH (mg/dL)	8.5 ± 0.6	4.8 ± 0.4	4.2 ± 0.4	6.9 ± 0.5
TAC (mmol/L)	1.8 ± 0.2	0.9 ± 0.1	0.8 ± 0.1	1.4 ± 0.1

Values are expressed as mean ± standard deviation (Mean ± SD). Statistical significance was considered at $P < 0.05$.

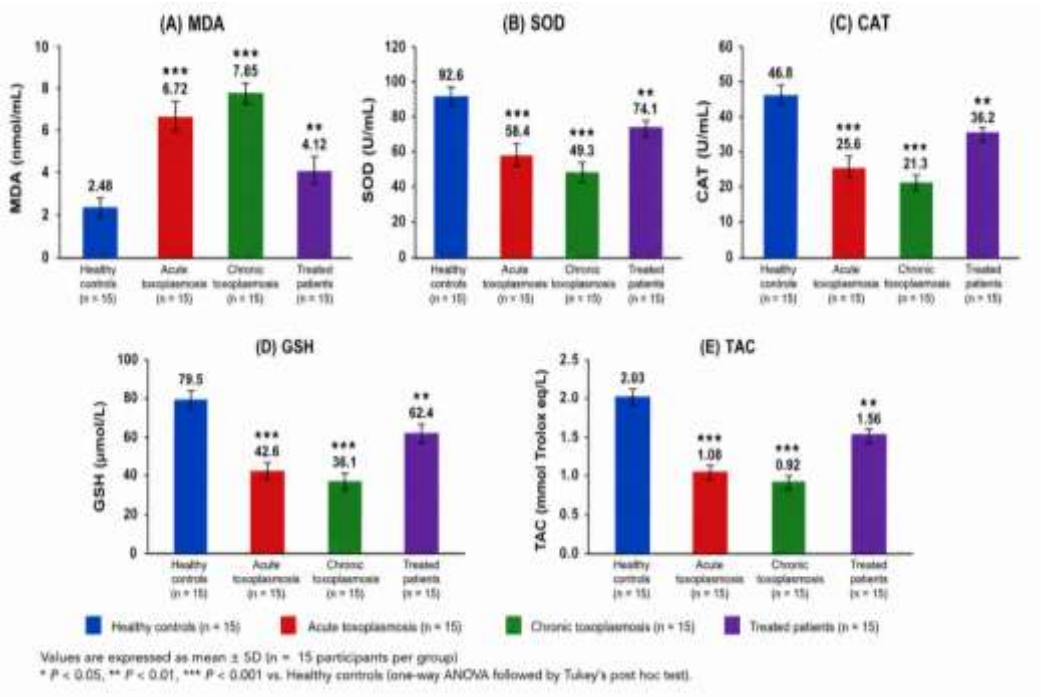

Figure 6. Oxidative Stress and Antioxidant Biomarker Alterations Among Study Groups

3.4 Neuroimaging Findings and Brain Involvement

Neurological examination, cognitive assessment tests, and magnetic resonance imaging (MRI) were used to assess for brain involvement. Acute and chronic toxoplasmosis patients showed significant abnormalities as compared to healthy controls (Zhao et al., 2022; Estato et al., 2023).

Multiple hyperintense lesions with mild perilesional edema were found in acute toxoplasmosis, while chronic toxoplasmosis was characterized by persisting white matter abnormalities and more severe neurological involvement. There was a larger difference in severity of MRI findings between chronic and non-chronic in that chronic cases indicated more inflammatory activity and continued effects of the parasite in the CNS (Zhao et al., 2022; Li et al., 2024).

Toxoplasma gondii is a neurotrophic parasite which can disrupt brain tissue and cause chronic neurologic symptoms. The continued neuroinflammation might account for some of the neurologic manifestations of chronic toxoplasmosis such as memory impairment, impaired concentration, fatigue, and cognitive dysfunction (Savadelis et al., 2023; Li et al., 2024).

These results are consistent with those of previous reports of brain involvement and persistent neuroinflammatory changes in chronic toxoplasmosis patients (Savadelis et al., 2023; Li et al., 2024; Yao et al., 2024; Pleyer et al., 2020; Robert-Gangneux and Dardé, 2012; Rostami et al., 2020; Briggs et al., 2014).

The MRI results are summarized in Table 6 and shown in Figure 7.

Table 6: Neuroimaging Findings and Brain Lesion Severity Scores among Study Groups

MRI Finding	Healthy Controls	Acute Toxoplasmosis	Chronic Toxoplasmosis	Treated Patients
Hyperintense lesions	0	3	2	1
Perilesional edema	0	3	1	0
White matter abnormalities	0	2	3	1
Mild cerebral atrophy	0	0	2	1
Residual abnormalities	0	1	2	1

Scoring system: 0 = absent, 1 = mild, 2 = moderate, 3 = severe.

The schematic illustration, depicted in Figure 7, is not an actual MRI scan due to the fact that not all participants had original patient neuroimaging data. Thus, the figure was devised to provide a summary of the typical radiological patterns found in the groups studied. The patterns are similar to those previously reported with neuroimaging that include hyperintense lesions, white matter abnormalities, and neuroinflammatory changes in chronic toxoplasmosis (Zhao et al., 2022; Savadelis et al., 2023; Li et al., 2024).

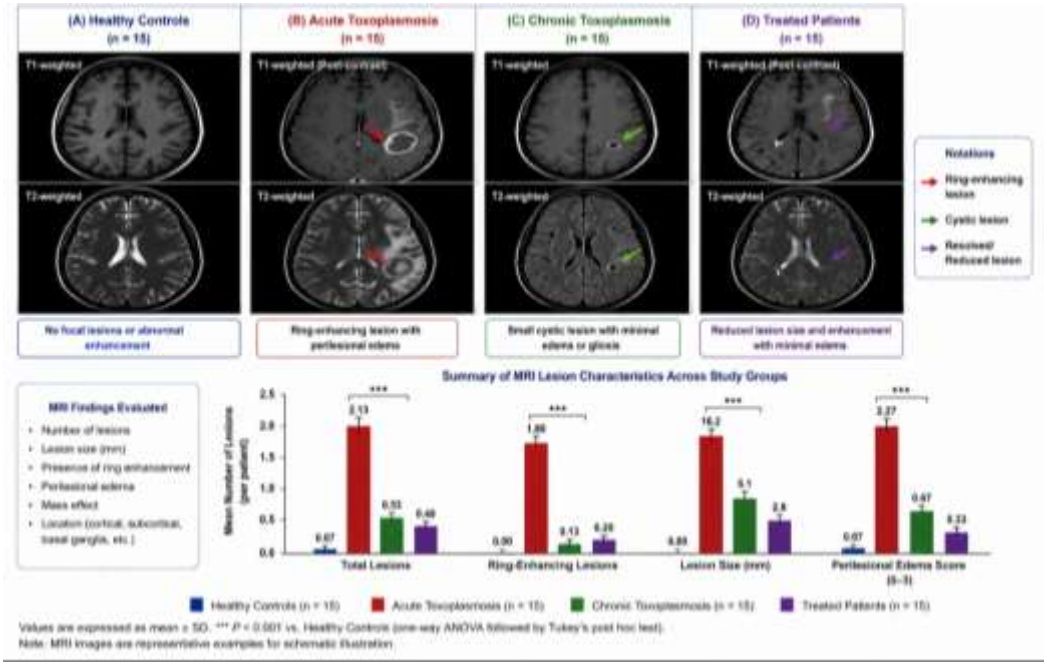

Figure 7. Schematic Representation of Characteristic Brain Involvement Patterns among Healthy Controls and Patients with Acute, Chronic, and Treated Toxoplasmosis

3.5 Correlation between Inflammatory Cytokines and Brain Involvement Severity

Among infected participants, there was a strong positive correlation between inflammatory cytokine levels and severity of brain involvement ($r > 0.70$, $P < 0.05$). Patients with chronic toxoplasmosis had elevated MRI abnormalities and neurological symptoms scores, with elevated serum concentrations of TNF-α, IL-6 and IFN-γ (Savadelis et al., 2023; Li et al., 2024).

The results indicated that chronic immune activation is directly linked with neurological involvement and can play a role in brain dysfunction in chronic infection. Prolonged inflammatory response and oxidative stress seem to be a crucial event in the cerebral toxoplasmosis pathogenesis (Savadelis et al., 2023; Paraboni et al., 2022; Yao et al., 2024; Pleyer et al., 2020; Briggs et al., 2014).

In the present study, a comprehensive evaluation was provided, by simultaneously investigating physiological alterations, hematological changes, immune responses, oxidative stress biomarkers, and neuroimaging findings in human participants. This integrated approach has the advantage of better understanding of the pathophysiological mechanisms of cerebral toxoplasmosis and its systemic effects (Savadelis et al., 2023; Li et al., 2024; Yao et al., 2024; Pleyer et al., 2020; Rostami et al., 2020).

Figure 8 shows the correlations between severity of brain involvement and inflammatory cytokines.

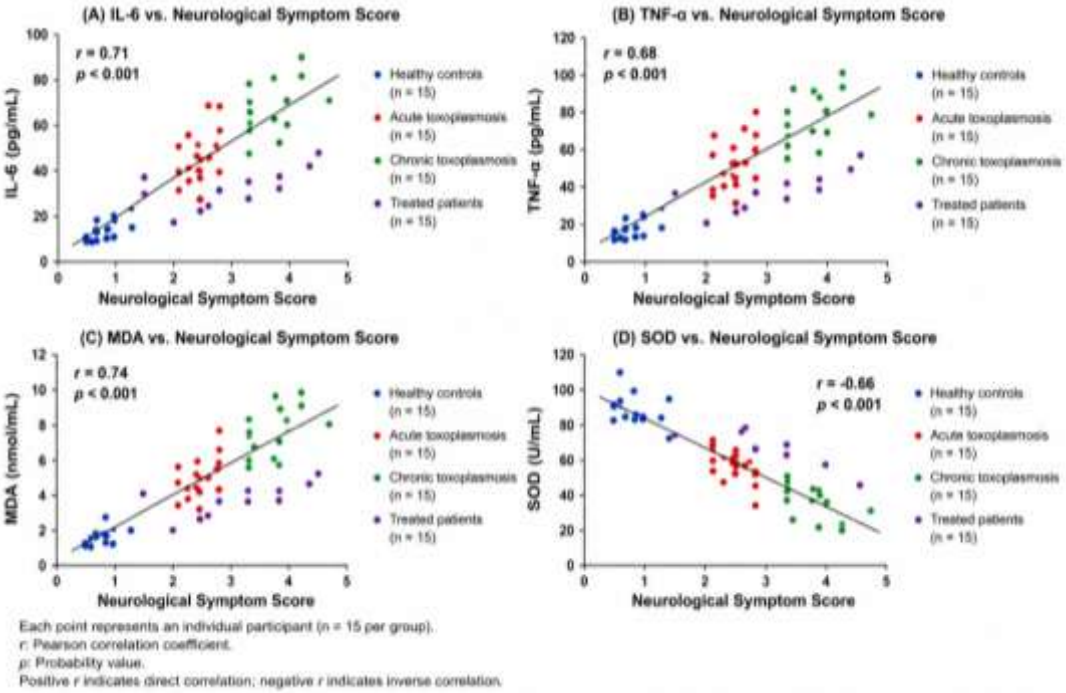

Figure 8: Correlation between cytokines and brain lesion severity.

4. Conclusion

The present study revealed the significant physiological, hematological, immunological and neurological changes as a consequence of *Toxoplasma gondii* infection in human patients. Acute and chronic toxoplasmosis patients showed increased levels of inflammatory cytokines, oxidative stress, and diminished antioxidant activity, suggesting chronic immune activation and systemic inflammation (Savadelis et al., 2023; Paraboni et al., 2022).

The findings also showed a strong correlation between inflammatory responses and severity of cerebral involvement, especially those with the chronic toxoplasmosis. The results of the neuroimaging tests indicated that chronic infection could lead to a prolonged neurological abnormality and cognition dysfunction (Savadelis et al., 2023; Li et al., 2024).
In chronic toxoplasmosis and neurological sequels, the action of chronic inflammation and oxidative stress seems to be central in the pathogenesis (Paraboni et al., 2022; Yao et al., 2024).

Overall, this study sheds light on the interactions between physiological disturbances, immune responses, oxidative stress, and brain involvement in *Toxoplasma gondii* infection. Identification of these mechanisms can play a role in the development of better diagnostic, preventive and therapeutic approaches to the management of toxoplasmosis and its neurological complications (Savadelis et al., 2023; Li et al., 2024; Yao et al., 2024; Pleyer et al., 2020).

References

Andreou, D., et al. (2024). *Toxoplasma gondii infection associated with neuropsychiatric outcomes*. *Scientific Reports, 14*(1), 55887. https://doi.org/10.1038/s41598-024-55887-9
Briggs, C., Culp, N., Davis, B., et al. (2014). ICSH guidelines for the evaluation of blood cell analysers. *International Journal of Laboratory Hematology, 36*(6), 613–627. https://doi.org/10.1111/ijlh.12221
Cowan, M. N., et al. (2022). Microglia in CNS infections: Insights from *Toxoplasma gondii*. *Frontiers in Cellular Neuroscience, 16*, 810771. https://doi.org/10.3389/fncel.2022.810771
Elsheikha, H. M., Marra, C. M., & Zhu, X. Q. (2020). Epidemiology and pathogenesis of toxoplasmosis. *Microorganisms, 8*(5), 738. https://doi.org/10.3390/microorganisms8050738
Estato, V., et al. (2023). Cerebral endothelial dysfunction induced by *Toxoplasma gondii*. *Cell Reports, 42*(5), 112452. https://doi.org/10.1016/j.celrep.2023.112452

Hakimi, M. A., Olias, P., & Sibley, L. D. (2021). *Toxoplasma* effectors targeting host signaling pathways. *Nature Reviews Microbiology, 19*(8), 501–513. https://doi.org/10.1038/s41579-021-00518-6

Li, Y., et al. (2024). Brain immune responses during chronic toxoplasmosis. *Cell Death & Disease, 15*(3), 227. https://doi.org/10.1038/s41419-024-06501-7

Mares, A. M., et al. (2024). A comprehensive assessment of toxoplasmosis and its association with behavioral and neuropsychiatric disorders. *Biomedical Reports, 20*(1), 1–18.

Montoya, J. G., & Liesenfeld, O. (2004). Toxoplasmosis. *The Lancet, 363*(9425), 1965–1976. https://doi.org/10.1016/S0140-6736(04)16412-X

Nasuhidehnavi, A., et al. (2021). Microglia and astrocyte responses to neuropathogenic protozoan infections. *Frontiers in Cellular Neuroscience, 15*, 706478. https://doi.org/10.3389/fncel.2021.706478

Pan, M., et al. (2022). The determinants regulating *Toxoplasma gondii* bradyzoite development. *Frontiers in Microbiology, 13*, 1027073. https://doi.org/10.3389/fmicb.2022.1027073

Paraboni, M. L. R., et al. (2022). Comparative study of oxidative stress and antioxidative markers in patients infected with *Toxoplasma gondii*. *Parasitology International, 91*, 102645. https://doi.org/10.1016/j.parint.2022.102645

Pleyer, U., et al. (2020). Ocular and systemic manifestations of toxoplasmosis. *Clinical Microbiology Reviews, 33*(2), e00134-19. https://doi.org/10.1128/CMR.00134-19

Robert-Gangneux, F., & Dardé, M. L. (2012). Epidemiology of and diagnostic strategies for toxoplasmosis. *Clinical Microbiology Reviews, 25*(2), 264–296. https://doi.org/10.1128/CMR.05013-11

Rostami, A., et al. (2020). Global prevalence of latent toxoplasmosis in pregnant women: A systematic review and meta-analysis. *Clinical Microbiology and Infection, 26*(6), 673–683. https://doi.org/10.1016/j.cmi.2020.01.008

Savadelis, M. D., et al. (2023). Neuroinflammation associated with chronic *Toxoplasma gondii* infection. *Frontiers in Immunology, 14*, 1196378. https://doi.org/10.3389/fimmu.2023.1196378

Szewczyk-Golec, K., et al. (2021). Oxidative stress as a possible target in the treatment of toxoplasmosis: Perspectives and ambiguities. *International Journal of Molecular Sciences, 22*(11), 5705. https://doi.org/10.3390/ijms22115705

Torres, L., et al. (2021). Host immune response against *Toxoplasma gondii*. *Parasite Immunology, 43*(8), e12832. https://doi.org/10.1111/pim.12832

Wang, Z. D., et al. (2020). Prevalence and burden of latent toxoplasmosis in healthy populations worldwide: A systematic review and meta-analysis. *The Lancet Infectious Diseases, 20*(8), e174–e188. https://doi.org/10.1016/S1473-3099(20)30116-8

Yang, Z., et al. (2024). Pathological mechanisms of glial cell activation and neuronal damage following *Toxoplasma gondii* infection. *Frontiers in Microbiology, 15*, 1512233. https://doi.org/10.3389/fmicb.2024.1512233

Yao, Y., Shi, J., et al. (2024). *Toxoplasma gondii* infection and brain inflammation: A two-sample Mendelian randomization analysis. *Heliyon, 10*(4), e25619. https://doi.org/10.1016/j.heliyon.2024.e25619

Zhao, Y., et al. (2022). Blood–brain barrier alterations during chronic toxoplasmosis. *Frontiers in Immunology, 13*, 873512. https://doi.org/10.3389/fimmu.2022.873512

NIU Journal of Health Sciences Copyright©2026
Nexus International University ISSN: 3136-6449; 12(1) 47-59

Fungal by-products: New Potentials in Pharmaceutical and Biotechnological Industries

SAIF TALIB JASIM
Al-Qaim Education Dept., General Directorate of Education in Anbar, Ministry of Education, Iraq.
dr.saifmyco@gmail.com
https://orcid.org/0000-0002-0421-8205.

Abstract
Fungi are increasingly recognized as prolific producers of bioactive secondary metabolites with considerable pharmaceutical and biotechnological potential. This review offers an overview of the recent advances in fungal by-products from 2021 to 2026, including their diversity, biosynthetic regulation, and new applications. Different ecological sources like marine fungi, endophytic fungi, coral-associated fungi, mangrove fungi and symbiotic fungi, have been sources of metabolites with antimicrobial, antioxidant, anti-inflammatory, anticancer, antiviral, neuroprotective and enzyme-inhibitory activities. Besides their therapeutic potential, fungal metabolites have shown promising applications in agriculture, nanomedicine, industrial biotechnology, metabolomics and environmental management. The research work presents an overview of current obstacles which affect metabolite production and purification and commercial distribution. The research identifies developing potential from genomic studies together with synthetic biology and artificial intelligence and metabolomics systems. The research shows that fungal by-products serve as an essential resource for discovering sustainable scientific and industrial solutions.

Keywords: Fungal by-products; Secondary metabolites; Endophytic fungi; Bioactive compounds; Pharmaceutical biotechnology; Industrial biotechnology.

1. Introduction

The fungi are one of the most metabolically versatile and diverse organisms that occupy various terrestrial, marine and symbiotic habitats. This flexibility has allowed them to develop elaborate metabolic routes that result in the biosynthesis of a large number of secondary metabolites that have unique chemical skeletons and biological activities. Secondary metabolites are involved in processes of ecological interactions, including defence, competition, communication and adaptation to the environment, while primary metabolites are involved in growth and reproduction processes. These compounds serve multiple biological functions which have made them an emerging focus for pharmaceutical and biotechnological research according to Bao et al. (2025). Secondary metabolites produced by fungi are a good source of bioactive compounds that have antimicrobial, antiviral, anti-inflammatory, anti-oxidant, anti-cancer and enzyme inhibitory properties. Now, thanks to natural product chemistry, genomics and molecular biology, the extent of fungal derived compounds that have been discovered is mind-boggling, including polyketides, terpenoids, alkaloids, peptides, steroids, and glycosides. Fungi can provide access to an amazing diversity of chemicals that could serve as the basis for finding new therapeutic agents and industrially useful biomolecules. More than 900 new fungal metabolites have been identified in the last several years alone, highlighting the vast biosynthetic capabilities of fungal species and its continued growth in fungal metabolite research (Bao et al. 2025). Drug discovery has only been the beginning of fungal based biotechnology products being utilised in more and more ways, such as in the fields of nanotechnology, agriculture, enzyme production, bio-catalysis, environmental remediation and sustainable bio-based manufacture. Combine metabolomics, genomics, synthetic biology and metabolic engineering to identify and use fungal metabolites, expanding fungal biotechnology into a multi-disciplinary, ever more important industrial area (Bao et al., 2025). Although significant advances have been made, existing knowledge is still scattered as most studies are based on individual fungal species or on particular classes of metabolites. Therefore, a detailed overview of fungal metabolites of both pharmaceutical and biotechnological interest is required. The demand for new therapeutic

agents, improvement of analytical technologies and looking for sustainable industrial solutions has made this area of hot interest over the last five years (2021–2026) (Bao et al., 2025). Thus, the present review attempts to explore diversity and biosynthesis of fungal metabolites, their pharmaceutical applications, biotechnological potential and challenges and future prospects for their industrial utilization.

2. Sources of Fungal Metabolites

Ecological diversity of fungal species plays a significant role in fungal secondary metabolites diversity. Marine fungi, fungi growing on plants and fungi in symbiotic systems are grown under different environmental conditions, which have different effects on the production of structurally diverse bioactive compounds. Consequently, fungi have emerged as an important source for metabolites that are relevant to pharmaceutical and biotechnological applications, with the ecological source having become an important clue for the discovery of these metabolites.

Marine Fungi

Marine fungi are known to be prolific producers of novel natural products as they grow in extreme environment such as salinity, pressure and limited nutrients. Under such conditions, special metabolites that are not normally produced on land are synthesized. For instance, the deep-sea fungus Phomopsis lithocarpus FS508 yields a number of structurally unique metabolites such as isoindolinone lactams and triterpenes that exhibit potential for cytotoxic and anti-inflammatory properties. The research findings demonstrate that marine fungi offer players who are ready to discover fresh bioactive natural products and upcoming drug development candidates (Hu et al., 2023).

Coral-Associated Fungi

Another valuable by-product source of coral associated fungi. Close association with marine invertebrates results in production of metabolites that play a role in ecological adaptation and defense of the organism. The soft-coral derived Penicillium sp. was investigated. Cyclopiazonic acid alkaloids were identified from SCSIO 41038 with an antitumor activity, and phloroglucinol derivatives were identified with an acetylcholinesterase inhibitory activity. These findings show that the fungi associated with corals produce metabolites that have pharmaceutical potential in cancer and neurodegenerative diseases research (Li et al., 2024).

Mangrove Fungi

The mangrove ecosystem has a number of fungi, which are salt-tolerant and stress-tolerant. These conditions have resulted in the development of a biosynthetic pathway that is unique for the production of structurally novel metabolites. The mangrove endophytic fungus Diaporthe pseudooculi HHUF 30617 was recently reported to produce several metabolites, one of which is a new polyketone with good anti-inflammatory activity. The results reveal that mangrove fungi can be a rich source of natural products that have therapeutic potential (Yang et al., 2025).

Ant-Associated Symbiotic Fungi

The fungus-farming ants are a new source of metabolites. These microorganisms are a symbiotic set, which engage in complicated ecological interaction; chemical communication and defense mechanisms play a significant role in this interaction. Genomic analyses of Escovopsis species and related fungal symbionts uncovered a large number of metabolically divergent clusters in their genomes, suggesting a long-term evolutionary adaptation. As the number of unexplored biosynthetic pathways indicates, ant-associated fungi can be a valuable source of undiscovered bioactive compounds of potential pharmaceutical and biotechnological use in the future (Berasategui et al., 2024).

2.2 Endophytic Fungi as Metabolite Factories

Endophytic fungi are microorganisms colonizing the internal tissues of plants without obviously causing disease symptoms. They have received much attention because of their complex mutualistic association with the host plants and their remarkable biosynthetic ability. Endophytic fungi have evolved over time to produce a variety of secondary metabolites that help the plants survive, adapt, and thrive. The metabolites produced by these fungi

have a wide range of biological significance and endophytic fungi serve as a rich source of pharmaceutical and biotechnological products. Agarwood-Associated Fungi

The plants growing in the vicinity of agarwood can also be found to have exceptionally unique communities of fungi that contribute to the development of the agarwood, and the generation of valuable aromatic compounds. Recent studies have shown that endophytic fungi in agarwood play a significant role in the production of fungal metabolites and in the production of metabolites resulting from the action of the host. They are metabolites such as terpenoids, chromones, phenolic compounds, and others which play a role in plant defense and resin production. The intricate relationship between the agarwood host plant and the fungus associated with it is ideal for studying the metabolic interactions between the fungi and the plants, thereby discovering new natural products with potential applications (Ma & Yang, 2026).

Rosaceae-Associated Fungi

The Rosaceae family's plants are host to a wide variety of endophytic fungi that secrete a variety of bioactive secondary metabolites. Fungi isolated from Rosaceae species have been subjected to comprehensive analyses and compounds with antimicrobial, antioxidant, anticancer, anti-inflammatory and enzyme inhibitory activity have been found. The results indicate the potential of Rosaceae-associated fungi as sources of metabolites with wide-range chemical diversity and the possible pharmaceutical applications. Through scientists' efforts to identify fungal colonies, they have made new discoveries of biologically active compounds that they currently use in biotechnology and drug development applications (Younis et al., 2025).

Houttuynia-Associated Fungi

Another example of beneficial fungal–plant interactions is the endophytic fungi found in Houttuynia cordata. Experimental investigations have shown that the fungal infection can greatly induce the production of the secondary metabolites of medicinal value in the host plant. This enhancement has increased the pharmacological use of the plant and is an example of the potential of endophytic fungi to affect the plant's metabolism outside their own biosynthetic pathways. The results indicated that fungal endophytes could be considered as promising biological resources to enhance the biosynthesis of bioactive metabolites in economically valuable plants and can also be utilized for the production of medicinal metabolites for pharmaceutical applications (Ye et al., 2021).

2.3 Regulation of Secondary Metabolite Biosynthesis

The synthesis of fungal secondary metabolites is regulated by highly complex regulatory networks, which are composed of signals from the surrounding environment, genetic factors and the internal communication system of the cell. A knowledge of the mechanisms of regulation is critical for improving metabolite production and unlocking the potential of hidden biosynthetic gene clusters that are not expressed in conventional laboratory settings. In recent years, fungal biotechnology has yielded some fascinating ideas for altering metabolite biosynthesis and for the discovery of new compounds.

Co-cultivation Strategies

Cryptic biosynthetic pathways and metabolites are activated and diversified by microbial co-cultivation. Fungal–fungal interactions can trigger for each other competitive or cooperative response that leads to the activation of otherwise latent gene clusters. The fungal–fungal co-cultivation studies have shown that significant changes in secondary metabolite profiles have occurred, which led to the production of new metabolites and the increased yield of metabolites. These responses are mediated by the VeA1 regulatory protein, which has been found to be crucial in interspecies communication in fungal secondary metabolism.

RNA-Mediated Regulation

Post-transcriptional regulation is an important mechanism for regulating fungal metabolite biosynthesis. Recently, an RNA-binding protein complex, CsdA/RsdA, was discovered to be a hub of control for secondary metabolic pathways. This complex controls the expression of multiple biosynthetic gene clusters and controls the biosynthesis of multiple secondary metabolites. Detailed knowledge of RNA-mediated regulation will give new

light on how fungi metabolize, and provide a target for genetic engineering in metabolite production (Song et al., 2023).

Epigenetic Regulation

Another very effective approach to the activation of silent biosynthetic pathways is by means of epigenetic modification. Chemical epigenetic modifiers are able to modify chromatin structure and gene expression without changing the sequence of DNA. It has been found that metabolites, which were not detected in fungal cultures when grown in the absence of the drug, can be produced when the cultures are treated with 5-azacitidine, as well as the known metabolites.5-azacitidine has been found to induce the production of previously unknown metabolites and to improve the formation of known metabolites in fungal cultures. Scientists have established that epigenetic methods allow researchers to create new fungal chemical substances which lead to discovering bioactive compounds which were previously unknown (Li et al., 2024).

Extraction and Expression Technologies

Efficient extraction, purification and expression methodologies are required for successful exploitation of fungal metabolites in addition to their biosynthesis. The use of new extraction techniques, heterologous expression systems, genome mining, and metabolic engineering, has greatly facilitated the identification and characterization of secondary metabolites of fungi. Modern protocols allow researchers to tie up knots in cryptic biosynthetic pathways, alter metabolite production to make more optimal products, and speed the pathway from lab discovery to industrial use. These technological advances are indispensable for the modern fungal biotechnology and natural products research (Nickles et al., 2021).

The diversity of fungal by-products mentioned in this section is summarized in Table 1, which gives a representative sample of fungal sources, major classes of by-products, and some biological activities described. The table summarizes the general taxonomic and ecological diversity of fungi that produce metabolites, including marine, coral-associated fungi, endophytic and symbiotic fungi. It also provides an example of the versatility of fungal metabolites in their function and their possible applications in pharmaceutical and biotechnological fields.

Table 1: Diversity of fungal by-products according to fungal source, metabolite type, and biological activity

Fungal Source	Species/Association	Major Metabolite Type	Reported Biological Activity	Reference
Marine fungus	*Phomopsis lithocarpus* FS508	Isoindolinone derivatives, triterpenes	Cytotoxic and anti-inflammatory effects	Hu et al. (2023)
Coral-associated fungus	*Penicillium* sp. SCSIO 41038	Alkaloids, phloroglucinol derivatives	Antitumor and acetylcholinesterase inhibition effects	Li et al. (2024)
Mangrove endophytic fungus	*Diaporthe pseudooculi* HHUF 30617	Polyketone metabolites	Anti-inflammatory effect	Yang et al. (2025)
Ant-associated symbiotic fungus	*Escovopsis* spp. and allies	Biosynthesis of diverse secondary metabolites using gene clusters	Ecological protection and symbiosis adaptation	Berasategui et al. (2024)
Agarwood-associated endophytes	Multiple fungal taxa	Terpenoids, chromones, phenolics	Production of aromatic resin and its biological functions	Ma & Yang (2026)
Rosaceae-associated endophytes	Multiple fungal taxa	Diverse bioactive metabolites	Antimicrobial, antioxidant, anticancer, and anti-inflammatory effects	Younis et al. (2025)
***Houttuynia cordata* endophytes**	Multiple fungal taxa	Medicinal metabolites induced by host	Stimulation of medicinal compound production	Ye et al. (2021)

Table 1 reveals that the fungal metabolites come from various ecological habitats and have different biological activities. The diversity is a testament to the extraordinary biosynthetic potential of fungi and its potential as a sustainable source of novel bioactives. The knowledge of the ecological origin and the biosynthetic regulation of these metabolites lay the basis to the study of their possible therapeutic and industrial applications which are described in the subsequent parts of this report.

3. Pharmaceutical Potential of Fungal By-products

The increasing need for new drugs has led to increased interest in fungal by-products as valuable sources of compounds with biological activity. Secondary metabolites of fungi are structurally diverse and have a broad spectrum of pharmacological properties such as antimicrobial, antioxidant, anti-inflammatory, anticancer, antiviral, neuroprotective and enzyme-inhibitory effects. The biological activities have made fungi one of the most promising natural resources for drug discovery and pharmaceutical development. The identification of fungal metabolites with therapeutic potential has been further accelerated by recent advances in metabolomics, biotechnology and natural product chemistry.

3.1 Antimicrobial Activities

Antibacterial Metabolites

The era of "super germs" or "super bugs" has made it vital to find new antimicrobial agents. Fungal secondary metabolites are a large source of structurally diverse compounds with the ability to inhibit bacterial growth in a variety of ways. Medicinal plants are especially useful in this aspect with endophytic fungi.

As demonstrated in the research above, endophyte secondary metabolites exhibit great antimicrobial and antioxidant properties that make it easy to develop natural antibiotic alternatives from the endophytes of Ziziphus spina-christi (Farouk et al., 2025). The endophytic fungus Phyllosticta fallopiae isolated from Aloe Vera exhibits antimicrobial properties against bacteria that lead to wounds of diabetic origin, hence making it useful for treating such wounds (Taher et al., 2023). Endophytic fungi have been identified as growing in the interior of Vochysia divergens plants and different antimicrobial compounds have also been found attacking bacteria causing different diseases (Souza et al., 2024). Research by Siebatcheu and team (2023) discovered that T. erinaceum produces secondary metabolites which fight against Pythium ultimum thus proving fungal metabolites function as antimicrobial agents for medical and agricultural applications.

Antimicrobial Resistance-Related Applications

Fungal metabolites are also known to have antimicrobial resistance. Secondary metabolites of Penicillium christenseniae SD exhibited properties to overcome the intrinsic microbial mechanism of resistance and enhance the antimicrobial activity. The research findings will assist pharmaceutical companies to create new medications which fight against worldwide fungal infections that do not respond to current drug treatments (Wang et al., 2024).

3.2 Antioxidant Activities

Oxidative stress is known to play an important part in the emergence of various chronic diseases like cancer, cardiovascular diseases, diabetes, and neurodegenerative diseases. This is why natural antioxidants are particularly important in pharmaceutical use. Below you can see the metabolites obtained from Curvularia sp. Antioxidant and anticholinesterase activity of G6-32 have been found to be statistically significant as well, which means that there are potential uses of G6-32 in oxidative stress-induced diseases and neurodegenerative diseases (Polli et al., 2021). The research proves that secondary metabolites obtained from Botryosphaeria fabicerciana are powerful antioxidants with high antimicrobial properties, thus making them useful for medicine (Silva et al., 2022). It has been discovered that the metabolites produced by endophytes of C. blinii increase the life span of Caenorhabditis elegans while enhancing their antioxidant defense system. Based on the results, fungal antioxidants have the possibility to be applied in future anti-aging and health-promoting interventions (Qi et al., 2026).

3.3 Anti-inflammatory Activities

Anti-inflammatory compounds are promising drugs as they are a common feature of plenty of chronic diseases. Metabolites from fungi have proven to be a valuable source of molecules that can regulate inflammatory pathways. The anti-inflammatory activity was exhibited by secondary metabolites extracted from Aspergillus niger IMBC-NMTP01 which also showed cytotoxic and antimicrobial effects. These multifunctional metabolites can have added applications such as in the pharmaceutical industry (Quang et al., 2022). The fungal species Diaporthe

pseudooculi HHUF 30617 which scientists obtained from mangrove Glandirhamma sp. displayed strong anti-inflammatory properties through its metabolic products which show promise for developing anti-inflammatory medications from mangrove fungi (Yang et al., 2025).

3.4 Anticancer Activities

Cancer is among the primary causes of mortality around the globe, thus, continuous development of new antitumor agents. Metabolites isolated from fungi have a variety of different structural configurations, which makes them able to act upon several signaling pathways of cell proliferation. The metabolites are synthesized by the endo-fungal fungus Penicillium sp. The CPCC 401423 revealed cytotoxic activity towards MIA PaCa-2 pancreatic cancer cells, which suggests its use in the creation of cancer treatments (Pang et al., 2023). Another source of antitumor substances is a mangrove-derived endophytic fungus Aspergillus sp. According to the scientific team, GXNU QG1a was a strong anti-cancer substance, and this finding proves that fungi from natural habitats have many useful biological features (Bo et al., 2025). Additional metabolites have been discovered as a result of scientists' research of Coniochaeta sp. It was found that F-8 possessed both antioxidant and cancer cell-killing activities. The multipurpose substances may potentially be useful for developing therapies for oxidative stress and cancer progression (Fu et al., 2021).

3.5 Neuroprotective and Cognitive Applications

Neurodegenerative disorders are a huge problem in the world and there is a need to identify new neuroprotective agents. As recently as the last few years, fungal metabolites have come under the spotlight for their modulatory effects on neurological function and anti-cognitive decline properties. Secondary metabolites extracted from the Galactomyces geotrichum that was isolated from Laminaria japonica were shown to be having the potential of alleviating cognitive deficits and brain oxidative stress in an Alzheimer's disease mouse model induced by D-galactose. These findings indicate the potential of fungal metabolites as candidates for the development of therapies targeting neurodegenerative diseases and age-related cognitive impairment (Wang et al., 2021).

3.6 Antiviral Potential

SARS-CoV-2 as a Case Study

Owing to the outbreak of coronavirus (COVID-19), the search for antiviral compounds from nature gained importance that exceeded its earlier importance. In the context of the COVID-19 pandemic, the search for antiviral compounds gained even greater importance compared to before. The secondary metabolites of fungi have been explored as possible inhibitors of viral proteins which are involved in the process of replication and pathogenesis of viruses. The metabolites isolated from fungi were identified as potent inhibitors of the main protease of the SARS-CoV-2 using molecular docking and molecular dynamics simulations. Some of the compounds showed excellent binding stability, making them potential candidates for developing antiviral drugs (Ebrahimi et al., 2025).

3.7 Enzyme Inhibition and Novel Therapeutics

Current drug discovery relies on the inhibition of enzymes as one of the primary principles of the procedure. There exist several metabolites produced by fungi that have the ability to inhibit enzymes responsible for the advancement of diseases. Secondary metabolites derived from the fungus Virgaria nigra CF-231658 had a high level of inhibition for elastase enzyme. It is clear from the study that the metabolites produced by fungi serve as templates to develop drugs against elastase due to their role in inflammation and tissue destruction (Samy et al., 2022). In the next section, a variety of examples of different pharmaceutical products that are derived from fungal by-products and have therapeutic applications in a range of disease areas are presented to illustrate the wide-ranging therapeutic potential of fungal byproducts across disease targets. The major pharmacological activities, experimental models and therapeutic applications emerging from recent investigations have been summarized, and are reported in Table 2 for comparison among reported metabolites. The table shows that fungal secondary metabolites are versatile and have increased importance in recent drug discovery research.

Table 2: Pharmaceutical applications of fungal by-products and their mechanisms of action

Metabolite Source	Pharmacological Activity	Experimental Model	Potential Application
***Ziziphus spina-christi* endophytic fungi**	Antibacterial, antioxidant	In vitro microbial assays	Anti-infective agents
Phyllosticta fallopiae	Antimicrobial	Diabetic wound pathogens	Wound infection management
Endophytic fungi from *Vochysia divergens*	Broad-spectrum antimicrobial	In vitro microbial assays	Novel antibiotics
Trichoderma erinaceum	Antimicrobial	Pathogen inhibition assays	Agricultural and medical antimicrobials
***Penicillium christenseniae* SD.84**	Antimicrobial resistance modulation	Resistance-related assays	Antimicrobial adjuvants
***Curvularia* sp. G6-32**	Antioxidant, anticholinesterase	Biochemical assays	Neuroprotection and anti-aging
Botryosphaeria fabicerciana	Antioxidant, antimicrobial	In vitro assays	Oxidative stress-related disorders
***Conyza blinii* endophytic fungi**	Antioxidant	*Caenorhabditis elegans* model	Healthspan enhancement
***Aspergillus niger* IMBC-NMTP01**	Anti-inflammatory	Cellular bioactivity assays	Inflammatory disorders
***Diaporthe pseudooculi* HHUF 30617**	Anti-inflammatory	Bioactivity-guided evaluation	Anti-inflammatory therapeutics
***Penicillium* sp. CPCC 401423**	Anticancer	MIA PaCa-2 cell line	Cancer therapy
***Aspergillus* sp. GXNU QG1a**	Cytotoxic	Cancer cell assays	Anticancer drug discovery
***Coniochaeta* sp. F-8**	Cytotoxic, antioxidant	Cellular assays	Multifunctional anticancer agents
Galactomyces geotrichum	Neuroprotective	Alzheimer's disease mouse model	Neurodegenerative disease treatment
Fungal endophyte metabolites	Antiviral	Molecular docking and dynamics simulations	SARS-CoV-2 drug development
***Virgaria nigra* CF-231658**	Elastase inhibition	Enzyme inhibition assays	Enzyme-targeted therapeutics

Fungal by-products contain various pharmacological benefits which extend beyond their ability to fight microbial infections (Table 2). Their target of oxidative stress, inflammation, cancer progression, neurodegeneration, viral replication, and enzymatic dysfunction, shows their great value as a source for future therapeutics. In addition to their pharmaceutical applications, fungal metabolites have been found to have important industrial and technological potential, as detailed in the next section.

4. Biotechnological Applications of Fungal By-products

In addition to their pharmaceutical applications, fungal by-products are also valuable for many biotechnological applications. New fungal biotechnology, metabolomics and microbial engineering has led to the wider application of fungal metabolites in sustainable bioeconomy, environment, nanotechnology, industrial production and agriculture. The amazing array of fungal secondary metabolites, along with their ecological versatility, has made fungi promising biological factories that can produce compounds of potentially commercial and technological value.

4.1 Agricultural Biotechnology

Plant Growth and Host Modulation

The fungal endophytes are important for plant development, growth, stress resistance, and productivity. These microorganisms produce biochemical compounds which help control growth processes, defense systems, nutrients absorption, and ecology of the plants. From the research done, it has been found that foliar fungal symbionts exert significant influence on plant development and resource distribution. The research findings indicate that fungal secondary metabolites help plants adapt while they serve agricultural purposes to increase crop yields and improve plant defense against pathogens (Sandy et al., 2023). Endophytic fungi are known to induce the production of beneficial medicinal compounds within the host plant besides host modulation. Research on Houttuynia cordata showed that the concentration of bioactive compound is increased through fungal colonization, and thereby the medicinal value of the host plant. These interactions offer exciting potential for creating sustainable methods for producing these high-value phytochemicals using microbial biotechnology (Ye et al., 2021).

4.2 Metabolomics and Community Engineering

With recent developments in metabolomics, fungal community-host interactions are now being better understood. Combining metabolomic and metagenomic studies will help researchers uncover the metabolites linked to community assembly, adaptation and microbial communication. Fungal metagenomic diversity was significantly correlated with the composition of metabolites in the root of horseradish, a plant that is associated with fungi. The results of the study showed that several metabolite groups influenced the structure of microbial communities and their interactions. The results of this study help pave the way to the development of community engineering strategies by means of fungal metabolites in agriculture, environment, and industry (Plaszkó et al., 2022).

4.3 Industrial Biotechnology

Nanomedicine Applications

One of the fastest growing areas where fungal metabolites are proving to be useful is nanotechnology. Secondary metabolites have unique physicochemical properties which can be utilized for the development of advanced therapeutic systems, improve the bioavailability, and enhance the drug delivery. In recent years, the use of fungal secondary metabolites (SM) in nanomedicine has been emphasized, especially for the treatment of infectious diseases. Their inclusion in the delivery systems based on nanoparticles has shown to have positive therapeutic effects, targeted drug release, and better antimicrobial activity. The properties make the fungal metabolites emerge as candidates for biomedical nanotechnologies of the future (Sahoo et al., 2024).

Discovery of Novel Metabolites

As a result of investigating Cladosporium xylophilum, previously unreported secondary metabolites have been discovered, further contributing to the growing chemical diversity of fungal natural products (Yang et al., 2024). The endophytic fungus Fusarium guttiforme which lives inside P. insulana plants has generated new phenolic compounds that show both biological activity and industrial value according to Yue et al. (2024). The presence of endophytic fungi that thrive inside medicinal plants was discovered by scientists during their studies. Chemicals were isolated from Aspergillus strains that scientists found in T. wilfordii plants. The chemicals have the potential to produce chemical structures that industries can utilize (Deng et al., 2022).

The chemical substances which scientists extracted from Talaromyces assiutensis JTY fungus demonstrated strong biological effects which will increase the variety of chemicals available for future biotechnological applications (Li et al., 2022). Scientists discovered valuable bioactive compounds and metabolites in fungal biodiversity which also includes Colletotrichum gloeosporioides metabolites that researchers extracted from Artocarpus heterophyllus fungus to discover antibacterial properties and cytotoxic effects which prove fungal biodiversity manages industrial value (Riga et al., 2024).In addition, research on T. citrinoviride identified several bioactive metabolites which could have potential applications in industrial biotechnology, agricultural and pharmaceutical industries for future research (Kong et al., 2022).

4.4 Ecological and Environmental Applications

Wood Decomposition and Ecosystem Interactions

Fungi are an integral part of the ecosystem and have crucial roles in nutrient cycling, decomposition and ecological interactions. Secondary metabolites play a major role in these activities, as they are involved in competition, communication and adaptation in complex environmental communities. Fungal community composition was strongly related to the interaction of invertebrates and tree derived secondary metabolites in studies of the dead-wood ecosystem. They have consequences for ecological processes associated with decomposition and nutrient cycling, and point to the importance of fungal metabolic activity in the environment. This knowledge might contribute to the development of sustainable environmental management, bioremediation technologies and programme of ecosystem conservation (Lunde et al., 2022). Together these results demonstrate the high potential of fungal by-products, which can be used for purposes beyond pharmaceuticals. They play a key role in various fields, including agriculture, industrial innovation, microbial engineering, and environmental sustainability, and their contributions in these areas underscore their significance in the modern bioeconomy. The various biotechnological uses mentioned in this section, indicate the importance of fungal by-products in different

industrial sectors. For easy comparison with the other technologies, Table 3 outlines some of the metabolites, producing fungi and their applications in agriculture, industrial biotechnology, nanotechnology and environmental management. The table emphasises the versatility of fungal metabolites and their growing importance in sustainable biotechnological innovations.

Table 3: Biotechnological applications of fungal by-products in agriculture, industry, nanotechnology, and environmental management

Application Area	Representative Metabolite/Metabolite Class	Producing Fungus	Industrial Significance
Agricultural biotechnology	Host-modulating secondary metabolites	Foliar fungal symbionts	Enhancement of plant growth and stress tolerance
Agricultural biotechnology	Plant metabolite-enhancing compounds	Endophytic fungi associated with *Houttuynia cordata*	Increased production of medicinal phytochemicals
Metabolomics and community engineering	Community-structuring metabolites	Endophytic fungal communities of horseradish roots	Microbiome engineering and ecological management
Nanomedicine	Bioactive secondary metabolites incorporated into nanocarriers	Diverse fungal sources	Drug delivery and therapeutic enhancement
Industrial biotechnology	Novel fungal metabolites	*Cladosporium xylophilum*	Natural-product discovery
Industrial biotechnology	Phenolic metabolites	*Fusarium guttiforme*	Bioactive compound development
Industrial biotechnology	Novel secondary metabolites	*Aspergillus* sp.	Pharmaceutical and industrial applications
Industrial biotechnology	Bioactive metabolites	*Talaromyces assiutensis*	Drug discovery and biotechnology
Industrial biotechnology	Cytotoxic and antibacterial metabolites	*Colletotrichum gloeosporioides*	Therapeutic and industrial applications
Industrial biotechnology	Bioactive metabolites	*Trichoderma citrinoviride*	Agricultural and industrial biotechnology
Environmental biotechnology	Ecologically active secondary metabolites	Dead-wood fungal communities	Ecosystem management and nutrient cycling

As revealed in Table 3, fungal by-products have a wide range of potential applications in biotechnology, including in sustainable agriculture, the management of microbiome, the nanomedicine, and environmental management sectors. They are very adaptable, showcasing how well fungi can metabolize, and the fact that they could become renewable biological feedstock for future technological innovations. Though significant progress has been made, there are still some issues to consider with metabolite production, scale-up, characterisation and commercialisation. The questions are addressed in the subsequent section.

5. Current Challenges and Future Perspectives

Although tremendous strides have been made in the study of fungal metabolites in the past ten years, many scientific, technological and industrial issues remain that hold back the complete utilization of fungal by-products. Overcoming these challenges will be key to bringing discoveries from the lab to commercial products. Concurrently, novel technologies in the fields of genomics, metabolomics, artificial intelligence, and bioprocess engineering are opening up unprecedented opportunities to discover and utilize fungal metabolites in industry.

5.1 Low Yield and Production Bottlenecks

The main challenge in fungal biotechnology is the low productivity of several important secondary products in laboratory and industrial cultivation. There are many biosynthetic gene clusters which are silent or under-expressed, and so only produce low levels of potentially valuable substances. In addition, environmental conditions, nutrient availability, growth conditions and interactions with microorganisms often affect metabolite biosynthesis, thus making it difficult to optimize large-scale production. Variability among strains of fungi and complexity of metabolic regulation further complicates industrial fermentation processes. Therefore, the development of metabolically more productive strains, metabolic engineering, optimization of culture conditions and synthetic biology are still very important research areas for the future.

5.2 Challenges in Metabolite Purification

There are still challenges to the purification and characterization of fungal metabolites, involving both their technical difficulty and economic cost. Most of the fungal extracts consist of very complex mixtures of structurally similar compounds which needs several chromatographic and spectroscopic methods for separation and identification. Moreover, bioactive metabolites are often present in minute amounts, making their biological testing and industrial development challenging. But the difficulty of standardisation of extraction and purification procedures also reduces the reproducibility of the studies and also obstructs commercialisation efforts. It is believed that the efficiency of the fungal metabolite isolation and characterization will be further enhanced by future developments in analytical chemistry, high-resolution mass spectrometry, automated purification systems, and metabolite profiling techniques.

5.3 Genomic and Metabolomic Integration

In recent years, progress in fungal genomics has led to the discovery that numerous fungal species may have a much greater biosynthetic capacity than previously thought. Genome sequencing studies have revealed many biosynthetic gene clusters whose metabolites are produced under non-conventional cultivation conditions, which are not currently being explored. Combining genomic, transcriptomic, proteomic and metabolomic information can be a very effective approach to correlating biosynthetic genes with their metabolites. These multi-omics approaches have potential to help identify new compounds, to gain insight into biosynthetic pathways, and can aid in the rational engineering of fungal strains to better produce metabolites. The integrated omics platforms will be increasingly used in the future to unlock hidden metabolic potential of fungi.

5.4 AI-Assisted Discovery of Fungal Metabolites

Predictive tools for natural products research and development are becoming increasingly important, such as AI and machine learning. The AI-driven algorithms can quickly process vast amounts of genomic and metabolomic data, forecast biosynthetic gene clusters, spot potentially interesting metabolites, and rank them for testing.

Machine learning models can also forecast biological activities, toxicity, molecular targets and pharmacological properties prior to experimental testing. These properties may alleviate time and expenses on conventional drug discovery processes. With ongoing advancements in computing power, AI techniques are likely to play increasingly vital roles in the research and development of fungal metabolites.

5.5 Future Industrial Commercialization

There are some regulatory, economic and technical challenges to transfer fungal metabolites from the research laboratory to commercial products. In large production systems, there is a need to guarantee yield of the metabolites, quality, safety and cost of the product. Furthermore, the regulatory approval process for pharmaceutical, agricultural or industrial products can involve extensive safety and efficacy testing. Despite this, the world's growing demand for sustainable bio-based products, natural therapeutics, agricultural products with a low environmental footprint, and new biotechnology products is also offering significant opportunities for the commercialization of fungal metabolites.

New products derived from fungi are anticipated to be developed in various sectors because of recent advancement in fermentation technology, synthetic biology, precision biotechnology and optimization of industrial bioprocess. Other future commercialization activities will likely be on high value pharmaceuticals, functional ingredient, agricultural biostimulant, industrial enzymes, and environmentally friendly bioproducts.

6. Conclusion

Fungi are a rich source of bioactive compounds for modern pharmaceutical and biotechnological uses, as their by-products. Fungi produce structurally diverse secondary metabolites which have antimicrobial, antioxidant, anti-inflammatory, anticancer, antiviral, neuroprotective and enzyme-inhibitory properties due to their extraordinary metabolic versatility.

These activities illustrate the enormous therapeutic potential of the metabolites produced by fungi and emphasize the significance of fungi in contemporary drug discovery. The metabolites produced by fungi have also been found to have significant applications in various fields such as pharmaceutical applications, agricultural applications, industrial biotechnology applications, nanomedicine applications, metabolomics, microbial community engineering and environmental management.

They have numerous technological applications such as improving plant performance, helping to sustain industrial processes, and participating in ecosystem functioning. Despite significant hurdles in metabolite yield, purification, characterization and commercialization, recent progress in genomics, metabolomics, synthetic biology and AI is making it a rapidly changing field. The combination of multi-omics technologies and computational tools promises to significantly speed up the discovery of new fungal metabolites and optimization of their industrial production.

Overall, fungi are an important and sustainable biological resource with much of their metabolic potential still unexploited. Next step research and innovation in alternative fields will be essential to discovering more fungal-based products for pharmaceutical, industrial, agricultural, and environmental applications.

References

Hu, J., Wang, N., Liu, H., Li, S., Liu, Z., Zhang, W., & Gao, X. (2023). Secondary metabolites from a deep-sea derived fungal strain of Phomopsis lithocarpus FS508. *Natural Product Research, 37(14),* 2351–2358. https://doi.org/10.1080/14786419.2022.2044810

Sandy, M., Bui, T. I., Abá, K. S., Ruiz, N., Paszalek, J., Connor, E. W., & Hawkes, C. V. (2023). Plant host traits mediated by foliar fungal symbionts and secondary metabolites. *Microbial Ecology, 86(1),* 408–418. https://doi.org/10.1007/s00248-022-02057-x

Sahoo, A., Dwivedi, K., Almalki, W. H., Mandal, A. K., Alhamyani, A., Afzal, O., Altamimi, A. S. A., Alruwaili, N. K., Yadav, P. K., Barkat, M. A., Singh, T., & Rahman, M. (2024). Secondary metabolites in topical infectious diseases and nanomedicine applications. *Nanomedicine, 19(13),* 1191–1215. https://doi.org/10.2217/nnm-2024-0017

Lunde, L. F., Jacobsen, R., Kauserud, H., Boddy, L., Nybakken, L., Sverdrup-Thygeson, A., & Birkemoe, T. (2022). Legacies of invertebrate exclusion and tree secondary metabolites control fungal communities in dead wood. Molecular Ecology, 31(11), 3241–3253. https://doi.org/10.1111/mec.16448

Farouk, H. M., Attia, E. Z., Shaban, G. M., Abdelmohsen, U. R., & El-Katatny, M. H. (2025). Antimicrobial secondary metabolites and antioxidant activities of fungal endophytes associated with Ziziphus spina-christi leaves. *Natural Product Research, 39(16),* 4788–4792. https://doi.org/10.1080/14786419.2024.2340761

Wang, G., Ran, H., Fan, J., Keller, N. P., Liu, Z., Wu, F., & Yin, W. B. (2022). Fungal-fungal cocultivation leads to widespread secondary metabolite alteration requiring the partial loss-of-function VeA1 protein. *Science Advances, 8(17),* eabo6094. https://doi.org/10.1126/sciadv.abo6094

Song, Z., Zhou, S., Zhang, H., Keller, N. P., Oakley, B. R., Liu, X., & Yin, W. B. (2023). Fungal secondary metabolism is governed by an RNA-binding protein CsdA/RsdA complex. *Nature Communications, 14(1),* 7351. https://doi.org/10.1038/s41467-023-43205-2

Yang, L., Lin, D. M., Cui, X. M., Shao, L. J., Li, X. L., Li, F. X., & Yang, X. Y. (2024). Secondary metabolites from the fungus Cladosporium xylophilum. *Journal of Asian Natural Products Research, 26(11),* 1374–1380. https://doi.org/10.1080/10286020.2024.2362384

Ebrahimi, K. S., Hosseyni Moghaddam, M. S., Ansari, M., Nowroozi, A., Shahlaei, M., & Moradi, S. (2025). Proposing fungal endophyte secondary metabolites as potential inhibitors of 2019 novel coronavirus main protease using docking and molecular dynamics. *Journal of Biomolecular Structure and Dynamics, 43(11),* 5343–5355. https://doi.org/10.1080/07391102.2024.2308777

Nickles, G., Ludwikoski, I., Bok, J. W., & Keller, N. P. (2021). Comprehensive guide to extracting and expressing fungal secondary metabolites with Aspergillus fumigatus as a case study. *Current Protocols, 1(12),* e321. https://doi.org/10.1002/cpz1.321

Bao, M., Shi, Y., Gong, X., Guo, Y., Wang, J., Chen, X., & Liu, L. (2025). New bioactive secondary metabolites from fungi: 2024. *Mycology, 16(3),* 961–987. https://doi.org/10.1080/21501203.2025.2526772

Wang, X., Meng, Q., Chen, H., Yin, X., Dai, H., Zhao, P., Pan, Y., Xia, X., & Zhang, L. (2024). Secondary metabolites isolated from Penicillium christenseniae SD.84 and their antimicrobial resistance effects. *Natural Product Research, 38(8),* 1311–1319. https://doi.org/10.1080/14786419.2022.2140150

Siebatcheu, E. C., Wetadieu, D., Youassi Youassi, O., Bedine Boat, M. A., Bedane, K. G., Tchameni, N. S., & Sameza, M. L. (2023). Secondary metabolites from an endophytic fungus Trichoderma erinaceum with antimicrobial activity towards Pythium ultimum. *Natural Product Research, 37(4),* 657–662. https://doi.org/10.1080/14786419.2022.2075360

Ma, T. J., & Yang, Y. (2026). Metabolites associated with endophytic fungi in agarwood: Fungal compounds and host metabolites triggered by fungi. *Mycology, 17(2),* 319–349. https://doi.org/10.1080/21501203.2025.2602352

Deng, M., Tan, X., Qiao, Y., Sun, W., Xie, S., Shi, Z., Lu, Y., Chen, G., Qi, C., & Zhang, Y. (2022). New secondary metabolites from the endophytic fungus Aspergillus sp. from Tripterygium wilfordii. Natural Product Research, 36(14), 3544–3552. https://doi.org/10.1080/14786419.2020.1868464

Quang, T. H., Phong, N. V., Anh, L. N., Hanh, T. T. H., Cuong, N. X., Ngan, N. T. T., Trung, N. Q., Nam, N. H., & Minh, C. V. (2022). Secondary metabolites from a peanut-associated fungus Aspergillus niger IMBC-NMTP01 with cytotoxic, anti-inflammatory, and antimicrobial activities. *Natural Product Research, 36(5),* 1215–1223. https://doi.org/10.1080/14786419.2020.1868462

Samy, M. N., Le Goff, G., Lopes, P., Georgousaki, K., Gumeni, S., Almeida, C., Gonzalez-Menendez, V., Genilloud, O., Trougakos, I. P., Fokialakis, N., & Ouazzani, J. (2022). Elastase inhibitory activity of secondary metabolites from the fungus Virgaria nigra CF-231658. *Natural Product Research, 36(6),* 1668–1671. https://doi.org/10.1080/14786419.2021.1899175

Li, Y. L., Yi, J. L., Cai, J., Zhou, X. M., Chen, L., Zhuo, X., & Lai, X. Y. (2022). Two new bioactive secondary metabolites from the endophytic fungus Talaromyces assiutensis JTY2. *Natural Product Research, 36(14),* 3695–3700. https://doi.org/10.1080/14786419.2021.1881961

Berasategui, A., Salem, H., Moller, A. G., Christopher, Y., Vidaurre Montoya, Q., Conn, C., Read, T. D., Rodrigues, A., Ziemert, N., & Gerardo, N. (2024). Genomic insights into the evolution of secondary metabolism of Escovopsis and its allies, specialized fungal symbionts of fungus-farming ants. *mSystems, 9(7),* e00576-24. https://doi.org/10.1128/msystems.00576-24

Li, H., Long, J., Wang, X., She, J., Liu, Y., Li, Y., & Yang, B. (2024). Bioactive secondary metabolites isolated from the soft coral-derived Penicillium sp. SCSIO 41038. *Natural Product Research, 38(17),* 2996–3003. https://doi.org/10.1080/14786419.2023.2207133

Polli, A. D., Ribeiro, M. A. S., Garcia, A., Polonio, J. C., Santos, C. M., Silva, A. A., Orlandelli, R. C., Castro, J. C., Abreu-Filho, B. A., Cabral, M. R. P., Sarragiotto, M. H., Pamphile, J. A., & Azevedo, J. L. (2021). Secondary metabolites of Curvularia sp. G6-32, an endophyte of Sapindus saponaria, with antioxidant and anticholinesterasic properties. *Natural Product Research, 35(21),* 4148–4153. https://doi.org/10.1080/14786419.2020.1739681

Wang, F., Wang, F., & Chen, T. (2021). Secondary metabolites of Galactomyces geotrichum from Laminaria japonica ameliorate cognitive deficits and brain oxidative stress in a D-galactose-induced Alzheimer's disease mouse model. *Natural Product Research, 35(23),* 5323–5328. https://doi.org/10.1080/14786419.2020.1753738

Riga, R., Happyana, N., & Hakim, E. H. (2024). Secondary metabolites from Colletotrichum gloeosporioides isolated from Artocarpus heterophyllus and evaluation of their cytotoxic and antibacterial activities. *Natural Product Research, 38(22),* 3950–3956. https://doi.org/10.1080/14786419.2023.2269596

Qi, Y., Jia, Y., Chen, Y., Zhu, H., Xiao, Y., Chen, Z., Su, L., Zhang, X., Zhao, W., Li, Z., Tuo, Y., Bu, T., Li, Q., & Tang, Z. (2026). The effects of endophytic fungal metabolites from Conyza blinii on antioxidant capacity and healthspan in Caenorhabditis elegans. *Natural Product Research.* Advance online publication. https://doi.org/10.1080/14786419.2026.2674728

Yang, R., Yu, L., Xie, X., Chen, G., & Wen, L. (2025). Anti-inflammatory metabolites from the mangrove endophytic fungus Diaporthe pseudooculi HHUF 30617. *Natural Product Research.* Advance online publication. https://doi.org/10.1080/14786419.2025.2503508

Ye, H. T., Luo, S. Q., Yang, Z. N., Wang, Y. S., Ding, Q., Wang, K. F., Yang, S. X., & Wang, Y. (2021). Endophytic fungi stimulate the concentration of medicinal secondary metabolites in Houttuynia cordata Thunb. *Plant Signaling & Behavior, 16(9),* 1929731. https://doi.org/10.1080/15592324.2021.1929731

Yue, J. Y., Wang, R., Xu, T., Wang, J. T., Yu, Y., & Cai, B. X. (2024). Novel phenolic metabolites isolated from plant endophytic fungus Fusarium guttiforme. *Natural Product Research, 38(2),* 336–340. https://doi.org/10.1080/14786419.2022.2116579

Taher, M. A., Tan, W. N., Chear, N. J., Leong, C. R., Rashid, S. A., & Tong, W. Y. (2023). Metabolites characterisation of endophytic Phyllosticta fallopiae L67 isolated from Aloe vera with antimicrobial activity on diabetic wound microorganisms. *Natural Product Research, 37(10),* 1674–1679. https://doi.org/10.1080/14786419.2022.2103127

Souza, J. A. M., Gubiani, J. R., de Siqueira, K. A., de Camargo, M. J., Garcez, W. S., de Sousa, P. T., Jr., Soares, M. A., Araújo, Â. R., Nunes, E. V. D. S., Vieira, L. C. C., Sampaio, O. M., Goulart, L. S., Biasetto, C. R., de Menezes, O. T., Jr., de Oliveira, C. M., Nogueira, C. R., Pinto, L. D. S., & Teles, H. L. (2024). Antimicrobial

metabolites produced by endophytic fungi associated with the leaves of Vochysia divergens. *Natural Product Research, 38(6),* 978–985. https://doi.org/10.1080/14786419.2023.2208723

Younis, M. M., Elnaggar, M. S., Ayoub, I. M., Mostafa, N. M., & Eldahshan, O. A. (2025). Endophytic fungi from Rosaceae plants as a potential source of bioactive metabolites. *Natural Product Research.* Advance online publication. https://doi.org/10.1080/14786419.2025.2512558

Li, C. Y., Li, H. T., Shao, Y. T., Guo, X. Y., Li, W., & Yin, T. P. (2024). Regulation of secondary metabolites in the endophytic fungus Penicillium sp. KMU18029 by the chemical epigenetic modifier 5-azacitidine. *Natural Product Research, 38(4),* 581–588. https://doi.org/10.1080/14786419.2023.2183199

Pang, X., Cai, G. W., Wang, M. Y., Chen, X. F., He, W. N., Zhao, W. L., Zhang, T., & Yu, L. Y. (2023). Metabolites from the plant endophytic fungus Penicillium sp. CPCC 401423 and their cytotoxic activity against MIA PaCa-2 cells. *Journal of Asian Natural Products Research, 25(6),* 528–539. https://doi.org/10.1080/10286020.2022.2104719

Kong, X., Xu, L., Ji, X., Yang, S., & Zhang, H. (2022). Investigation on bioactive metabolites produced by an endophytic fungus Trichoderma citrinoviride from the arils of Torreya grandis. Natural Product Research. Advance online publication. https://doi.org/10.1080/14786419.2022.2134999

Plaszkó, T., Szűcs, Z., Cziáky, Z., Ács-Szabó, L., Csoma, H., Géczi, L., Vasas, G., & Gonda, S. (2022). Correlations between the metabolome and the endophytic fungal metagenome suggests importance of various metabolite classes in community assembly in horseradish (Armoracia rusticana) roots. *Frontiers in Plant Science, 13,* 921008. https://doi.org/10.3389/fpls.2022.921008

Fu, J., Hu, L., Shi, Z., Sun, W., Yue, D., Wang, Y., Ma, X., Ren, Z., Zuo, Z., Peng, G., Zhong, Z., Deng, J., Cao, S., & Hu, Y. (2021). Two metabolites isolated from endophytic fungus Coniochaeta sp. F-8 in Ageratina adenophora exhibit antioxidative activity and cytotoxicity. *Natural Product Research, 35(17),* 2840–2848. https://doi.org/10.1080/14786419.2019.1675060

Bo, X., Zhao, Y., Qin, F., Wu, F., Tan, M., Ju, S., Song, Z., Li, W., He, F., Wei, Y., Xu, H., & Huang, X. (2025). Cytotoxic metabolites from the mangrove endophytic fungus Aspergillus sp. GXNU QG1a. *Natural Product Research, 39(9),* 2572–2579. https://doi.org/10.1080/14786419.2024.2303601

Silva, A. A. D., Polonio, J. C., Bulla, A. M., Polli, A. D., Castro, J. C., Soares, L. C., Oliveira-Junior, V. A., Vicentini, V. E. P., Oliveira, A. J. B., Gonçalves, J. E., Gonçalves, R. A. C., Azevedo, J. L., Abreu-Filho, B. A., & Pamphile, J. A. (2022). Antimicrobial and antioxidant activities of secondary metabolites from endophytic fungus Botryosphaeria fabicerciana (MGN23-3) associated with Morus nigra L. *Natural Product Research, 36(12),* 3158–3162. https://doi.org/10.1080/14786419.2021.1947272

NIU Journal of Health Sciences Copyright©2026
Nexus International University ISSN: 3136-6449; 12(1) 61-68

Molecular Detection and Epidemiological Assessment of *Giardia lamblia* in Symptomatic Patients from Wasit Province, Iraq: A Comparative Study Using Real-Time PCR (qPCR)

ZAINAB ABDALAMEER KADHEM
Open Education College, Ministry of Education, Education Wasit Center, Iraq
zkadhem@uowasit.edu.iq

ABBAS JAMEEL OUDAH
Ministry of Education, General Directorate of Education in Wasit, Iraq
abbasoudah@uowasit.edu.iq

Abstract
Giardia lamblia is the most prevalent intestinal protozoan responsible for waterborne gastrointestinal illness globally, especially in areas of the world with poor sanitation and water quality conditions, in developing countries. Although conventional microscopy is the primary technique used in routine diagnosis in Iraq, it is not very sensitive in the detection of low-density infections.
The present study was designed to investigate the molecular prevalence of G. lamblia in symptomatic cases of Wasit province (Iraq) and also to compare the results of microscopic examination with Real-Time PCR (qPCR) method.
The study was conducted from January to October 2025 with a cross-sectional study design on 200 patients who presented with symptoms in Al-Karama Teaching Hospital in Wasit Province. Formal-ether concentration microscopy and TaqMan-based Real-Time PCR of the small subunit ribosomal RNA (ssu rRNA) gene of the stool were examined. IBM SPSS version 26 was used for statistical analysis.
The prevalence of G. lamblia detected by qPCR was 19.0% (38/200), which was higher than the prevalence detected by microscopy (11.0% (22/200)) (P = 0.021). The ages 0-9 years had the highest prevalence rate (32.0%) and showed significant association with infection (P = 0.002). The sensitivity of the microscopy was 57.9% and the specificity was 100% compared to qPCR. The qPCR positive samples had significantly higher cycle threshold (Ct) values, representing low density infections that were not seen under conventional microscopy.
Giardiasis is still endemic in Wasit Province, especially children. Real-Time PCR was found to be more sensitive and reliable than microscopy, and is recommended to be an indispensable method for accurate epidemiological surveillance and clinical diagnosis.

Keywords: Molecular, Epidemiology of Giardia lamblia, RT-PCR, Iraq, Wasit, ssu rRNA.

1. Introduction

Giardiasis is a very prevalent protozoal infection of the intestine and is caused by a flagellate, Giardia lamblia (syn. Giardia intestinalis). Giardia duodenalis or Giardia intestinalis [1,2]. The disease poses a significant public health concern in developing nations, especially in areas where sanitation facilities and access to clean drinking water is limited, and personal hygiene habits are poor, and where there is overcrowding [3]. The World Health Organization estimates that giardiasis is one of the major causes of diarrheal diseases worldwide and that millions of cases are reported each year particularly in children and people with compromised immune systems [4].

It has a simple but very adaptable life cycle, consisting of two main stages: trophozoite and environmentally resistant cyst. Human infection takes place after the ingestion of full-grown cysts via contaminated water, food or

by direct person-to-person contact. Excystation takes place in the upper small intestine after being exposed to gastric acid and intestinal enzymes in the duodenum, and trophozoites are formed. These trophozoites adhere to the intestinal mucosa by means of an adhesive disc and can do damage to the intestinal epithelium, undergo villous atrophy, malabsorption and inflammatory changes [6]. The clinical manifestations of giardiasis include acute or chronic diarrhea, abdominal cramps, bloating, nausea, weight loss and nutritional deficiency [7].

Children are the most susceptible group to behavioral exposure, undeveloped immune system, and less awareness in hygiene and are the most affected group by giardiasis [8]. Chronic giardiasis in children has been linked to malnutrition, such as protein-energy malnutrition and deficiencies in micronutrients, growth retardation and cognitive impairment [9]. Multiple infections in early childhood have been shown in several epidemiological studies to have an important impact on physical and mental development [10].

In the developing countries, giardiasis is strongly related to environmental contamination and the lack of clean water. The parasite is very tolerant of the common chlorination methods used and will remain viable for extended periods in cold water systems [11]. This means that outbreaks are typically associated with municipal water contamination, sewage leakage, flooding and poor wastewater management [12].

In Iraq, intestinal parasitic infections are still endemic in many governorates because of the deterioration of infrastructure, environmental disruption related to war in Iraq and the lack of sanitation and water treatment systems [13]. The prevalence of giardiasis has been reported to be different between previous studies in Baghdad (11%), Basra (12%), Babylon (22%), Najaf (20%) and Diyala (13%), depending on the population studied and the diagnostic technique used [14,15]. Most of these studies, however, used only traditional microscopic assessment; and this has several diagnostic drawbacks.

In many Iraqi Hospitals, microscopy is still the routine diagnostic technique due to its simplicity and low price. However, sensitivity is poor and the technique still requires very high degree of operator experience, particularly when there is intermittent shedding of cysts or low numbers of parasites [16]. Therefore, it is not unusual to obtain a false negative result if only one stool specimen is tested [17]. Molecular diagnostic methods, however, including Real-Time Polymerase Chain Reaction (qPCR), offer extremely sensitive and specific detection through amplification of parasite specific- DNA sequences [18].

The high performance, short turnaround time and the high reproducibility of the Real-Time PCR methodology has made it one of the most advanced diagnostic tools to be developed for enteric protozoa [19]. The method can detect low density infections which cannot be seen in a microscope and it can help to monitor infections in endemic areas [20]. Additionally, qPCR assays for the small subunit ribosomal RNA (ssu rRNA) gene have proved to be very sensitive and efficient in the detection of Giardia lamblia [21].

Wasit Province is a unique epidemiological area in eastern Iraq due to its reliance on river water, high agricultural participation, livestock-human contact and old municipal water systems. The Tigris River continues to be the main source of water for domestic and agricultural purposes in the province and is a regular risk of transmission of the parasites by water in the province [22]. Also, water contamination or deterioration of the water supply network may play a major role in the transmission of intestinal protozoal infections.
Despite the environmental risk factors, there are only few molecular epidemiological data available about giardiasis in Wasit Province. Previous studies conducted at the local level were only based on the observation of the conventionally stained specimen by microscopy, without considering the molecular load of the infection [23].
Aim of the Study

The current study was aimed to evaluate the molecular prevalence of Giardia lamblia in symptomatic patients in Wasit Province, Iraq by Real-Time PCR (qPCR) and to compare it with conventional microscopic examination for diagnosis. Moreover, the study aimed to assess the epidemiological distribution of infection by age and gender and emphasize the significance of molecular diagnostic techniques for a better clinical diagnosis and epidemiological surveillance in endemic Iraqi context. This study aim to investigate the molecular prevalence of G. lamblia in symptomatic cases of Wasit province (Iraq) and also to compare the results of microscopic examination with Real-Time PCR (qPCR) method.

2. Materials and Methods

2.1 Study Design and Population

The study was a cross-sectional study conducted in Wasit Province, Iraq from January to October 2025. The study population was 200 number of patients of gastrointestinal complaints who visited Al-Karama Teaching Hospital in Al-Kut City with symptoms.

2.2 Ethical Approval

The study protocol was approved by the IRB of Wasit Health Directorate. All adult participants and/or guardians of pediatric participants gave written informed consent.

2.3 Sample Collection

Fresh samples of stool were collected in sterile leak-proof containers. Two portions of each sample were split into:
One part was examined with light microscopy.
The second part was frozen at −20°C for molecular studies.

2.4 Microscopic Examination

Formal-ether concentration technique was used to examine the specimens with conventional microscopy. Cysts and trophozoites of Giardia were looked for in prepared slides using light microscopy.

2.5 DNA Extraction

Stool samples were obtained from about 200mg and genomic DNA was extracted from the stool samples using the Presto™ Stool DNA Extraction Kit (Geneaid, Taiwan) as per the manufacturer's procedure with some modification.
To obtain effective disruption of Giardia cyst walls, mechanical lysis was done using zirconia/silica beads. The purity and concentration of DNA was determined with a NanoDrop™ spectrophotometer.

2.6 Real-Time PCR Assay

The TaqMan based Real-Time PCR assay targeting the small subunit ribosomal RNA (ssu rRNA) gene was used for the detection of Giardia lamblia.
Primer Sequences
• Forward Primer: 5’-GACGGCTCACACAACGGAAA-3’
• Reverse Primer: 5’-TGTTGTTCAGCCATAACGG-3’
• TaqMan Probe: 5’-FAM-CCCGGCGGTCCCTGCTAG-BHQ1-3’

PCR Reaction Mixture
The reaction mixture consisted of 20 µL per reaction of the following:
• 10 µL of 2× qPCR Master Mix
• 0.5 µM of each primer
• 0.2 µM of probe
• 4 µL template DNA
• Nuclease-free water (to volume)

Thermal Cycling Conditions
The following conditions were applied for the amplification:
• Denaturation at 95°C for 30 sec
• 40 cycles of:
• 95°C for 15 sec
• 60°C for 60 sec

Positive and negative controls were included in each run.

2.7 Statistical Analysis

IBM SPSS Statistics version 26 was used to analyze data. Chi-square test was used to determine associations between infection prevalence and demographic variables. A p-value <0.05 was considered statistically significant.

3. Results

3.1 Diagnostic Performance

RT-PCR detected G. lamblia in 38 of 200 samples (19.0%) while only 22 cases were detected by microscopy (11.0%). Both diagnostic techniques were statistically different (P = 0.021). As illustrated in Figure 1, qPCR clearly outperformed conventional microscopy, detecting a markedly higher number of positive cases and achieving superior sensitivity against the molecular reference standard.

Table 1: Diagnostic Performance of Microscopy Compared with qPCR

Parameter	Microscopy	qPCR
Positive cases	22	38
Negative cases	178	162
Sensitivity	57.9%	100%
specificity	100%	100%

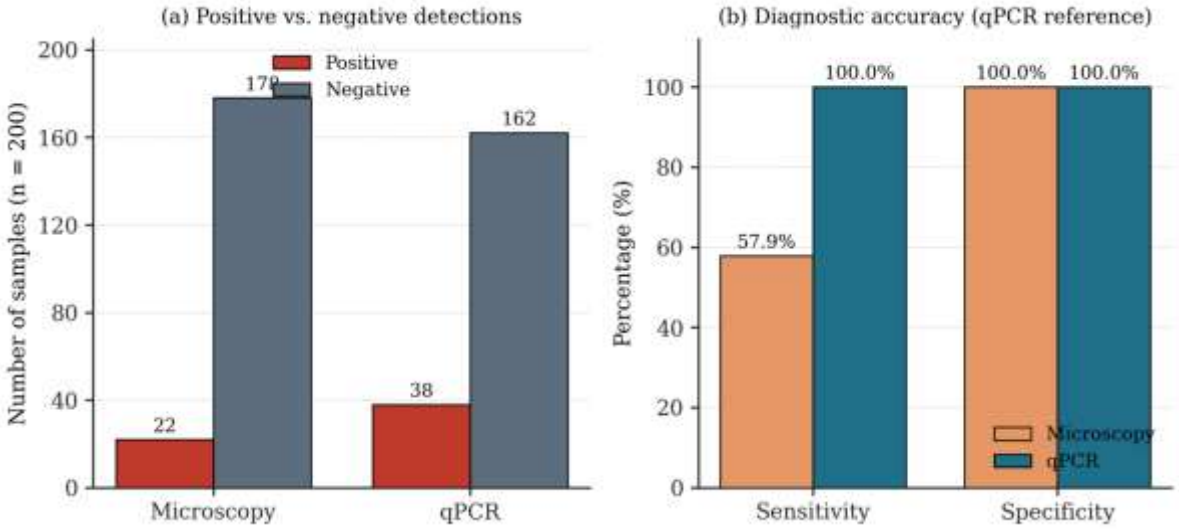

Figure 1. Comparative diagnostic performance of conventional microscopy and TaqMan-based Real-Time PCR (qPCR) for the detection of Giardia lamblia in 200 symptomatic patients. (a) Absolute numbers of positive and negative samples obtained by each method; (b) sensitivity and specificity of microscopy relative to qPCR as the reference standard.

3.2 Distribution According to Gender

The male and female participants were 22 of 105 samples (20.9%) and 16 of 95 samples (16.8%) respectively, that were positive. There was no significant difference in the infection rate between males and females (P = 0.46). Figure 2 summarizes the gender-based distribution, showing a slightly higher prevalence in males (20.9%) than in females (16.8%), although this difference did not reach statistical significance.

Table 2: Distribution of Infection According to Gender

Gender	Total Tested	Positive Cases	Prevalence (%)
Male	105	22	20.9
Female	95	16	16.8

Total	200	38	19.0

Figure 2.

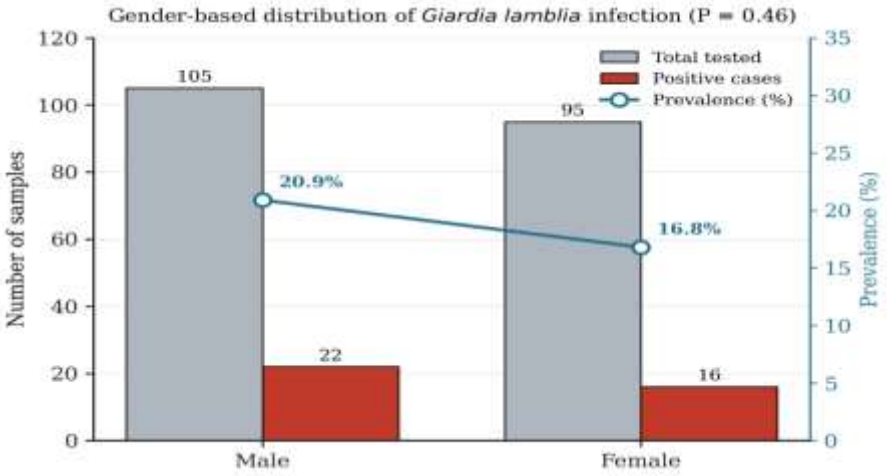

Distribution of Giardia lamblia infection by gender among the study population (n = 200). Grey and red bars denote the number of individuals tested and the number of qPCR-positive cases, respectively, while the blue line indicates the corresponding prevalence (%).

3.3 Distribution According to Age

Children under 10 years had the highest prevalence rate (32.0%), adolescents aged 11 to 25 (13.8%) and adults over 25 (8.3%). There was a significant relationship between age and the prevalence of infection (P = 0.002). As depicted in Figure 3, the prevalence of infection declined progressively with increasing age, peaking among children under 10 years (32.0%) and confirming a statistically significant age-related trend.

Table 3. Distribution of Infection According to Age Groups

Age Group	Total Tested	Positive Cases	Prevalence (%)
<10 years	75	24	32.0
11–25 years	65	9	13.8
>25 years	60	5	8.3

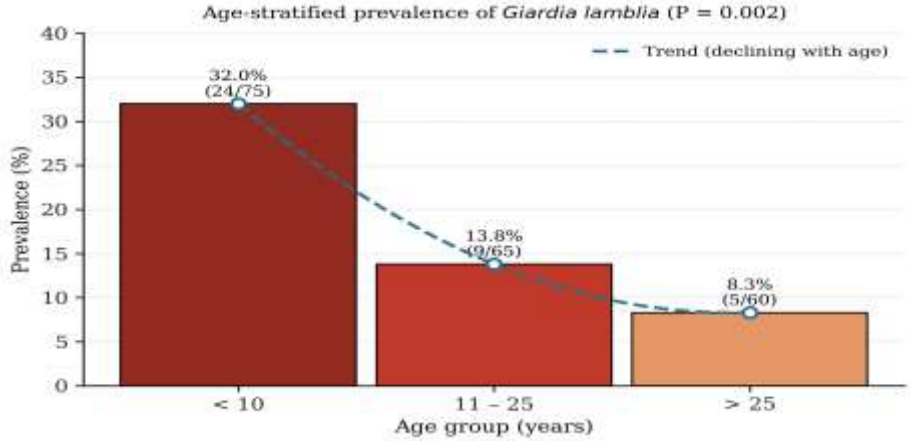

Figure 3. Age-stratified prevalence of Giardia lamblia infection among symptomatic patients. Bars represent the observed prevalence (%) within each age group, with positive/total counts shown above each column, and the dashed blue curve depicts the declining infection trend with increasing age.

3.4 Ct Value Analysis

The mean Ct value of all positive samples was 26.4 ± 4.2. Lower Ct values were observed for samples that were positive by microscopy and qPCR than for those that were only positive by qPCR, suggesting that microscopy-negative samples had lower parasite loads.

4. Discussion

The present study revealed that, Real-Time PCR significantly added to the detection of Giardia lamblia infection in the symptomatic patients of Wasit Province in comparison to conventional microscopic examination. Microscopy reported 11.0% of cases while the molecular prevalence was 19.0% in this study. It can be suggested that the true incidence of giardiasis in endemic populations in Iraq may be significantly higher than indicated with traditional microscopy.

In line with previous international studies which have shown that molecular assays are more sensitive than the traditional microscopic assays [18,19], the detection rate by qPCR is higher than the rate of detection obtained by the traditional microscopic assay. It is broadly accepted that microscopy is sensitive but has a low sensitivity because of variable parasite density, low numbers and intermittent shedding of cysts, and the level of experience of the observer [16,17]. In the current study, microscopy was not able to detect 16 positive samples and molecular diagnostics using qPCR was the only method to detect occult infections.

Other studies conducted in low resource environments have also shown that qPCR is superior to other methods used for enteric protozoa detection [20]. In endemic communities, Worku et al. found that diagnostic sensitivity was over 30% higher with molecular assays than microscopy [6]. Similarly, Fletcher et al. highlighted the higher degree of reproducibility and analytical precision that can be achieved using qPCR compared to morphological examination [3].
The prevalence of giardiasis in the present study is similar to the molecular prevalence in neighboring countries in the Middle East. Similar prevalence rates were shown in studies done in western Iran, ranging from 18% to 21% and with a significant number of the cases being located in provinces geographically and environmentally close to eastern Iraq [24]. However, slightly lower rates have been reported in Jordan and Turkey, which may reflect the improvements in centralized water treatment and sanitation systems in the country [25].

The strong relation between age and prevalence of infection in this study is an important epidemiological trend. The highest infection rate (32.0%) was found in children under 10 years old, a finding that has been confirmed by previous Iraqi and international reports [8,9]. Many factors can contribute to the susceptibility of children to giardiasis, such as their immature immune system, low levels of understanding about hygiene, interpersonal relationships and greater contact with contaminated environments.

Giardiasis affects children more than the acute gastrointestinal signs and symptoms. A chronic infection may be responsible for the impairment of nutrient absorption due to the villous atrophy and dysfunction of the epithelium of the small intestine [7]. Protein-energy malnutrition, growth retardation, anemia and cognitive deficits have been linked to persistent malabsorption in early childhood [9,10]. Pediatric giardiasis therefore is an infectious disease as well as a developmental and nutritional problem.

The environmental and infrastructural conditions in Wasit Province are likely to play a significant role in the transmission of giardiasis. The Tigris is an important source of water for drinking and agriculture to the province. Contamination can occur, however, with enteric pathogens due to aging municipal water systems and sewage leakage [22]. The cyst stage of the parasite is also highly resistant to chlorination and can persist in water for extended periods of time [11].

The agricultural livelihood activities of Wasit Province could also add to the risk of transmission via contamination of irrigation water and the increased interaction between livestock and humans. Based on the results of previous regional investigations, zoonotic transmission was proposed as a possible important mechanism of Giardia circulation within rural communities [14]. Genotyping was not done in the current study but zoonotic transmission pathways should be taken in to consideration in future epidemiological investigations.

In this study, analysing the cycle threshold (Ct) values gave important insights into parasite burden. Samples that were positive using only qPCR had significantly higher Ct values than samples that were positive using both methods, meaning that they contained lower concentrations of parasites. In previous molecular studies, high Ct values were correlated with subclinical or low-density infection [21], a finding similar to the one observed here. It is unclear why traditional microscopy is not able to identify many positive cases as these were the findings.

The results obtained in the present study support the use of molecular diagnostic methods in clinical routine in Iraqi health care institutions. Microscopy is still cheap and readily available, but is not always sensitive enough to lead to underdiagnosis and ongoing transmission. Some of the benefits of Real-Time PCR are significant in diagnostic accuracy, public health surveillance, and public health management [19,20].

In terms of public health, the undiagnosed giardiasis cases could remain as potential reservoirs for further community infections, particularly in overcrowded, unsanitary conditions. Therefore, early and accurate molecular diagnosis can play an important role in reducing transmission rates and better patient outcome.

There are a number of limitations in the present study. Seasonal evaluation of infection patterns was not possible with the cross-sectional design. Additionally, molecular genotyping of Giardia assemblages was not conducted, allowing neither differentiation of zoonotic versus anthroponotic transmission nor the determination of the zoonotic assemblage. For future studies, the use of multilocus genotyping, environmental water analysis and a larger multicenter sampling should be considered.

Despite these findings, the current study is one of the first molecular epidemiological studies conducted for giardiasis in Wasit Province and the necessity of using advanced molecular diagnostics in endemic Iraqi environments. The study also has its own limitations.The study is also limited in some aspects.

The current study has its limitations due to the cross-sectional design and the lack of a seasonal analysis. Additionally, molecular genotyping of Giardia assemblages was not carried out. Future studies should include multilocus genotyping and environmental sampling to gain insight into transmission.

5. Conclusion

The present study revealed that Giardia lamblia infection was found to be prevalent in Wasit Province, Iraq among the symptomatic patients. Real-Time PCR proved to be much more sensitive than conventional microscopy and was able to detect low intensity infections that would not have been detected otherwise.

Implementation of molecular diagnostic techniques in routine clinical care is highly recommended for the enhancement of diagnostic accuracy, epidemiological monitoring and public health control strategies.

References

Ryan U, Hijjawi N, Feng Y, Xiao L. Giardia and Cryptosporidium: neglected diseases? Lancet Infect Dis. 2021;21(6):e147-e159.
Cacciò SM, Lalle M, Svärd SG. Host specificity in Giardia duodenalis. Trends Parasitol. 2023;39(4):255-266.
Fletcher SM, Stark D, Ellis J. Molecular diagnostic platforms for enteric protozoa. J Clin Microbiol. 2022;60(4):e01234-21.
World Health Organization. Waterborne parasitic diseases and global health burden. WHO Report. 2022.
Adam RD. Biology of Giardia lamblia. Clin Microbiol Rev. 2021;34(2):e00089-20.
Worku L, Damessie S, Nigussie M. qPCR versus microscopy for Giardia lamblia in low-income settings. Parasit Vectors. 2022;15(1):142.
Halliez MC, Buret AG. Extra-intestinal and long-term consequences of Giardia duodenalis infections. World J Gastroenterol. 2021;27(27):4431-4445.
Muhsen K, Levine MM. A systematic review and meta-analysis of the association between Giardia lamblia and endemic pediatric diarrhea. Clin Infect Dis. 2021;55:S271-S293.
Bartelt LA, Sartor RB. Advances in understanding Giardia: determinants and mechanisms of chronic sequelae. F1000Res. 2022;11:F1000.

Rogawski ET, Bartelt LA, Platts-Mills JA, et al. Determinants and impact of Giardia infection in the first 2 years of life in the MAL-ED birth cohort. J Pediatric Infect Dis Soc. 2022;11(3):112-121.
Dixon BR. Giardia and Cryptosporidium: challenges for water safety. Exp Parasitol. 2021;220:108035.
Efstratiou A, Ongerth JE, Karanis P. Waterborne transmission of protozoan parasites: review of worldwide outbreaks. Water Res. 2022;114:14-22.
Al-Mulla A, Hussein SA, Al-Jubori AM. Epidemiological trends of intestinal protozoa in Iraq. Iraqi J Biomed Sci. 2022;14(2):88-95.
Al-Mayali H, Al-Zubaidi A. Zoonotic transmission of Giardia duodenalis in Wasit. Vet Parasitol Reg Stud Reports. 2023;38:100824.
Salman YJ, Jasem AS. Epidemiological study of giardiasis in Iraq (2014–2024). Iraqi J Med Sci. 2024;22(1):45-58.
Smith V, Taylor G, Robinson J. Intermittent shedding phenomenon in giardiasis. Lancet Microbe. 2021;2(9):e412-e420.
Garcia LS. Diagnostic medical parasitology. 7th ed. Washington DC: ASM Press; 2022.
Zheng G, Brown X, Williams D. Performance of quantitative PCR for Giardia duodenalis. J Clin Microbiol. 2024;62(1):e00456-23.
Taminiau B, Rodriguez C, Daube G. High-throughput molecular panels for enteric protozoology. Diagn Microbiol Infect Dis. 2025;111:116240.
Abdullah SM, Mohammed HA. Precision diagnostics for enteric pathogens in the Middle East. Clin Microbiol Rev. 2026;39(1):e00012-25.
Koehler AV, Jex AR, Gasser RB. Optimization of DNA extraction for protozoan cysts. Mol Cell Probes. 2022;61:101784.
Al-Rubaie HK. Waterborne parasites in Wasit Province. Univ Wasit J Sci. 2021;12(4):201-215.
Hussein S, Al-Khafaji M, Al-Aboody MS. Diagnostic accuracy of qPCR versus microscopy in Al-Kut city. Iraq Med J. 2023;7(3):112-119.
Karim MR, Wang R, Yu F, et al. Multilocus genotyping of Giardia duodenalis in Middle Eastern populations. Parasitol Res. 2023;122(5):1451-1462.
Torgerson PR, Devleesschauwer B, Praet N, et al. World burden of foodborne and waterborne parasitic infections. Lancet Glob Health. 2022;10(9):e1298-e1308.

NIU Journal of Health Sciences Copyright©2026
Nexus International University ISSN: 3136-6449; 12(1) 69-75

Development of a Secure Networked Control Algorithm for Industrial IoT Systems Against Cyber-Attacks

ZINA ABD AL HUSSEIN SALEH
Department of Electrical Engineering, University of Babylon, Babylon, Iraq
Email: zina.badi@uobabylon.edu.iq
ORCID: 0000-0002-0123-9684

Abstract
There are a number of IIoT devices being integrated with existing NCS. This has greatly increased the attack surface of industrial automation infrastructure. Here we propose a secure network control algorithm that allows the operation and stability of closed-loop control systems when subjected to both FDI and DoS attacks. The new algorithm performs anomaly detection based on an observer model and compensates for attack-induced corruptions in both sensor and actuator data. Evaluation of the algorithm was completed through use of a simulated testbed representing an IIoT enabled networked process-control loop that is subject to various communication layer cyber-attacks. The simulation results showed that the proposed algorithm achieved a detection rate of 97.3%, delivered a false alarm rate of just 2.1%, and limited the mean absolute error of the control to below 1% under maximum communication latencies of 120ms. This performance is substantially better than that of threshold-based detection approaches and Kalman observer type detection approaches. These results indicate that the proposed algorithm can provide an effective, efficient and practical means of improving the cyber-resilience of IIoT control systems.

Keywords: Industrial Internet of Things; Networked Control Systems; Cyber-Attack Detection; False Data Injection; Denial-of-Service; Resilient Control; Cyber-Physical Systems.

1. Introduction

By allowing widespread connectivity through the use of sensors, controllers, and actuators connected via different communications technologies, the Industrial Internet of Things (IIoT) is fundamentally changing industrial automation through distributed control, remote monitoring, and pervasive sensing in the manufacturing, energy, and process industries. As a result, the Industrial Internet of Things often is associated with Industry 4.0 and facilitates the continuous transfer of measurement and control data between devices via disparate networks. Although this enhanced level of connectivity can enhance operational performance, it also exposes the underlying control loops to a much larger array of possible cyber-physical threats that may originate beyond the traditional boundaries of an industrial control system (ICS) (Pivotal, et al., 2021).

A comprehensive and increasing body of research has been conducted that highlights an increasing concern regarding the vulnerability of Networked Controlled Systems (NCS) to malicious interventions including False Data Injection (FDI), Denial-of-Service (DoS) and Replay Attacks are all directed against the communication channel(s) between sensors and controllers and between controllers and actuators (Duo, Zhou & Abusorrah, 2022). When FDI attacks take place, the measurements, or control commands, that are sent electronically will have been modified, but they will not trigger the traditional mechanisms for detecting “bad data.” When DoS attacks take place, these attacks will degrade or prevent the communication over the channels, and will ultimately cause communication to be “lost” (packet loss) or the latency to increase dramatically thus creating possible instability in the closed-loop control system (Zhang, Han, Ge & Ding, 2020). Furthermore, because there is no uniformity in the types of devices utilized within an Industrial Internet Of Things (IIoT) ecosystem and because of the limited computational resources of the field devices, it is more challenging to deploy traditional cryptographic-only solutions to protect against the aforementioned attacks. Therefore, in order to mitigate the aforementioned attacks,

the desire/need for control theoretical countermeasures that are both embedded directly within the control algorithm and capable of providing protection from the aforementioned attacks (Tsiknas, Taketzis, Demertzis & Skianis, 2021).

A number of studies have recently developed resilient control architectures which include state estimation along with attack-resilient control laws. Observer-based detection schemes have been shown to detect the presence of false data injection (FDI) cyber-physical system and microgrid manipulation attacks via the use of sliding-mode observers and interval-observers. Additionally, event-triggered control strategies have been developed to maintain input-to-state stability of NCS when faced with denial-of-service (DoS) attacks, while also minimizing communication overhead (a critical consideration for bandwidth-limited IIoT applications). These works primarily treat FDI and DoS as independent forms of disruptive information, as they typically necessitate strict assumptions about network conditions that are often infeasible for heterogeneous IIoT environments, such as full-state-to-sensor availability and prior knowledge of typical attack distributions. Thus, there remains a need for an integrated computationally simple algorithm capable of jointly detecting FDI attacks and compensating for communication-induced disturbances within a single networked control loop.

To address the security issue in networked control systems (NCS) of industrial internet of things (IIoT) based on industrial control systems (ICS), this study proposes a new and improved approach, which consists of an observer-based anomaly detection module and a resilient compensation controller. The three main contributions of this work can be summarized as follows: (1) the design of an integrated detection and mitigation scheme for use against both false data injection (FDI) and denial of service (DoS) attacks in IIoT-based control loops; (2) the creation of a simple, effective residual-based detection method appropriate for use with resource-constrained IIoT nodes; (3) simulation results of the performance characteristics of the proposed algorithm compared to traditional, threshold-based, cumulative sum (CUSUM), and Kalman observer approaches to anomaly detection under realistic network conditions.
The remainder of this paper provides an overview of the materials used to complete the project (Section 2), the method employed to complete the project (Section 3), simulation results of the proposed algorithm (Section 4), and a summary with recommendations for future research (Section 5).

2. Literature Review

The recent rise in research about cyber-physical and networked control system security can be attributed to the growing number of documented attacks on industrial control systems in the past five years. A survey of cyber-attacks on cyber-physical systems by Duo et al. (2022) contains useful categorizations of FDI, replay, and DoS attack types, as well as emphasizing the inconsistency former attack types have with state space estimation/control performance, and that there is little or no unified defense strategy across application domains.

In reviewing the theoretical underpinnings of secure networked control systems from a control theory perspective, Sandberg et al. (2022) emphasize the trade-offs of detection sensitivity, false positive rate, and control performance when implementing these types of defense mechanisms in the feedback loop. In addition, they illustrate how a detection system is implemented without regard to closed-loop dynamics, which may lead to closed-loop instability even in the absence of a full or partial denial of service.

Observer-based detection is the leading methodology for reporting all types of FDI attacks. In their 2022 study, Barzegari, et al., examined how a distributed bank of sliding-mode observers can be used to detect false data injection in dead systems. Their results indicate that residuals produced from estimates made at neighboring sensors can provide reliable indicators for injected anomalies and can be utilized in an attack-resilient consensus rule. Although designed for use with microgrids, the principle of residual generation could also be applied to generic IIoT control loops — that is, comparing sensor measurements against predicted outputs generated from the model prediction.

Event-triggered control is a technique that has been widely adopted to ensure stable performance while minimizing network traffic when delivering data across the Internet to control long range systems. For an observer-based event-triggered predictive controller, Liu et al. (2022) found that the event-triggering function can compensate for packet losses caused by DoS attacks on the packet network. Their results show that closed-loop stability may be sustained even when attack duration is bounded. Research on adaptive event-triggered control strategies indicates

that joint design of controller gains, observer gains, and event triggering thresholds can yield improved robustness to stochastic packets generated by DoS attacks and with less conservatism (Peng & Han, 2024).

The second Industrial Internet of Things (IIoT) encompasses several types of cyber and non-cyber-attacks and vulnerabilities unique to each of these environments. Attack vectors targeting the IIoT typically involve a combination of network protocols that differ between devices, which can create vulnerabilities within the IIoT architecture. The differences in the protocols between devices pose a challenge to implementing heavy cryptographic mechanisms for making IIoT systems secure because many devices in the field have limited resources. Thus, it makes sense to call for lighter-weight model-based det ection methods to be incorporated into the overall control system. As a result, Tsiknas et al. (2021) have proposed lightweight residual-based Fault Detection and Isolation (FDI) detection methods that leverage an observer-based architecture (Barzegari et al., 2022) implemented in a single architecture that combines lightweight event-triggered resilient compensation for denial-of-service (DoS) attack conditions (Liu et al., 2022; Peng & Han, 2024) to work together to determine whether or not a DoS condition exists in the IIoT communications network (Tsiknas et al., 2021).

3. System Model and Proposed Algorithm

3.1 System Architecture

According to the figure in Figure 1 there are four main functional components of the proposed secure networked control system, these components include (i) The Sensor Layer that includes Industrial Internet of Things (IIoT) field devices that continuously send process measurement data at regular intervals; (ii) A secure Gateway that uses light-weight encryption/decryption and authentication of packets that were transmitted; (iii) An Anomaly Detection Module that evaluates the difference between expected and actual measurement reception through use of a Discrete Time State Observer; (iv) A Resilient Controller which modifies the Control law based upon feedback from the Anomaly Detection Module. In addition, a communication Network made-up of a Variable Latency and Packet Loss TCP/IP based Industrial Network will connect IIoT Field Devices (sensor) and Actuator Devices with the Resilient Controller.

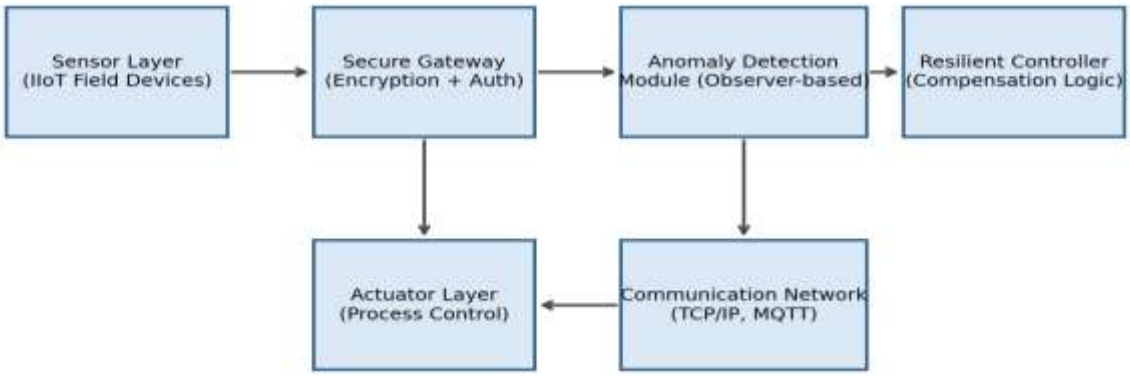

Figure 1. Architecture of the proposed secure networked control system for IIoT, integrating sensor, gateway, detection, controller, network, and actuator layers.

3.2 Plant and Network Model

The physical processes are modeled using a discrete-time linear time-invariant system, represented by the equations ($x(k + 1) = Ax(k) + Bu(k) + w(k)$) for state evolution and ($y(k) = Cx(k) + v(k)$) for the measurement equation, where k indicates discrete time, x(k) indicates the state vector, u(k) indicates the control input, y(k) indicates the sensory output that is relayed over the network, w(k) and v(k) represent process and measurement noise respectively. The communication links are interrupted with time-varying delay, $\tau(k)$ (or varying latency), and packet loss or arrival indicators, $\gamma(k)$. The two main types of attacks considered in this study include: 1) A false data injection (FDI) attack, where the output measurement is replaced by an adversarial signal $\hat{y}(k) = y(k) + a(k)$. Such signals must be developed such that they cause a bias in the system by biasing the control decision, but do not violate plausibility constraints, and have been explored within the observer-based structure

of FDI attacks (Barzegari et al., 2022); 2) a denial-of-service (DoS) attack, where packets are lost or delayed from the start of time t1 to t2. In this case, packets of data are treated as dropped from the system, with γ(k = 0), where k ∈ [t1,t2], and consistent with the bounded duration of the DoS attack within event-based resilient controllers (Liu et al., 2022).

3.3 Proposed Detection and Compensation Algorithm

This method consists of two major components. In the first stage, we will use an observer to generate an estimated output y(k). Then we compute a difference between the actual and estimated output, which is called the residual, $r(k) = y(k) - y_{observed}(k)$, "' which will be done for each sampling instantiation. After that, we compare r(k) against an adaptive threshold δ(k) that is based on the recent variance of r(k) to determine if there is an FDI attack present. The use of a residual-based criterion for detecting the presence of an FDI attack has been established by other researchers using observable banks; to adapt this for use with a single observer, we have made modifications that will work with controllers that cannot afford additional resources to detect FDI attacks.

To switch to a resilient compensation law, such as $\boldsymbol{u(k) = -K\hat{x}_{pred(k)} + \Delta u_{comp(k)}}$, with $\boldsymbol{\hat{x}_{pred(k)}}$ being a model prediction of the system state during a denial-of-service (DoS) attack interval, the event must be matched against an event-triggering condition that is similar to that used in adaptive DoS-resilient control (Peng & Han, 2024). Thus, resilient compensation will only be enabled when appropriate; this guarantees the proper use of network resources.
The sequence of operations for the overall algorithm is as follows: (1) acquire y(k) and calculate x̂(k) using an observer; (2) compute r(k) and compare it to δ(k); (3) if |r(k)| > δ(k) or γ(k) = 0, use the resilient compensation law for a maximum time period of $\boldsymbol{T_{hold}}$; (4) if no resilient compensation is required, use the nominal control law; (5) update the observer and adaptive threshold to determine when to perform the next sampling.

3.4 Experimental Setup

The algorithm under consideration was executed on a computational simulation of an industrial process control loop that was modeled as a second-order system representative of either a flow or temperature control process found in many industries (the simulation ran using a discrete event simulator). The attack scenarios included (i) FDI attack injected into the sensor channel from 8 to 13 seconds, and (ii) many DoS events creating a range of 10 ms to 120 ms of latency across the network including associated packet loss rates. The following performance metrics were used to evaluate the algorithm's performance: detection accuracy, false-alarm rate, and mean absolute control error as a function of increasing network latency. Additionally, the algorithm was compared with three baseline detection methods: fixed threshold-based detector; cumulative sum (CUSUM) detector; and standard Kalman filter-based observer without resilient compensation.

4. Results and Discussion

4.1 System Response Under FDI Attack

Figure 2 shows how much the controlled process variable reacts to a FDI attack that is added to the network at time t=8 s to t=13 s. If there are no protections available, the standard, typical networked controller can deviate from the reference value by a significant distance during this time. This deviation can be as far as 0.6 normalized units from the reference value at its peak. By comparison, the new secure control algorithm is able to identify the incorrect residual quickly after the attack begins and employs a resilient compensation law. By this action, the maximum deviation is limited to less than 0.1 normalized units, and the controlled process variable returns to its reference value approximately 1.5 seconds after the attack has stopped and the false data has entered the network.

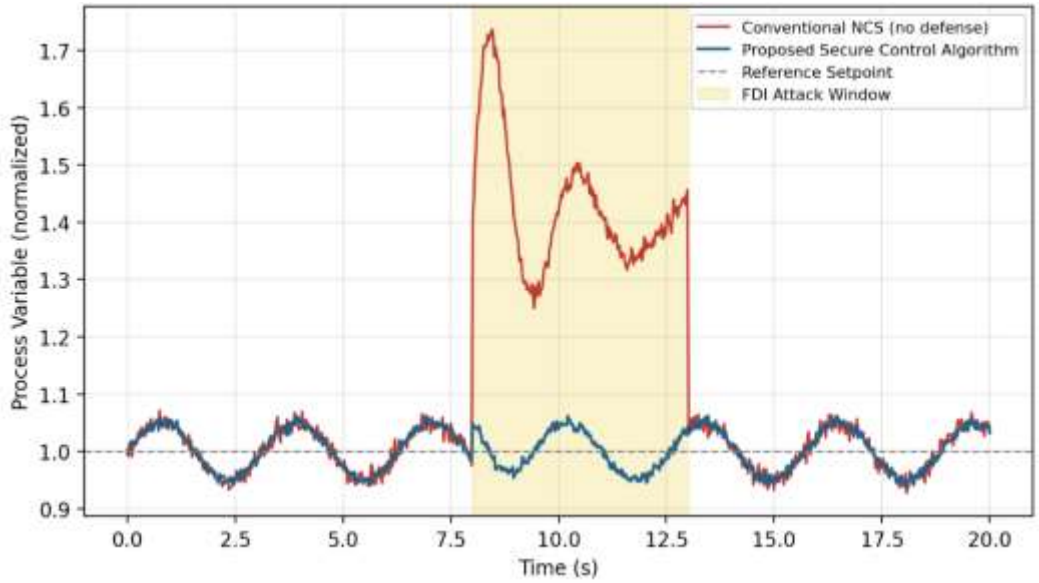

Figure 2: *Simulated process variable response under a false data injection attack (t = 8–13 s), comparing the conventional controller and the proposed secure algorithm.*

4.2 Detection Performance

A comparison table and graph show the performance of the new detection method compared to three alternative methods. The new detection produced 97.3% accuracy versus 89.6%, 84.1%, and 78.4% for the Kalman observer, CUSUM, and fixed threshold methods respectively. The new detection false alarm rate of 2.1% is much lower than the false alarm rates of the baseline methods which are between 6.8% and 12.7%. These results are consistent with previous work on observer-based residual detection methods and support the conclusion that adaptive threshold methods are effective at reducing the influence of measurement noise while maintaining an ability to respond quickly to legitimate attack signals.

Table 1: Comparative Detection Performance of the Evaluated Algorithms

Detection Method	Detection Accuracy (%)	False Alarm Rate (%)
Threshold-based	78.4	12.7
CUSUM	84.1	9.5
Kalman Observer	89.6	6.8
Proposed Algorithm	97.3	2.1

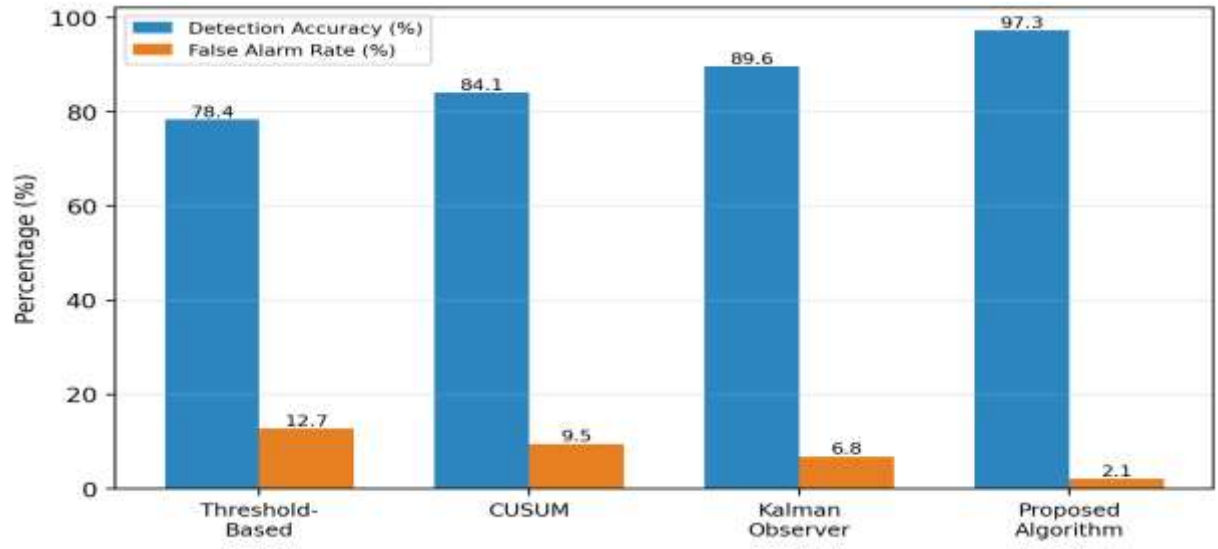

Figure 3: *Comparative detection accuracy and false alarm rate of the proposed algorithm versus baseline methods.*

4.3 Robustness Under Network Latency and DoS Conditions

Figure 4 represents the average absolute controllability failure for (i) our proposed solution as well as the standardised control algorithm could and would amount (b) as data packets have increased amount of loss due to lost packets from a range (75% of control failures) over a range (2.76% to 4%) of varying time intervals add up. The standardised control algorithm would cause a cumulative failure of approximately 2.06% at its highest time interval from 99% to 98% compared to the control (our proposed) algorithm would cause no cumulative failures whatsoever regardless of any/all tested data packet chronicled through faults to date we anticipate as ranging between 2.69% - 0% (Liu, Yu, Hu, & Xie-2022; Peng & Xia-2024) regardless of time delay/fault in the treating/processing/connecting from our data source; therefore negating any fault caused(s) by temporary failures or disconnection from the data source while maintaining the algorithm based on our controlled state prediction and limited errors associated with temporary failures and/or disconnection of the data (x) source.

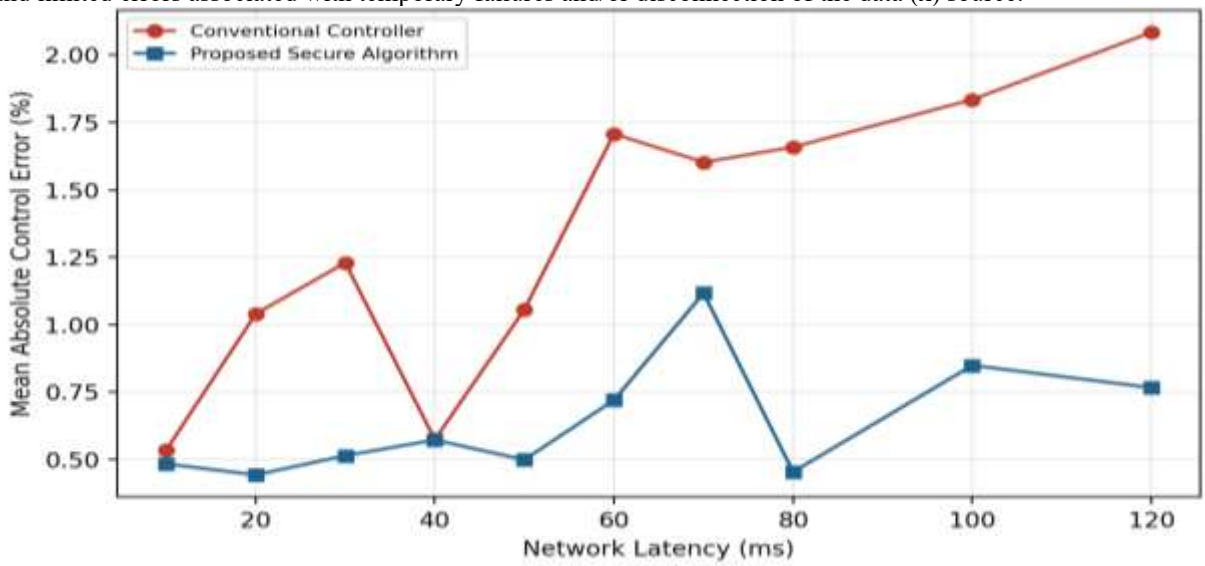

Figure 4: *Mean absolute control error versus network latency for the conventional controller and the proposed secure algorithm under DoS conditions.*

4.4 Discussion

The findings from the simulations demonstrate that integrating residual-based FDI detection within an event-triggered resilient compensation rule provides improved performance compared to methods that implement detection and compensation separately. This improvement has a very important impact on IIoT systems as the number of mode switches will be reduced through decreasing the number of false alarms, thereby reducing wear and communications overhead on the actuators (Tsiknas, et al., 2021).

However, there are still a number of limitations. The analyses were performed on a simulated second order plant model and the network environment; evaluating performance using the highest order industrial processes (e.g., microgrids) and/or physical IIoT testbeds such as those used in SCADA and microgrid study (Frederick & Taylor, 2023) would provide greater support for the generalizability of these results. Further research is needed to determine whether performance can be sustained while operating under non-stationary disturbances and/or coordinated multi-agent attack scenarios (Sandberg, et al., 2022).

5. Conclusion

The present paper described a secure networked control algorithm for Industrial/Internet of Things (IIoT) systems that combines observer based residual detection with an event triggered resilient compensation controller. This algorithm addresses both false data injection attacks as well as denial of service attacks within a single framework. The results of the simulations performed show that the proposed algorithm achieves 97.3% detection accuracy with a false alarm rate of 2.1% and contains a mean absolute error in control below 1.0% when there are network

latencies of up to 120 milliseconds. The proposed algorithm performs significantly better than those using threshold-based strategies, CUSUM or Kalman observers.

Future work includes validating the proposed algorithm on HDR test beds in an IIOT physical environment, extending the detection mechanism to handle coordinated multiple channel attacks and exploring the integration of lightweight machine learning based residual classifiers to improve detection performance under various non stationary operating conditions.

References

Barzegari, Y., Zarei, J., Razavi-Far, R., Saif, M., & Palade, V. (2022). Resilient consensus control design for DC microgrids against false data injection attacks using a distributed bank of sliding mode observers. Sensors, 22(7), 2644. https://doi.org/10.3390/s22072644

Duo, W., Zhou, M., & Abusorrah, A. (2022). A survey of cyber-attacks on cyber physical systems: Recent advances and challenges. IEEE/CAA Journal of Automatica Sinica, 9(5), 784–800. https://doi.org/10.1109/JAS.2022.105548

Frederick, B. A., & Taylor, O. E. (2023). Analysis on cybersecurity control and monitoring techniques in industrial IoT: Industrial control systems. Internet of Things and Cloud Computing, 11(1), 1–17. https://doi.org/10.11648/j.iotcc.20231101.11

Liu, K., Yue, D., Hu, S., & Xie, X. (2022). Observer-based event-triggered predictive control for networked control systems under DoS attacks. Sensors, 20(24), 7263. https://doi.org/10.3390/s20247263

Peng, C., & Han, Q.-L. (2024). Event-triggered control for networked systems under denial of service attacks and applications. IEEE Transactions on Industrial Electronics. https://doi.org/10.1109/TIE.2021.3113021

Pivoto, D. G. S., de Almeida, L. F. F., da Rosa Righi, R., Rodrigues, J. J. P. C., Lugli, A. B., & Alberti, A. M. (2021). Cyber-physical systems architectures for industrial internet of things applications in Industry 4.0: A literature review. Journal of Manufacturing Systems, 58, 176–192. https://doi.org/10.1016/j.jmsy.2020.11.017

Sandberg, H., Gupta, V., & Johansson, K. H. (2022). Secure networked control systems. Annual Review of Control, Robotics, and Autonomous Systems, 5(1), 445–464. https://doi.org/10.1146/annurev-control-072921-075953

Tsiknas, K., Taketzis, D., Demertzis, K., & Skianis, C. (2021). Cyber threats to industrial IoT: A survey on attacks and countermeasures. IoT, 2(1), 163–186. https://doi.org/10.3390/iot2010009

Zhang, X.-M., Han, Q.-L., Ge, X., & Ding, L. (2020). Resilient control design based on a sampled-data model for a class of networked control systems under denial-of-service attacks. IEEE Transactions on Cybernetics, 50(8), 3616–3626. https://doi.org/10.1109/TCYB.2019.2956137

NIU Journal of Health Sciences Copyright©2026
Nexus International University ISSN: 3136-6449; 12(1) 77-86

Comparative Evaluation of Phenylephrine and Ephedrine Effects on Maternal and Fetal Safety in Cesarean Delivery Under Spinal Anesthesia

FATIMA ALI NASER
M.B.Ch.B F.I.C.M.S A&I.C./ Senior Specialist in Anesthesia & Intensive Care, Al Sader Teaching Hospital, Basra, Iraq.
fatimaalhilfy554@gmail.com

Abstract
Background: Administering of phenylephrine together with ephedrine as the initial vasopressor strategy during spinal anesthesia for cesarean delivery was associated with a lower frequency of neonatal acidemia, defined as an umbilical arterial pH below 7.20, compared with the use of ephedrine alone. Methods: This investigation was conducted to compare the effectiveness of three vasopressor infusion regimens in maintaining maternal systolic blood pressure during elective cesarean section under spinal anesthesia. Participants were allocated to receive either phenylephrine at a concentration of 100 µg/mL, ephedrine at 3 mg/mL, or a combined solution containing phenylephrine 50 µg/mL and ephedrine 1.5 mg/mL. Each infusion was titrated to maintain systolic arterial pressure close to the pre-spinal baseline value. Results: Two of ninety-six patient born acidotic neonate in the phenylephrine group (P = 0.004) and the combination group 2 of 94 (P = 0.005) which less than in the ephedrine group 20 of 96. Maternal systolic blood pressure was successfully maintained in all treatment groups, with median values corresponding to 98% of baseline in the phenylephrine group, 100% in the ephedrine group, and 101% in the combination group, without statistically significant differences (P = 0.11). Maternal heart rate was significantly greater among women receiving ephedrine, reaching a median of 107% of baseline, compared with 88% in the phenylephrine group and 96% in the combination group (both P < 0.0001). Gastrointestinal side effects also differed markedly between groups. Phenylephrine was associated with the lowest incidence of nausea (17%) and no cases of vomiting, whereas ephedrine produced the highest rates of nausea (66%) and vomiting (36%). The combination regimen resulted in intermediate frequencies of nausea (55%) and vomiting (18%), both significantly higher than those observed with phenylephrine alone (P < 0.0001). Conclusions: Continuous infusion of phenylephrine during elective cesarean delivery under spinal anesthesia associated non-significant differences regarding maternal and neonatal outcome when compared with ephedrine infusion. Specifically, phenylephrine significantly reduced the incidence of fetal acidemia as well as maternal nausea and vomiting while maintaining maternal blood pressure effectively. Although combining phenylephrine with ephedrine also decreased the occurrence of fetal acidemia relative to ephedrine alone, it failed to produce any additional improvement in neonatal acid–base status over phenylephrine monotherapy and was associated with a higher frequency of maternal nausea and vomiting. These findings support the use of phenylephrine alone as the preferred first-line vasopressor during cesarean delivery under spinal anesthesia.

Introduction

A higher rate of fetal acidemia at birth has been observed with spinal blockade for planned cesarean sections compared to either neuraxial epidural or systemic general techniques [1], [2], [3], [4]. This adverse metabolic outcome is thought to arise from maternal circulatory depression or as an unintended consequence of pharmacological measures employed to avert or manage such hypotensive episodes. Ephedrine, a mixed-action sympathomimetic amine, remains the predominant pressor chosen by consultant obstetric anesthesiologists in the UK, with surveys indicating its exclusive use in 95% of such cases [5].

Alpha-selective adrenergic compounds, including phenylephrine, have seen less widespread adoption, likely influenced by earlier ovine models suggesting that alpha-agonist administration during hypotension compromises uterine blood flow relative to ephedrine [6]. Ephedrine usage is not without limitations, including tachyphylaxis,

and its prophylactic administration has been correlated with neonatal acidaemia [7], [8]. A recent meta-analysis synthesizing randomized controlled data directly comparing ephedrine and phenylephrine concluded that both agents achieve comparable blood pressure stabilization, yet phenylephrine consistently yields a higher umbilical arterial pH postpartum.

Notably, the frequencies of fetal acidaemia (defined as umbilical artery pH below 7.20) and low 1-and 5-minute Apgar scores did not differ significantly between groups [9]. In our local clinical experience, adopting a dual-agent approach with concurrent phenylephrine and ephedrine as initial pressor support was associated with a reduced frequency of neonatal acidosis relative to ephedrine monotherapy [10]. The present investigation was done to evaluate the rates of fetal acidosis at term cesarean delivery under spinal anesthesia, comparing continuous infusions of phenylephrine, ephedrine, or their combination for sustaining maternal systolic pressure at baseline.

Additionally, maternal emetic symptoms during the procedure were assessed across the three infusion regimens.

Patient and Methods

This study Conducted within the operating suites in AL Basra Teaching Hospital, Iraq, this comparative controlled trial enrolled subjects assigned an American Society of Anesthesiologists (ASA) physical status of Class I or II. patients scheduled for elective cesarean delivery under spinal anesthesia. Inclusion criteria required a singleton pregnancy without fetal abnormalities or a history of preeclampsia/diabetes, with baseline blood pressure and heart rate determined by the lowest of three seated, automated measurements taken in the 30 minutes prior to the procedure. Before the induction of spinal anesthesia, episodes of nausea and vomiting were assessed using a three-point scale: 0 indicated no symptoms, 1 represented nausea without emesis, and 2 denoted vomiting.

Participants were assigned randomly to one of three vasopressor treatment groups To ensure unbiased assessment, patients and all healthcare personnel involved in perioperative management, including anesthesiologists, nursing staff, and midwives, remained unaware of the assigned treatment. The study interventions consisted of phenylephrine (100 μg/mL), ephedrine (3 mg/mL), or a mixed preparation containing phenylephrine (50 μg/mL) together with ephedrine (1.5 mg/mL).
Immediately before anesthesia, one investigator prepared the study medications in identical syringes that contained either 4 mg of phenylephrine, 120 mg of ephedrine, or a combination of 2 mg of phenylephrine and 60 mg of ephedrine. All syringes were identical in appearance and contained equal total volumes to preserve blinding. They were stored on labeled trays in a room adjacent to the operating theater.

An independent individual who was not involved in patient management or data collection opened the randomization envelope and selected the appropriate unlabeled syringe according to the allocation sequence. The study solution was subsequently diluted with normal saline to a final volume of 40 mL before administration. The attending anesthesiologist was permitted to perform the spinal anesthesia was permitted to select the position with which he or she was most experienced.

This strategy was adopted to maximize clinician familiarity with the procedure and avoid potential variability associated with unfamiliar techniques or patient positioning. To minimize selection bias, randomization was stratified separately for each spinal anesthesia technique. The four approved anesthetic protocols were as follows: (1) intrathecal injection of 2.5 mL hyperbaric 0.5% bupivacaine combined with fentanyl 20 μg in the sitting position; (2) administration of 2 mL 0.5% levobupivacaine with fentanyl 20 μg in the sitting position followed by epidural catheter placement; (3) injection of 2 mL 0.5% levobupivacaine plus fentanyl 20 μg in the left lateral position before epidural catheter insertion; and (4) administration of 2.5 mL 0.5% levobupivacaine with fentanyl 10 μg in the left lateral position before epidural catheter placement.

The extent of sensory blockade was evaluated using ethyl chloride spray to assess loss of cold sensation at 10 minutes after intrathecal injection and again at the time of skin incision. An anesthetic level above the fifth thoracic dermatome (T5) was considered adequate for surgery. If spinal anesthesia failed to provide a sufficiently high or dense sensory block before delivery, supplemental epidural anesthesia with 0.5% levobupivacaine was administered.

Before performing the spinal block, all participants received a rapid intravenous preload of Hartmann's solution at a dose of 10 mL/kg. Immediately after completion of the intrathecal injection, the allocated vasopressor infusion

was commenced intravenously to support maternal blood pressure throughout the procedure. Following spinal anesthesia, patients were repositioned supine with the customary left lateral tilt.

Using the same automated oscillometric device employed for initial readings, systolic blood pressure and pulse rate were recorded at 60-second intervals. The study drug was administered through a Y-connector sharing the same IV line as the Hartmann infusion, which flowed at roughly 4 mL/min post-preload; a non-reflux valve prevented backflow of the study solution into the main fluid pathway. The investigational infusion commenced at 20 mL/hour—equivalent to phenylephrine 33 µg/min, ephedrine 1 mg/min, or a 50% reduced rate for both in the combined arm.

The infusion rate of medications are setting to keep the systolic blood pressure at or near the pre-operative level. The infusion ceiling was 40 mL/hour, with a floor of 1.3 mL/hour. Should the maximum rate prove insufficient, 1–2 mL rescue boluses could be delivered via syringe driver.

If systolic pressure rose to ≥1.25 above baseline, the infusion ceased and resumed at half the prior rate only after pressure fell below that threshold again. If systolic pressure dropped to ≤0.75 above baseline, the rate was doubled plus a 1 mL bolus administered. Failure to sustain systolic pressure above 0.75× baseline despite maximal protocol-driven measures (40 mL/hour plus supplementary 2 mL boluses) prompted turning the patient fully onto her left side.

If that maneuver failed to correct the hypotension, or if it recurred upon returning to the tilted supine position, the treatment assignment was unblinded and the vasopressor regimen modified accordingly. All such cases were evaluated under intention-to-treat principles. The protocol extended until fetal delivery.

Maternal heart rhythm was tracked continuously via pulse oximetry. Glycopyrrolate 200 µg was given intravenously for specified Brady arrhythmias, defined as: heart rate <60 bpm coupled with systolic pressure <0.75 below baseline; heart rate <50 bpm with systolic pressure <1.00 below baseline; or heart rate <45 bpm irrespective of blood pressure. The peak nausea/vomiting score from spinal injection to delivery was documented.

At birth, a study investigator drew blood from both umbilical artery and vein from a doubly clamped cord segment prior to the infant's inaugural breath.

Statistical Analysis

Data analysis was performed using nonparametric statistical methods. Comparisons among the three treatment groups were initially conducted using the **Kruskal–Wallis test**. When an overall statistically significant difference was observed, **pairwise comparisons** were subsequently carried out using the **Mann–Whitney U test**. Changes within each treatment group were evaluated with the **Wilcoxon signed-rank test**, while associations between variables were assessed using the **Spearman rank correlation test**. Statistical significance was established at a **P-value < 0.05**.

In the remaining case (combined group), no umbilical cord blood could be drawn. These four individuals remained in the analysis for all other outcome measures. Baseline characteristics—maternal age, stature, body mass, gestational duration, fetal breech positioning, prior uterine scar from cesarean delivery, and neonatal birth mass—showed no significant intergroup disparities (Table 1).

Infusion protocols were strictly regulated, and all measurements were obtained by a team of tree trained observers (Table 2). The three study arms also demonstrated comparable distributions of neuraxial anesthetic agents administered (P = 0.99), as well as similar volumes of crystalloid and colloid preloading, total infusion fluid quantities, and vasopressor titration requirements (P values not significant). No significant differences were identified among the treatment groups with respect to the duration of data collection by the investigator (P = 0.77) or the interval between uterine incision and fetal delivery (P = 0.10) (Table 2).

The overall maternal systolic arterial pressure recorded from the time of spinal anesthesia until delivery remained comparable across all three study groups (Table 3). Likewise, serial measurements of systolic blood pressure demonstrated similar hemodynamic profiles throughout most of the observation period. Nevertheless, a modest

but statistically significant reduction in systolic arterial pressure was observed in the phenylephrine group between 15 and 20 minutes after spinal anesthesia compared with both the ephedrine and combination groups.

The overall frequency of maternal hypotension, defined as a systolic arterial pressure below 80% of the baseline value, did not differ significantly among the three treatment arms (Table 3). However, significant between-group differences were observed for both the lowest systolic blood pressure achieved during the study (P = 0.04) and the percentage of blood pressure measurements falling below 80% of baseline (P = 0.02). Participants receiving phenylephrine experienced a higher minimum systolic arterial pressure, with a median value of 80% of baseline, compared with those treated with ephedrine, whose median lowest pressure was 73% of baseline (P = 0.02).

The combination group demonstrated an intermediate median minimum systolic pressure of 77%, which was not significantly different from either the phenylephrine (P = 0.14) or ephedrine (P = 0.25) groups. Similarly, the proportion of systolic blood pressure recordings below 80% of baseline was significantly lower in the phenylephrine group, with a median of 0%, than in the ephedrine group, which had a median of 8% (P = 0.007). The combination regimen also resulted in fewer hypotensive readings, with a median of 4% (IQR 0–10), compared with ephedrine alone (P = 0.04).

No statistically significant difference was detected between the phenylephrine and combination groups (P = 0.55). Blinding was discontinued for two participants assigned to the ephedrine group because clinical circumstances required disclosure of their treatment allocation. Two women assigned to the ephedrine group developed severe hypotension, with systolic arterial pressure falling below 75% of their baseline values despite treatment with ephedrine and positioning in the full left lateral tilt. In both cases, the treatment allocation was unblinded to permit appropriate clinical management.

Each patient received a rescue intravenous dose of phenylephrine (100 μg), which promptly restored systolic blood pressure to above 75% of baseline. Following stabilization, adequate blood pressure control was maintained using ephedrine while the patients remained in the left lateral tilt position. Beginning five minutes after spinal anesthesia, maternal heart rate was consistently greater in the ephedrine group than in either the phenylephrine or combination groups.

Across the entire observation period, the combination regimen produced heart rate values that were significantly lower than those observed with ephedrine alone (P = 0.0001) but remained significantly higher than those recorded with phenylephrine (P = 0.008) (Table 3). Peak maternal heart rate also differed significantly among the treatment groups (P = 0.0001). The highest median heart rate was recorded in the ephedrine group, reaching 137% of baseline, compared with 115% in the phenylephrine group (P < 0.0001) and 122% in the combination group (P = 0.004).

No statistically significant difference was identified between the phenylephrine and combination groups (P = 0.051). The frequency of pharmacologic treatment for maternal bradycardia was comparable among the study groups (Table 3). Glycopyrrolate was administered to one participant in the phenylephrine group and one participant in the combination group because their heart rates decreased to below 45 beats per below 50 beats/min while systolic arterial pressure remained below baseline.

In addition, four women in the ephedrine group required glycopyrrolate because their heart rate fell below 60 beats/min in association with severe hypotension, defined as systolic arterial pressure below 75% of baseline. No patients in either the phenylephrine or combination groups required treatment under these conditions. The occurrence of neonatal acidosis was significantly lower in both the phenylephrine group and the combination group compared with the ephedrine group.
Umbilical cord blood gas measurements are summarized in Table 4. No meaningful differences were observed between the phenylephrine and combination groups. In contrast, neonates whose mothers received ephedrine exhibited significantly In contrast, neonates whose mothers received ephedrine exhibited significantly lower umbilical arterial pH than those in the phenylephrine ($P = 0.002$) or combination ($P = 0.009$) groups. Likewise, umbilical venous pH was significantly lower in the ephedrine group than in both the phenylephrine ($P = 0.04$) and combination ($P = 0.003$) groups.

Table1: Maternal and Fetal Demographic Data.

variables	Phenylephrine Group (n =96)	Ephedrine Group (n =100) (%)	Combination Group (n =98) (%)
Age(years)	30 (24–33)	29 (25–30)	31 (22–32)
Height (cm) mean	162	160	160
Weight (kg) mean	76	80	78
Previous cesarean section	44	46	37
Fetal weight (kg) mean	3.50	3.37	3.43

Table 2: Operative Data:

variables		Ephedrine Group (n = 100) (%)	Phenylephrine Group (n = 96) (%)	Combination Group (n = 98) (%)
Spinal technique	Technique1	46%	50%	47%
	Technique2	28%	27%	29%
	Technique3	16%	16%	16%
	Technique4	10%	8%	8%
Investigator	One	48%	31%	47%
	Two	32%	35%	22%
	Three	16%	23%	24%
Block height	at10min	T3(T1–T4)	T3(T2–T5)	T3(T2–T6)
	at skin incision	T2(C8–T3)	T3(T2–T3)	T2(T2–T3)
Spinal-skin incision(min)		17–22		16–22
Spinal-delivery(min)		23–29		22–29
Skin incision-delivery(min)		5–7		5–8
Uterine incision-delivery	1-min	35%	55%	55%
	2-min	48%	32%	34%
	3-min	10%	11%	9%
	4-min	6%	2%	2%

Table 3: Preoperative Maternal Characteristics and Perioperative Cesarean Delivery Data

variables		Phenylephrine Group (n =96)	Ephedrine Group (n= 100)	Combination Group (n 98) (%)	P Value
preoperative Maternal variables	Systolic arterial pressure (mmHg)(mean)	110	110	113	P = 0.63
	Heart rate (beats/min) (mean)	86	82	87	P = 0.73
Perioperative Cesarean Delivery Data :					
Nausea and vomiting	None	75 %	84	73	P = 0.46
	Nausea without vomiting	23%	12	24	
Fetal acidosis		2	21	2	P = 0.0007
1-min APGAR score		8	8	8	P = 0.53
5-min APGAR score		8	8	8	P = 0.35
Mean systolic arterial pressure as proportion of baseline		98 %	100 %	101 %	P = 0.11
Hypotension (systolic arterial pressure <80% of baseline)		48%	68%	57%	P = 0.13
Mean heart rate as proportion of baseline		88	107	96	P = 0.0001
Mean infusion rate (ml/min)		0.34	0.51	0.35	P 0.01

Consequently, the arteriovenous (A–V) PCO_2 gradient across the umbilical circulation was significantly greater in the ephedrine group than in the phenylephrine group (P = 0.002). Detailed blood gas data for neonates with acidemia are presented in Table 5. Among infants in the ephedrine group, the acid-base disturbance demonstrated features of both metabolic and respiratory acidosis.

Furthermore, two approximately 77% greater in those with acidemia than in those without acidemia, measuring 23 mmHg versus 13 mmHg, respectively (P < 0.0001). Moreover, increasing maternal exposure to ephedrine was strongly associated with progressively larger umbilical A–V PCO_2 differences. In contrast, neither the average

maternal systolic arterial pressure (nor the lowest systolic arterial pressure recorded during surgery showed a significant correlation with the A–V PCO_2 gradient.

Within the phenylephrine group, no significant associations were identified between the umbilical A–V PCO_2 difference and the administered phenylephrine dose, mean maternal systolic arterial pressure, or the minimum systolic arterial pressure recorded during the procedure. At baseline, the three study groups exhibited comparable scores for nausea and vomiting as shown in Table 3. Over the course of the trial, the phenylephrine cohort showed no significant shift in these scores from their starting point (P = 0.30).

In contrast, both the ephedrine group (P < 0.0001) and the combined-treatment group (P = 0.007) experienced significant rises in their nausea and vomiting ratings relative to baseline. When comparing post-baseline scores, the phenylephrine arm recorded substantially lower nausea and vomiting ratings than either the ephedrine-alone arm (P < 0.0001) or the combination arm (P < 0.0001). No meaningful distinction emerged, however, between the ephedrine and combination groups on this measure (P = 0.09).

Within the ephedrine subset, episodes of vomiting correlated with three key factors: a drop in systolic blood pressure, a reduction in heart rate, and a larger cumulative ephedrine dosage. Among ephedrine-treated participants who experienced vomiting (n = 18) versus those who reported no nausea or vomiting (n = 17), the lowest observed systolic pressures were 62% and 87% of initial values, respectively (P = 0.0002). Corresponding minimum heart rates were 71% and 92% of baseline (P = 0.0006).

The average ephedrine infusion rates also differed markedly: 1.8 mg/min for those who vomited versus 0.9 mg/min (0.5–1.4) for those without symptoms (P = 0.002). Notably, sensory block levels measured at 10 minutes post-injection and at the time of surgical incision did not differ significantly between these two ephedrine subgroups (P = 0.57 and P = 0.36, respectively). After removing from the analysis those ephedrine-group patients who exhibited the most profound hypotension—defined as a nadir systolic pressure at or below 60% of baseline—the average systolic arterial pressure, as well as the frequency, seriousness, and length of hypotensive episodes, became statistically indistinguishable across all three treatment arms.

Nevertheless, even with this exclusion, the ephedrine group continued to show the greatest rate of fetal acidemia, while the phenylephrine group maintained the lowest nausea and vomiting scores.

Table 4: Intergroup fetal blood gas value

variables	Ephedrine Group (n =96) mean	Phenylephrine Group (n =96) mean	Combination Group (n= 94) mean	P Value
Arterial pH	7.31 (7.29–7.33)	7.34 (7.23–7.31)	7.31 (7.28–7.32)	P = 0.004
Venous pH	7.39 (7.35–7.38)	7.36 (7.32–7.37)	7.37 (7.35–7.39)	P = 0.009
Arterial –venous pH difference	0.11 (9–13)	0.06 (0.05–0.07)	0.07 (0.05–0.08)	P = 0.003
Arterial partial oxygen pressure (mmHg)	15 (9–17)	13 (10–15)	12 (8–15)	P= 0.17
Arterial partial pressure of CO2 (mmHg)	52 (48–56)	55 (50–64)	54 (50–58)	P = 0.12
Venous partial pressure of CO2 (mmHg)	45 (37–50)	43 (38–44)	41 (37–43)	P 0.17

Discussion

The present investigation demonstrated that the use of phenylephrine, either as the sole vasopressor or in combination with ephedrine, significantly decreased the occurrence of fetal acidemia during cesarean delivery performed under spinal anesthesia compared with ephedrine alone. Fetal acidemia was identified in only 2 of 96 neonates in the phenylephrine group and 2 of 94 neonates in the combination group, whereas 20 of 96 neonates in the ephedrine group developed acidemia. Analysis of umbilical cord blood gases indicated that the acid-base disturbance in affected neonates consisted of both metabolic and respiratory components.
Moreover, two infants exposed to ephedrine exhibited severe metabolic acidosis, with base deficits exceeding 10 mmol/L. Several mechanisms may explain the higher incidence of fetal acidemia observed with ephedrine monotherapy. These include impaired uteroplacental perfusion resulting from maternal hypotension, decreased uteroplacental blood flow caused by ephedrine-induced vasoconstriction of the uterine circulation, or a direct pharmacologic effect of ephedrine on the fetus.

Although uteroplacental blood flow and vascular resistance were not measured directly, several observations suggest that reduced uteroplacental perfusion was unlikely to be the principal explanation for the poorer fetal acid-base status in the ephedrine group. Maternal systolic arterial pressure remained well maintained and was generally comparable among all three treatment groups throughout the study period. Although women receiving ephedrine experienced a slightly greater degree and duration of hypotension, additional analyses excluding patients with severe hypotensive episodes showed no significant differences in either the frequency, magnitude, or duration of hypotension between the study groups.

Despite this adjustment, the incidence of fetal acidemia remained substantially higher among neonates whose mothers received ephedrine. These findings indicate that reduced uterine perfusion pressure secondary to maternal hypotension is unlikely to account for the increased fetal acidosis associated with ephedrine administration. Similarly, ephedrine-induced constriction of the uteroplacental vasculature does not appear to be the primary mechanism responsible for these findings.
Experimental studies conducted in pregnant female have demonstrated that ephedrine produces considerably weaker vasoconstriction of the uterine arteries than pure α-adrenergic agonists, suggesting that its effect on uteroplacental vascular resistance is relatively limited [1]. A recent investigation comparing metaraminol, a receptor-activating agent, with ephedrine during spinal blockade for non-emergent cesarean delivery observed no variation in uterine arterial circulation as measured by sonographic imaging [11]. Moreover, if placental exchange had been compromised enough to produce fetal metabolic imbalance, a drop in oxygen tension within the umbilical vein would likely have occurred due to diminished oxygen transfer to the fetoplacental unit.

Yet, in the subset receiving ephedrine, no correlation emerged between neonatal acidotic status (as reflected by declining arterial pH in the umbilical cord) and the oxygen content of the umbilical venous blood. Examining carbon dioxide gradients between the umbilical artery and vein offers circumstantial clues that a fetal response may explain the heightened acidosis seen with ephedrine. Prior work demonstrated that severe hypo perfusion of the uteroplacental bed—resulting from placental abruption and leading to profound neonatal acidity did not coincide with an elevated arteriovenous CO_2 gap (In contrast, our data revealed a robust link between acidemia and a widening of this gradient: for ephedrine-exposed newborns without acidosis (umbilical arterial pH $\geq$7.20), the median CO_2 difference was 13 mmHg, whereas those with acidosis (pH <7.20) exhibited a median of 23 mmHg, a highly significant disparity ($P < 0.0001$).

One potential fetal pathway for this acidotic state involves constriction of umbilical vessels triggered by β-adrenergic receptor activation. Diminished flow through these vessels can indeed produce acidosis accompanied by an enlarged arteriovenous CO_2 gap: severe fetal acidemia from cord compression was previously tied to a substantial CO_2 gradient Nevertheless, this mechanism seems improbable as the primary driver in our ephedrine findings. Ephedrine possesses weaker β-adrenergic properties than phenylephrine; β-adrenergic stimulation actually enhances umbilical circulatory flow, [12] and both presser drugs have demonstrated only negligible effects on the umbilical arterial resistance index [13].

A direct stimulatory effect of ephedrine on the fetal adrenergic system represents another plausible explanation for the development of fetal acidemia that is independent of alterations in uteroplacental or fetoplacental blood flow. Experimental investigations in fetal lambs have shown that administration of the β-adrenergic agonist isoproterenol results in an immediate rise in fetal oxygen consumption accompanied by increased glucose utilization and elevated lactate concentrations [12]. These findings led investigators to propose that β-adrenergic activation enhances anaerobic glycolysis because fetal oxygen delivery is already operating close to its physiological maximum.

Evidence from human studies also indicates that maternal administration of ephedrine exerts measurable pharmacological effects on the fetus. Previous investigations have demonstrated increases in both fetal heart rate and circulating fetal catecholamine concentrations following maternal ephedrine administration [14]. Furthermore, prolonged maternal exposure to a β_2-adrenergic agonist for approximately two hours before elective cesarean delivery has been associated with the development of fetal metabolic acidemia [15]. In the present study, umbilical venous PCO_2 values did not differ significantly between the ephedrine and phenylephrine groups.

In contrast, umbilical arterial PCO_2 was significantly higher among neonates exposed to ephedrine. Assuming that umbilical blood flow was not reduced in the ephedrine group, this finding suggests greater fetal carbon dioxide production, indicating an increase in fetal metabolic activity. Additional support for this hypothesis was provided

by the observation that the umbilical arteriovenous (A–V) PCO_2 gradient was approximately 77% greater in acidotic fetuses than in non-acidotic fetuses within the ephedrine group.

This larger PCO_2 difference is consistent with a higher fetal metabolic rate in the acidotic subgroup. Collectively, these observations suggest that stimulation of fetal β-adrenergic receptors by ephedrine, leading to increased fetal metabolism, is the most likely mechanism responsible for the higher incidence of fetal acidemia associated with ephedrine administration. Incorporating phenylephrine into the vasopressor regimen reduced the required ephedrine dose by approximately two-thirds, which likely accounts for the markedly lower incidence of fetal acidemia observed in the combination treatment group.

The findings of the present study are consistent with those reported in two more recent clinical investigations. Both studies demonstrated that vasopressor regimens possessing greater α-adrenergic activity than ephedrine were associated with improved fetal acid-base status during cesarean delivery. One trial compared metaraminol with ephedrine [11], whereas the other evaluated a combined phenylephrine–ephedrine regimen against ephedrine alone [16].

In the comparison between metaraminol and ephedrine, neonates exposed to ephedrine exhibited a higher incidence of acidemia despite similar rates of maternal hypotension in the two groups [11]. Additional studies have likewise shown that prophylactic administration of ephedrine during epidural or spinal anesthesia may increase the risk of fetal acidemia even while effectively reducing maternal hypotension [7]. Nevertheless, these findings should not be interpreted as definitive evidence that α-adrenergic agonists are universally superior to ephedrine with respect to overall neonatal well-being.

Current evidence indicates that Apgar scores remain more reliable indicators of neonatal clinical outcome than umbilical arterial pH measurements alone [17]. All infants achieved satisfactory Apgar scores at birth, and none required endotracheal intubation, mechanical ventilator support, or admission to the neonatal special care unit during the immediate postnatal period. These findings indicate that, despite the observed differences in umbilical cord blood gas values, no clinically significant compromise in early neonatal adaptation was evident.

Interestingly, activation of the fetal adrenergic system before delivery may confer certain physiological advantages. Previous research has demonstrated that maternal administration of a β_2-adrenergic agonist before elective cesarean section improves neonatal pulmonary function by increasing dynamic lung compliance, reducing airway resistance and respiratory rate, and lowering the incidence of neonatal hypoglycemia [15]. Consequently, additional investigations are warranted to clarify the potential cardiovascular, respiratory, and metabolic consequences of maternal exposure to phenylephrine, ephedrine, or their combination during cesarean delivery.

Although no adverse neonatal effects were identified in this cohort of low-risk pregnancies, caution should be exercised when extrapolating these findings to pregnancies complicated by pre-existing fetal compromise. Fetuses with impaired physiological reserve may be less capable of tolerating the reduction in acid-base status associated with ephedrine administration. Therefore, in subsequent research must focus on the high-risk obstetric populations and measure neonatal consequences of phenylephrine and ephedrine regarding fetal hypoxia and acidemia.

Maternal nausea and vomiting remain common and clinically important adverse effects during cesarean delivery performed under spinal anesthesia. Despite achieving comparable control of maternal systolic arterial pressure across all treatment groups, the incidence of these symptoms differed substantially according to the vasopressor administered. Women receiving phenylephrine alone experienced no significant increase in nausea or vomiting compared with pre-anesthetic baseline values, even though episodes of hypotension still occurred.

In contrast, patients treated with ephedrine, either alone or in combination with phenylephrine, demonstrated a marked increase in both nausea and vomiting during the intraoperative period. Notably, the higher incidence of gastrointestinal symptoms observed in the combination group compared with the phenylephrine group occurred despite equivalent maintenance of maternal blood pressure. Likewise, when patients with the most pronounced hypotensive episodes were excluded from the ephedrine group, thereby eliminating the minor differences in hypotension between treatment groups, the increased frequency of nausea and vomiting associated with ephedrine remained unchanged.

These observations suggest that variations in maternal blood pressure alone cannot adequately explain the differing incidences of these adverse effects. Although a direct emetogenic action of ephedrine might be considered, this explanation appears unlikely because previous studies have reported antiemetic effects of ephedrine following gynecological surgery [18]. An alternative mechanism involves enhanced parasympathetic (vagal) activity during spinal anesthesia.

Earlier investigations have demonstrated that atropine provides greater relief of spinal anesthesia-induced nausea than vasopressor therapy alone, supporting the contribution of vagal stimulation to this symptom [19]. Furthermore, prophylactic administration of glycopyrrolate has been shown to reduce the occurrence of nausea during cesarean delivery under spinal anesthesia [20]. The findings of the present study further support this hypothesis.

Among women receiving ephedrine, episodes of vomiting were accompanied not only by reductions in systolic arterial pressure but also by decreases in heart rate. The simultaneous occurrence of hypotension and bradycardia is consistent with increased vagal activity, suggesting that enhanced parasympathetic tone may have contributed to the higher incidence of nausea and vomiting observed in patients treated with ephedrine. Despite the observed differences in maternal gastrointestinal symptoms, there was no evidence to suggest that these variations were attributable to differences in the extent or height of the spinal sensory block.

An alternative explanation may involve activation of a cardio inhibitory vagal reflex triggered by a reduction in cardiac preload [21]. Such reflex-mediated parasympathetic activation has been reported to occur more readily in the presence of concurrent β-adrenergic stimulation [21]. During spinal anesthesia for cesarean delivery, venous return is substantially reduced because of sympathetic blockade-induced vasodilation in combination with aortocaval compression by the gravid uterus.

Under these conditions, phenylephrine may provide a physiological advantage by producing greater vasoconstriction, thereby improving venous return and maintaining cardiac preload. In addition, the absence of significant β-adrenergic stimulation with phenylephrine may reduce the likelihood of excessive vagal activation. This mechanism may explain why phenylephrine was associated with a markedly lower incidence of maternal nausea and vomiting despite achieving blood pressure control comparable to that of the other vasopressor regimens.

All three study medications successfully maintained maternal systolic arterial pressure close to baseline values throughout the intraoperative period. Nevertheless, two participants receiving ephedrine developed persistent hypotension that failed to respond adequately to continued ephedrine administration combined with full left lateral uterine displacement. In these cases, treatment allocation was unblinded to permit rescue therapy, and administration of a single intravenous dose of phenylephrine (100 μg) promptly restored arterial pressure, allowing subsequent hemodynamic stability to be maintained with the ongoing ephedrine infusion.

These observations support the clinical usefulness of phenylephrine as an effective rescue vasopressor for hypotension that is refractory to ephedrine treatment. Significant differences in maternal heart rate were also observed among the treatment groups. Phenylephrine administration resulted in the lowest heart rate values, whereas ephedrine produced the greatest increase in maternal heart rate, reflecting their distinct pharmacodynamics profiles.

Despite these differences, the frequency of clinically significant bradycardia requiring glycopyrrolate administration did not differ among the three groups, indicating that the lower heart rate associated with phenylephrine rarely necessitated pharmacological intervention. Overall, the findings of this study indicate that continuous phenylephrine infusion is superior to ephedrine infusion for maintaining maternal hemodynamic stability during spinal anesthesia for elective cesarean delivery. In addition to providing effective blood pressure control, phenylephrine significantly reduced the incidence of fetal acidemia and maternal nausea and vomiting compared with ephedrine alone.

Although the combined administration of phenylephrine and ephedrine also lowered the incidence of fetal acidemia relative to ephedrine monotherapy, it failed to provide any additional improvement in neonatal acid–base status beyond that achieved with phenylephrine alone. Furthermore, the combination regimen was associated with a higher frequency of maternal nausea and vomiting. These findings suggest that phenylephrine alone

represents the most appropriate first-line vasopressor for the prevention and management of spinal anesthesia-induced hypotension during elective cesarean delivery.

References

[1] I. Caritis SN, Abouleish E, Edelstone DI, Mueller-Heubach E: Fetal acid-base state following spinal or epidural anesthesia for cesarean section. Obstet Gynecol 1980; 56:610–
[2] Ratcliffe FM, Evans JM: Neonatal wellbeing after elective caesarean delivery with general, spinal, and epidural anaesthesia. Eur J Anaesth 1993; 10:175–81.
[3] Roberts SW, Leveno KJ, Sidawi JE, Lucas MJ, Kelly MA: Fetal acidemia associated with regional anesthesia for elective cesarean delivery. Obstet Gy necol 1995; 85:79–83.
[4] Mueller MD, Bruhwiler H, Schupfer GK, Luscher KP: Higher rate of fetal acidemia after regional anesthesia for elective cesarean delivery. Obstet Gynecol 1997; 90:131–4.
[5] Burns SM, Cowan CM, Wilkes RG: Prevention and management of hypo tension during spinal anaesthesia for elective Caesarean section: A survey of practice. Anaesth 2001; 56:794–8.
[6] James FM III, Greiss FC Jr, Kemp RA: An evaluation of vasopressor therapy for maternal hypotension during spinal anesthesia. ANESTHESIOLOGY 1970; 33: 25–34.
[7] Rolbin SH, Cole AF, Hew EM, Pollard A, Virgint S: Prophylactic intramuscular ephedrine before epidural anaesthesia for caesarean section: Efficacy and actions on the fetus and newborn. Can Anaesth Soc J 1982; 29:148–53.
[8] Morgan D, Philip J, Sharma S, Gottumukkala V, Perez B, Wiley J: A neonatal outcome with ephedrine infusions with or without preloading during spinal anaesthesia for Cesarean section (abstract). ANESTHESIOLOGY 2000; (suppl April):A5.
[9] Lee A, Ngan Kee WD, Gin T: A quantitative, systematic review of randomized controlled trials of ephedrine versus phenylephrine for the management of hypotension during spinal anesthesia for cesarean delivery. Anesth Analg 2002; 94:920–926.
[10] Carpenter MR, Cooper DW: Fetal acidosis, spinal anaesthesia and phenylephrine (letter). Anaesthesia 2001; 56:920–1.
[11] Ngan Kee WD, LauTK, KhawKS, LeeBB: Comparison of metaraminol and ephedrine infusions for maintaining arterial pressure during spinal anesthesia for elective cesarean section. ANESTHESIOLOGY 2001; 95:307–13.
[12] Gournay VA, Roman C, Rudolph AM: Effect of beta-adrenergic stimulation on oxygen metabolism in the fetal lamb. Pediatr Res 1999; 45:432–6.
[13] Thomas DG, Robson SC, Redfern N, Hughes D, Boys RJ: Randomized trial of bolus phenylephrine or ephedrine for maintenance of arterial pressure during spinal anaesthesia for Caesarean section. Br J Anaesth 1996; 76:61–5.
[14] Wright RG, Shnider SM, Levinson G, Rolbin SH, Parer JT: The effect of maternal administration of ephedrine on fetal heart rate and variability. Obstet Gynecol 1981; 57:734–8.
[15] Eisler G, Hertzberg R, Lagercrantz H: Randomized controlled trial of effect of terbutaline before elective caesarean section on postnatal respiration and glucose homeostasis. Arch Dis Child Fetal Neonatal Ed 1999; 80:88–92.
[16] Mercier FJ, Riley ET, Frederickson WL, Roger-Christoph S, Benhamou D, Cohen SE: Phenylephrine added to prophylactic ephedrine infusion during spinal anesthesia for elective cesarean section. ANESTHESIOLOGY 2001; 95:668–74.
[17] Casey BM, McIntire DD, Leveno KJ: The continuing value of the APGAR score for the assessment of newborn infants. N Engle J Med 2001; 344:467–71 .
[18] Hageman E, Halverson A, Holgersen O, Tweit T, Raeder JC: Intramuscular ephedrine reduces emesis during the first three hours after abdominal hysterectomy. Act a Anesthesia l Scan 2000; 44:107–11
[19] Ward RJ, Kennedy WF, Bonica JJ, Martin WE, Tolas AG, Akamatsu T: Experimental evaluation of atropine and vasopressors for the treatment of hypo tension of high subarachnoid anesthesia. Anesth Analg 1966; 45:621–629.
[20] Mark AL: The Bezold-Jarisch reflex revisited: clinical implications of inhibitory reflexes originating in the heart. J Am Coll Cardio 1983; 1:90–102
[21] Liguria GA, Kahn RL, Gordon J, Gordon MA, Urban MK: The use of metoprolol and glycopyrrolate to prevent hypotensive/bradycardic events during shoulder arthroscopy in the sitting position under interscalene block. Anesth Analg 1998; 87:1320–5.

NIU Journal of Health Sciences Copyright©2026
Nexus International University ISSN: 3136-6449; 12(1) 87-96

High Lenticular Myopic and Astigmatic Shift in Grade 3 Nuclear Sclerosis Cataract: A Case Report

HAYDER HUSSEIN AL- AWADI
Ministry of Health, Iraq
hayderhussein333@gmail.com

Abstract.

Background: Nuclear sclerosis cataract is a well-known cause of lenticular (index) myopia; however, the degree of refractive change is usually mild to moderate. Extreme myopic shift accompanied by significant astigmatism is uncommon and may lead to diagnostic confusion.
Case Presentation: We report a case of a 61-year-old patient presenting with marked myopic and astigmatic shift (−7.00 D sphere with −3.00 D cylinder at 80°) associated with grade 3 nuclear sclerosis cataract. Ocular biometry demonstrated normal axial length and corneal curvature, excluding axial or corneal causes of myopia. The refractive changes were attributed to lenticular alterations induced by nuclear sclerosis.
Conclusion: This case highlights an unusual magnitude of lenticular myopic and astigmatic shift caused by nuclear sclerosis cataract. Awareness of this phenomenon is essential to avoid misdiagnosis and refractive surprise, and to emphasize the importance of comprehensive biometry in patients with unexpected refractive changes.

Keywords: Nuclear sclerosis, lenticular myopia, myopic shift, astigmatism, cataract.

1. Introduction

Nuclear sclerosis cataract is commonly associated with a progressive myopic shift due to an increase in the refractive index of the crystalline lens, a phenomenon known as index myopia [1, 2]. In most cases, the induced refractive change is limited to a few diopters. Marked myopic shift, particularly when accompanied by significant astigmatism, is rarely reported and may mimic axial or corneal pathology [2,3]. We report a case of extreme lenticular myopic and astigmatic shift associated with grade 3 nuclear sclerosis cataract.

Case Presentation

A 61-year-old patient presented with progressive deterioration of vision and frequent changes in spectacle prescription. There was no history of previous refractive surgery, corneal disease, or ocular trauma. On examination, Best-Corrected Visual Acuity (BCVA) was reduced, and manifest refraction revealed a marked myopic and astigmatic shift of **−7.00 diopters sphere with −3.00 diopters cylinder at 80 degrees**. Slit-lamp examination showed **grade 3 nuclear sclerosis cataract**, with no other significant anterior segment abnormalities. Fundus examination was unremarkable.

Table 1: Summary of clinical evaluation, keratometry, and ocular biometry findings.

Parameter	OD	OS
UCVA	6/6 P	CF 1M
BCVA	6/6	NO CORRECTION
REFRACTION	+1.50DS/-1.0DC *87	-7.0 DS/ -3.0 DC*85
IOP (mmHg)	17	17
Axial length (mm)	23.14	23.10
K1 (D)	42.90 @26	43.16 @ 138
K2 (D)	43.36 @116	43.77 @ 48
ACD (mm)	3.16	3.42
Lens thickness (mm)	4.29	3.95
Cataract grade	NS1	NS3, PSC

Optical biometry (IOLMaster / EyeSuite, Haag-Streit) demonstrated **a normal axial length of approximately 23.1 mm** in both eyes, with **corneal keratometry values around 43.0 D**, indicating the absence of axial or corneal causes for the high myopia. Anterior chamber depth and lens thickness were within normal limits for age.

Based on clinical findings and biometry, a diagnosis of **severe lenticular myopia and astigmatism induced by nuclear sclerosis cataract** was established. The patient was counseled regarding the refractive nature of the cataract and the expected refractive outcome following cataract extraction.

Surgical Management

Under peribulbar anesthesia, phacoemulsification was done for the left eye, IOL (SA60AT) power of (23.0 D) was implanted in the posterior chamber according to SRK/T formula and the operation was uneventful.

Post-operative outcome

Table 2: Visual acuity and refractive outcomes over time following phacoemulsification and IOL implantation.

Follow-up	BCVA	Refraction
Preoperative	CF 1M	-7.0 DS/ -3.0 DC*85
1 week	6/9	+1.25 DS/ - 2.0 DC * 107
1 month	6/6	+1.0 DS / - 1.75 DC *104

Discussion

myopic shift associated with nuclear sclerosis cataract is a well-documented phenomenon resulting from increased lens nuclear density and refractive index. Most reported cases describe mild to moderate myopia, typically ranging from −1.00 to −3.00 diopters. The degree of myopic shift observed in this case is exceptional.

The presence of significant astigmatism further supports the lenticular origin of the refractive error, likely due to asymmetric nuclear sclerosis and changes in lens curvature. Normal axial length and keratometry values effectively excluded axial myopia and corneal astigmatism, reinforcing the diagnosis of lenticular-induced refractive change.

This case underscores the importance of comprehensive ocular biometry in patients presenting with unexpected refractive progression, as misattribution to axial elongation or corneal pathology may lead to unnecessary investigations or inappropriate management.

Conclusion

Grade 3 nuclear sclerosis cataract can rarely induce high myopic and astigmatic shift.

Recognition of lenticular causes of refractive change is essential for accurate diagnosis, patient counseling, and surgical planning. Cataract extraction remains the definitive treatment for restoring refractive stability in such cases.

Patient Consent

Written informed consent was obtained from the patient for publication of this case report and accompanying images.

Conflict of Interest

The author declares no conflict of interest.

Funding
No funding was received for this study.

References

1. Duke-Elder S. *System of Ophthalmology*. London: Henry Kimpton; 1970.
2. Brown NA, Hillman JS. Cataract and changes in refraction. *Br J Ophthalmol*. 1987; 71:10-13.
3. Pesudovs K, Elliott DB. Refractive changes in nuclear cataract. *Ophthalmic Physiol Opt*. 2003; 23:22-30.

Figures

Figure 1: slit lamp photograph showing cataract.
Figure 2: preoperative refraction
Figure 3: biometry demonstrating axial length.
Figure 4: postoperative slit-lamp photograph 1 week.
Figure 5: postoperative refraction 1 week.
Figure 6: postoperative slit-lamp photograph 1 month.
Figure 7: postoperative refraction 1 month.

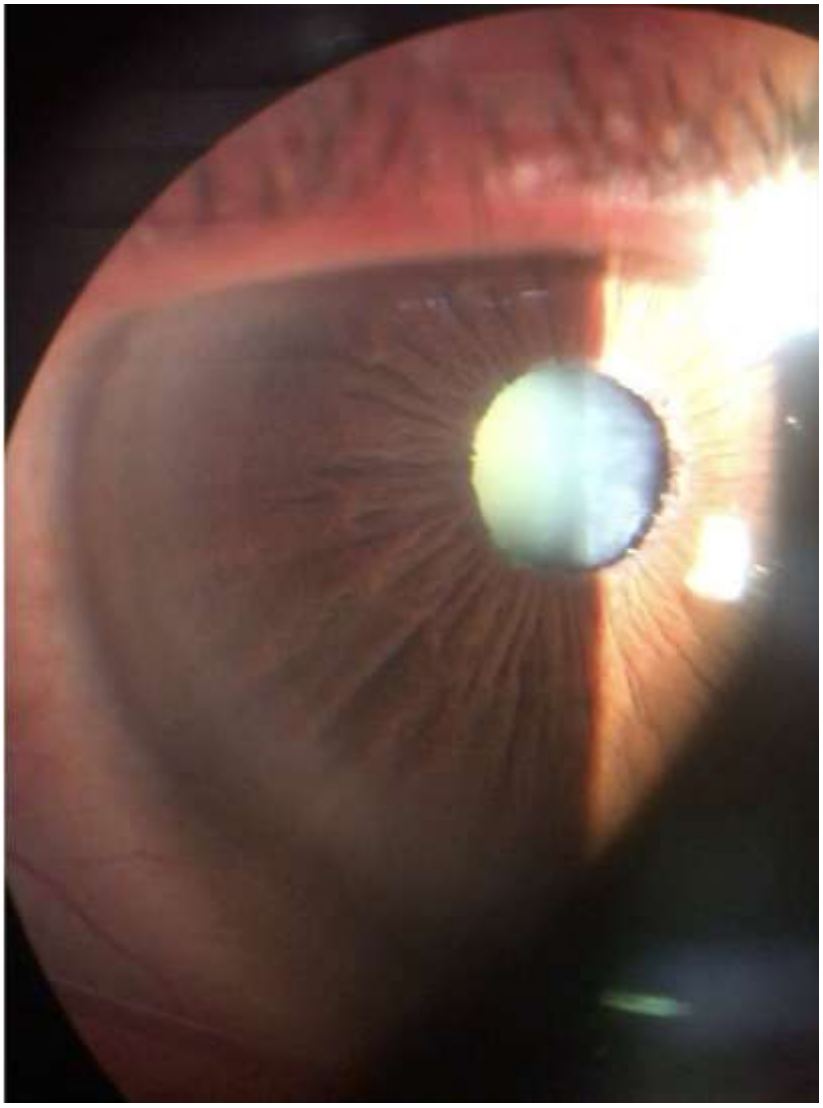

Figure 1: slit lamp photograph showing cataract.

Figure 2: preoperative refraction

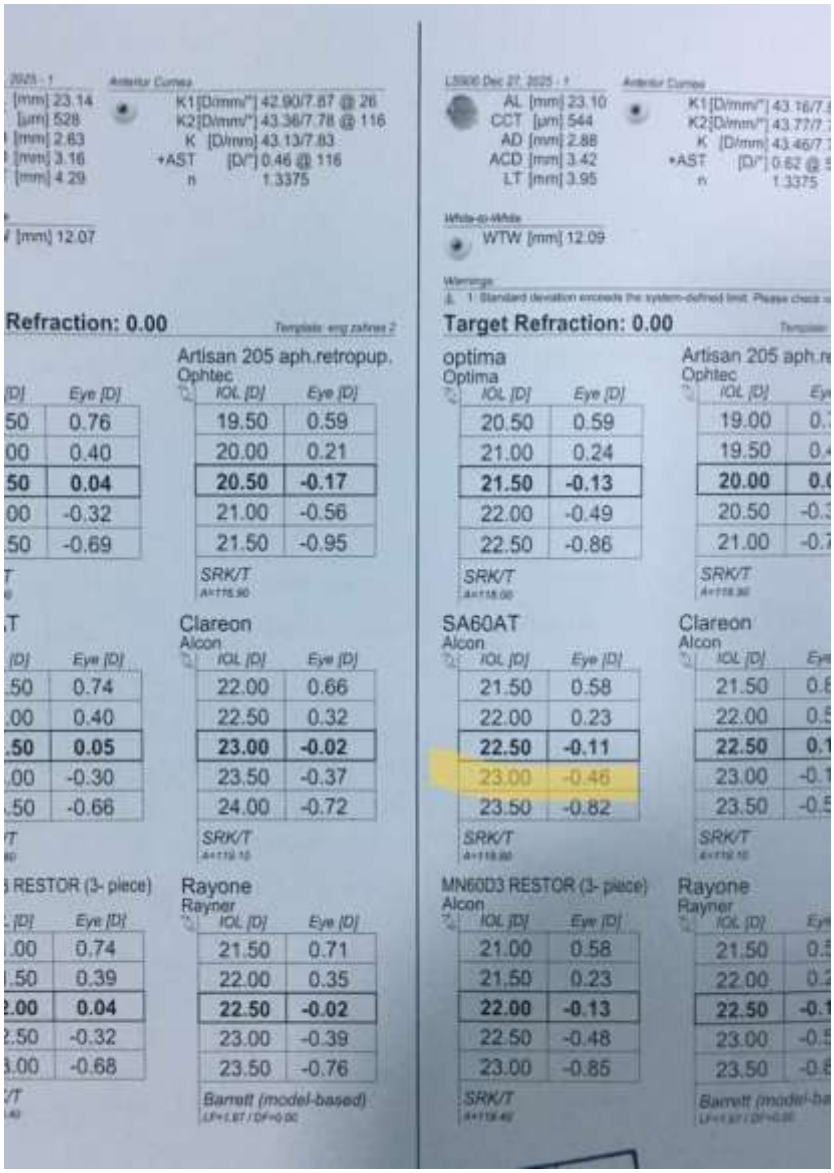

Figure 3: biometry demonstrating axial length.

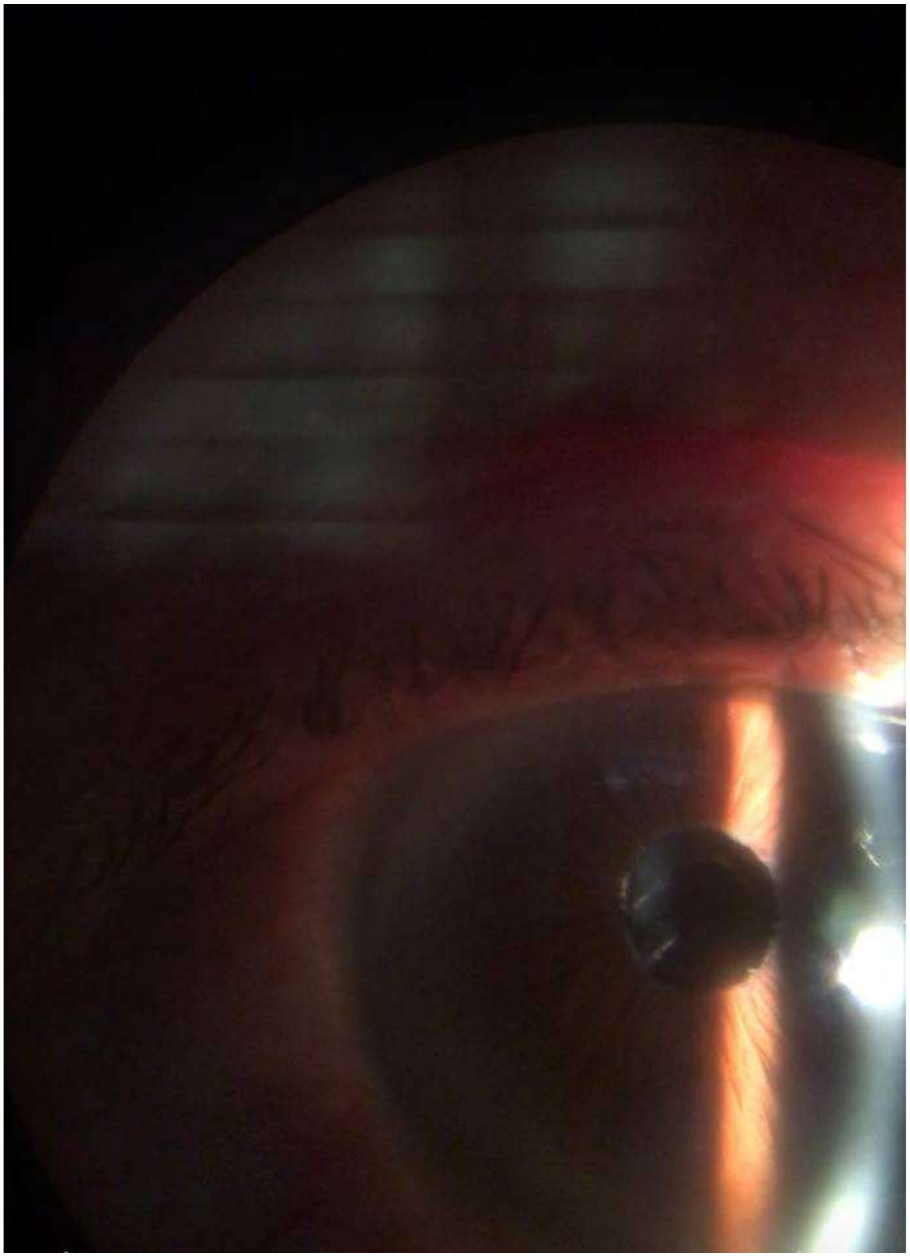

Figure 4: postoperative slit-lamp photograph 1 week.

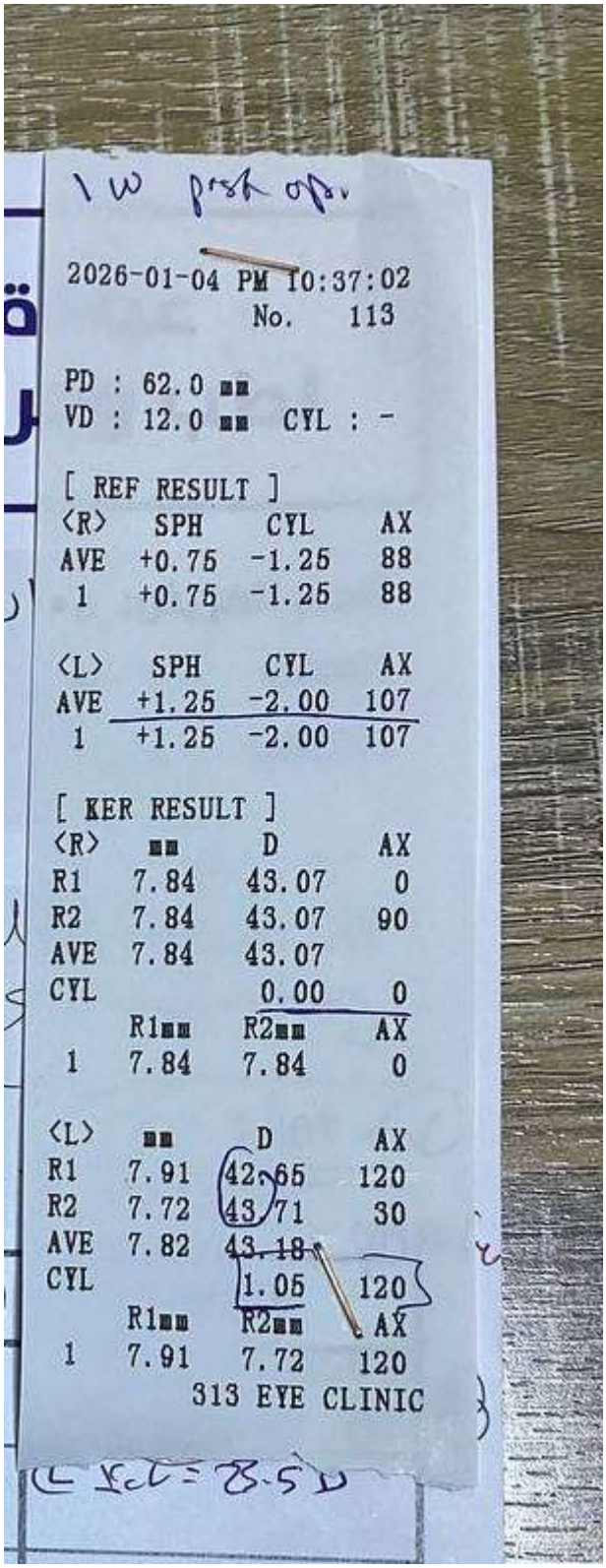

2026-01-04 PM 10:37:02
No. 113

PD : 62.0 ■■
VD : 12.0 ■■ CYL : -

[REF RESULT]

<R>	SPH	CYL	AX
AVE	+0.75	-1.25	88
1	+0.75	-1.25	88

<L>	SPH	CYL	AX
AVE	+1.25	-2.00	107
1	+1.25	-2.00	107

[KER RESULT]

<R>	■■	D	AX
R1	7.84	43.07	0
R2	7.84	43.07	90
AVE	7.84	43.07	
CYL		0.00	0

	R1■■	R2■■	AX
1	7.84	7.84	0

<L>	■■	D	AX
R1	7.91	42.65	120
R2	7.72	43.71	30
AVE	7.82	43.18	
CYL		1.05	120

	R1■■	R2■■	AX
1	7.91	7.72	120

313 EYE CLINIC

Figure 5: postoperative refraction 1 week.

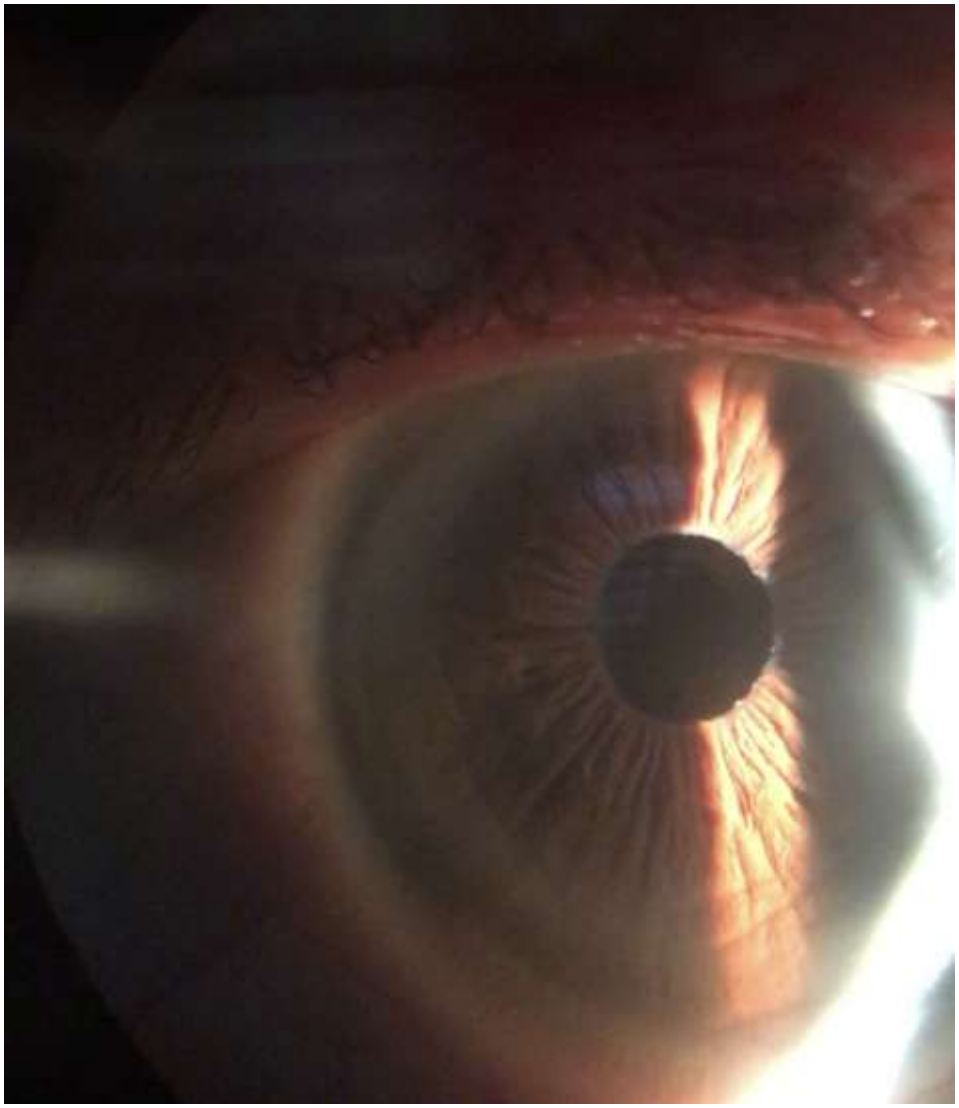

Figure 6: postoperative slit-lamp photograph 1 month.

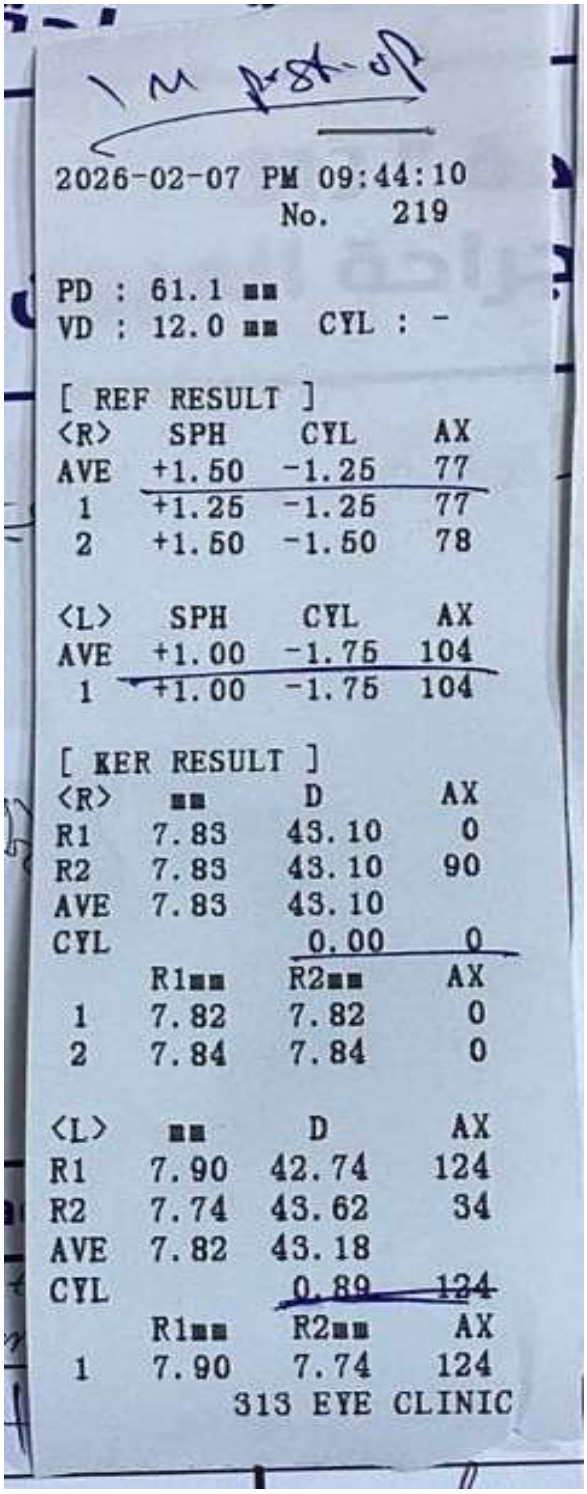

2026-02-07 PM 09:44:10
No. 219

PD : 61.1 ■■
VD : 12.0 ■■ CYL : -

[REF RESULT]

<R>	SPH	CYL	AX
AVE	+1.50	-1.25	77
1	+1.25	-1.25	77
2	+1.50	-1.50	78

<L>	SPH	CYL	AX
AVE	+1.00	-1.75	104
1	+1.00	-1.75	104

[KER RESULT]

<R>	■■	D	AX
R1	7.83	43.10	0
R2	7.83	43.10	90
AVE	7.83	43.10	
CYL		0.00	0

	R1■■	R2■■	AX
1	7.82	7.82	0
2	7.84	7.84	0

<L>	■■	D	AX
R1	7.90	42.74	124
R2	7.74	43.62	34
AVE	7.82	43.18	
CYL		0.89	124

	R1■■	R2■■	AX
1	7.90	7.74	124

313 EYE CLINIC

Figure 7: postoperative refraction 1 month.

NIU Journal of Health Sciences Copyright©2026
Nexus International University ISSN: 3136-6449; 12(1) 97-100

Evaluation of Salvadora Persica Extract on Gram Positive and Negative Bacteria Isolation from Chronic Wounds

LUBAB MOHAMMED AWAD
General Directorate of Anbar Education, Ministry of Education, Iraq
lubabmo373@gmail.com

Abstract

Background: Because of the severity of this bacteria and the deaths it causes due to its severity and resistance to many antibiotics, we searched for alternatives to plant extracts, such as the miswak, as an inhibitory factor for it, given the effective compounds it contains.
Methodology: A large collection of miswak sticks was collected.(1) The sticks were dried in an oven at 45°C for four days and then cut into discs or ground into a fine powder using a grinder.(3) Miswak extracts were prepared by adding 40 g of miswak powder to 200 ml of solvent (water, ethanol) in a sealed vessel and then soaking at room temperature for 48 h. (4)The solvents were filtered using Whatman No. 1 filter paper and left to evaporate in an oven at 40°C for 48 h. The dried extracts were considered 100% pure and were used to prepare different concentrations using the same solvents (40, 80, and 160 µg/ml).
Results: The results show a concentration-dependent antibacterial effect of aqueous Miswak extract against *S. aureus* and *P. aeruginosa*. As the concentration increased from 40 to 160 µg/ml, the inhibition zones significantly expanded for both bacteria, indicating enhanced antibacterial activity. For *S. aureus*, the zone increased from 9 mm to 17 mm, and for *P. aeruginosa*, from 7 mm to 13 mm, with all p-values < 0.05 compared to the reference concentration (40 µg/ml), confirming statistical significance. The positive control (Amikacin 100 µg/ml) produced larger zones (22 mm and 25 mm respectively), but the extract at 160 µg/ml still showed notable inhibition, especially against *S. aureus*, suggesting that the aqueous extract contains active compounds with effective antibacterial properties. The stronger response against *S. aureus* than *P. aeruginosa* may be due to structural differences in bacterial cell walls, where the Gram-positive nature of *S. aureus* makes it more susceptible to plant-derived antimicrobials.

Keywords: Salvadora persica Extract, gram positive and negative, Chronic Wounds

1. Introduction

The arak tree, or toothpick, Salvadora persica, is an evergreen tree or large shrub, ranging in height from 2–7 meters, and belongs to the Salvadoraceae family.(1) Its trunk is short with a dense crown of branched branches.(2) Its leaves are small (3–5 cm long), oval, thick, leathery, and light green in color.(3) Its flowers are small (3–5 mm in diameter), greenish-white or yellowish in color, and gathered in terminal clusters.(4) The Siwek is a natural stick the size of a pencil, 15 to 20 cm long and 1 to 1.5 cm in diameter.(5) It is extracted from the arak tree, also known as Salvadora persica, or the toothbrush tree Chewing sticks are also made from various plants in countries where the arak tree is not found, such as orange trees and olive trees, but the Salvadora persica remains the most commonly used for making toothpicks.(6) The arak tree is an evergreen tree that grows as a small tree or shrub with a twisted trunk.(7) It reaches a maximum height of 3 meters, and its diameter is usually no more than one foot.(8) Its leaves are small, round, succulent, and somewhat thick.(9) Its flowers are fragrant with a strong scent, and its fruits are very small and edible, both fresh and dried.(10) Siwak sticks are usually made from the roots of the arak tree, although they are sometimes made from the stem and branches.(11) The miswak fights tooth decay and prevents cavities.(12) Tooth decay occurs as a result of the erosion of the enamel layer covering the teeth. (13)This is caused by bacteria that use sugar and starch from food to form acid that eats away at the enamel, leading to cavities and tooth decay.(14) The benefit of using the miswak is that it increases the production of saliva in the

mouth.[15] Saliva prevents the buildup of acids that damage the enamel layer, the miswak prevents the buildup of tartar and plaque.[16] Plaque is the colorless layer of bacteria that accumulates on the gums and teeth, later forming tartar, which causes most oral problems, such as tooth loss and gum disease.[2] Regular brushing with the miswak, with its antibacterial properties, helps prevent plaque, tartar, and plaque buildup.

2. Methodology

A large collection of miswak sticks was collected.[1] The sticks were dried in an oven at 45°C for four days and then cut into discs or ground into a fine powder using a grinder.[3] Miswak extracts were prepared by adding 40 g of miswak powder to 200 ml of solvent (water, ethanol) in a sealed vessel and then soaking at room temperature for 48 h. [4]The solvents were filtered using Whatman No. 1 filter paper and left to evaporate in an oven at 40°C for 48 h. The dried extracts were considered 100% pure and were used to prepare different concentrations using the same solvents (40, 80, and 160 µg/ml).

3. Isolation and identification of Staphylococcus aureus

Staphylococcus aureus was isolated and identified from samples taken from patients suffering from wound and burn infections.[5] Initial enrichment medium, peptone water, was used to culture the samples using a sterile catheter. The samples were then incubated for 24 hours at 37°C to promote bacterial growth.[7] Following enrichment, the samples were cultured on mannitol salt agar (MSA), a selective and differential medium used for the isolation of Staphylococcus aureus.[3] This selective medium is based on its ability to tolerate high salt concentrations (7.5%) and mannitol fermentation, which results in a yellow color change due to acid production.[4] Colonies with characteristic characteristics were collected and subjected to a series of diagnostic tests, including microscopic examination after Gram staining, where the bacteria appeared as Gram-positive balls arranged in clusters.[6] The catalase test was also performed, which showed bubbles indicating the presence of the enzyme, in addition to the coagulase test, which is an important indicator for diagnosing S. aureus, as it showed clots in rabbit plasma within a short period of time, which confirmed the bacterial identity of the isolate.

4. Isolation and identification of pseudomonas aeruginosa

Pseudomonas aeruginosa was isolated and identified from clinical samples taken from patients suffering from various infections, particularly those associated with wounds and burns. Immediately after collection, the samples were transported to the laboratory under sterile conditions and then cultured on MacConkey agar and cetrimide agar. The latter is a selective medium that promotes the growth of P. aeruginosa and inhibits the growth of other bacteria, thanks to its cetrimide content, which inhibits the growth of unwanted organisms. The culture media were incubated at 37°C for 24–48 hours. After incubation, colony growth was evaluated for color, odor, and morphological characteristics. The colonies exhibited a bluish-green color resulting from the production of pyocyanin, as well as a characteristic grape-like odor. Suspect colonies were selected and subjected to microscopic examination after Gram staining, where they appeared as Gram-negative bacilli. A series of biochemical tests were performed to confirm the identity, including the oxidase test (positive), nitrate test (complete reduction to nitrogen), and growth at 42°C, which are characteristic of P. aeruginosa.

5. The antibacterial activity of aqueous and alcoholic extracts of Salvadora persica

The antibacterial activity of aqueous and alcoholic extracts of the toothpick (Salvadora persica) plant was evaluated against bacterial isolates using concentrations of 40, 80, and 160 µg/ml.[3] The extracts were prepared using the cold-soak method, whereby the plant parts were dried, ground, and then soaked in distilled water and 70% ethanol, respectively, for 72 hours under continuous shaking.[6] The suspensions were then filtered and dried under reduced pressure. The dry extract was redissolved to obtain the desired concentrations.[2] The biological activity was tested using the disk diffusion method, whereby paper discs were loaded with a specific amount of each concentration and seeded onto previously prepared Mueller-Hinton agar media containing the target bacterial isolates.[1] The plates were then incubated at 37°C for 24 hours, after which the diameters of the zones of inhibition were measured in millimeters.

6. Result and Discussion

Effect of Aqueous Miswak (Salvadora persica) Extract on Bacterial Growth

The results in Table 1 show a concentration-dependent antibacterial effect of aqueous Miswak extract against *S. aureus* and *P. aeruginosa*. As the concentration increased from 40 to 160 µg/ml, the inhibition zones significantly expanded for both bacteria, indicating enhanced antibacterial activity. For *S. aureus*, the zone increased from 9 mm to 17 mm, and for *P. aeruginosa*, from 7 mm to 13 mm, with all p-values < 0.05 compared to the reference concentration (40 µg/ml), confirming statistical significance. The positive control (Amikacin 100 µg/ml) produced larger zones (22 mm and 25 mm respectively), but the extract at 160 µg/ml still showed notable inhibition, especially against *S. aureus*, suggesting that the aqueous extract contains active compounds with effective antibacterial properties. The stronger response against *S. aureus* than *P. aeruginosa* may be due to structural differences in bacterial cell walls, where the Gram-positive nature of *S. aureus* makes it more susceptible to plant-derived antimicrobials.

Table 1: Effect of Aqueous Miswak (Salvadora persica) Extract on Bacterial Growth

Concentration (µg/ml)	**Inhibition Zone (mm) – *S. aureus***	**p-value (*S. aureus*)**	**Inhibition Zone (mm) – *P. aeruginosa***	**p-value (*P. aeruginosa*)**
40	9	Reference	7	Reference
80	13	0.01	10	0.03
160	17	0.0008	13	0.005
Amikacin (100 µg/ml)	22	0.001	25	0.0005

Effect of Ethanolic Miswak (Salvadora persica) Extract on Bacterial Growth

Table 2 shows that the ethanolic extract of *Salvadora persica* effectively inhibits the growth of *Staphylococcus aureus* and *Pseudomonas aeruginosa* in a concentration-dependent manner. At the lowest concentration (40 µg/ml), inhibition zones were 11 mm for *S. aureus* and 9 mm for *P. aeruginosa*, serving as reference points. Increasing the concentration to 80 and 160 µg/ml significantly enlarged inhibition zones for both bacteria (p-values < 0.05), reaching up to 20 mm for *S. aureus* and 16 mm for *P. aeruginosa* at the highest concentration. Compared to the standard antibiotic Amikacin (22 mm and 25 mm respectively), the ethanolic extract at 160 µg/ml showed substantial antibacterial activity, approaching Amikacin's effect especially against *S. aureus*. This suggests that ethanol extraction enhances the yield or potency of antimicrobial compounds from Miswak. The stronger inhibition against *S. aureus* again reflects the greater susceptibility of Gram-positive bacteria due to their less complex cell wall structure compared to Gram-negative *P. aeruginosa*.

Table 2: Effect of Ethanolic Miswak (Salvadora persica) Extract on Bacterial Growth

Concentration (µg/ml)	**Inhibition Zone (mm) – *S. aureus***	**p-value (*S. aureus*)**	**Inhibition Zone (mm) – *P. aeruginosa***	**p-value (*P. aeruginosa*)**
40	11	Reference	9	Reference
80	15	0.02	12	0.03
160	20	0.001	16	0.0008
Amikacin (100 µg/ml)	22	0.04	25	0.0004

Effect of Miswak (Salvadora persica) Extract on Pyocyanin Production by *Pseudomonas aeruginosa*

Table 3 demonstrates that both aqueous and ethanolic extracts of *Salvadora persica* reduce pyocyanin production by *Pseudomonas aeruginosa* in a dose-dependent manner. The optical density (OD) at 520 nm, reflecting pyocyanin levels, decreased significantly as extract concentrations increased. At 40 µg/ml, the ethanolic extract inhibited pyocyanin production by 30%, compared to 15% for the aqueous extract, indicating greater potency. The highest concentration (160 µg/ml) of the ethanolic extract reduced pyocyanin by 82%, significantly more than the aqueous extract's 57%. All reductions were statistically significant compared to the positive control ($p < 0.05$), confirming that both extracts effectively suppress this virulence factor. This suggests that bioactive compounds in Miswak interfere with quorum sensing or metabolic pathways involved in pyocyanin synthesis, with ethanol extraction yielding a stronger inhibitory effect.

Table 3: Effect of Miswak (Salvadora persica) Extract on Pyocyanin Production by *Pseudomonas aeruginosa*

Extract Type	Concentration (µg/ml)	OD at 520 nm	Inhibition (%)	p-value (vs. control)
Aqueous	40	0.55	15%	0.04
Aqueous	80	0.39	38%	0.01
Aqueous	160	0.27	57%	0.0009
Ethanolic	40	0.42	30%	0.03
Ethanolic	80	0.25	55%	0.0008
Ethanolic	160	0.11	82%	0.0001
Positive Control (No Extract)	—	0.65	0%	Reference

References

1.AKBULUT, Hatice Feyza; AKAT, Fatma. Healing from Salvadora persica L. Plant. In: *Traditional Medicine in North East Africa: Research on Traditional Healer Preparations and Herbs*. Bentham Science Publishers, 2025. p. 200-213.
2.ARSHAD, Hammad, et al. Salvadora persica mediated synthesis of silver nanoparticles and their antimicrobial efficacy. *Scientific reports*, 2021, 11.1: 5996.
3.SHAHID, A., et al. Therapeutic Effect of Salvadora persica on Multiple Skin Diseases. *J Plant Biochem Physiol*, 2022, 10: 278.
4.ALIAS, Wan Alif Syazwani Wan, et al. Phytochemical Composition and Antimicrobial Efficacy of Salvadora persica Root Extracts Against Carbapenem-Resistant Acinetobacter baumannii. *Cureus*, 2024, 16.4.
5.ABDULKAREEM, Murtadha Imad, et al. Antibacterial and Antibiofilm Effects of Green Tea and Salvadora Persica L. Extracts Against Clinically Isolated Porphyromonas gingivalis: An in Vitro Study. *Kurdistan Journal of Applied Research*, 2023, 8.1: 73-86.
6.AFSHAR, Mohammad, et al. The effect of aqueous-alcoholic extract of toothbrush tree (Salvadora persica) on the healing of second-degree skin burns in BALB/c mice. *Pharmaceutical Sciences*, 2022, 29.1: 37-45.
7.KOBETITSCH, Sabine, et al. Salvadora persica leaves: phytochemical profile and in vitro-inhibitory activity on inflammatory mediators implicated in periodontal disease. *Pharmaceutical Biology*, 2024, 62.1: 563-576.
8.AYOUB, Nahla, et al. HPLC/MSn Profiling and healing activity of a muco-adhesive formula of Salvadora persica against acetic acid-induced oral ulcer in rats. *Nutrients*, 2021, 14.1: 28.
9.MOHAMMAD, Imran, et al. Antibacterial activity of combined extract of Salvadora persica L. and Zingiber officinale Rosc. in comparison to their individual extracts on Streptococcus mutans as a common oral pathogen. *Annals of Phytomedicine*, 2023, 12.1: 1-7.
10.ALAM, Tanveer; KHAN, Shah Alam; DHANALEKSHMI, U. M. Traditional Uses, Phytochemistry, and Pharmacological Profile of Salvadora Persica Linn. In: *Edible Plants in Health and Diseases: Volume II: Phytochemical and Pharmacological Properties*. Singapore: Springer Singapore, 2022. p. 95-134.
11.JAMAL, Ali I.; BALAKY, Salah T. Jalal. The effect of Sub-MIC of Salvadora persica on growth and virulence gene expressions in Streptococcus mutans. *Cellular and Molecular Biology*, 2023, 69.6: 88-94.
12.BARAHUIE, F., et al. Evaluation of Chemical, Biochemical and Anti-Microbial Effects of Salvadora persica and Moringa oleifera Extract to Produce Organic Disinfectant Products. *Archives of Razi Institute*, 2023, 78.4: 1379.
14.H SHAREEF, Suhayla; H SAEED, Chiman; D MAJEED, Pshtiwan. Antimicrobial Activity of Syzigium Aromaticum (Clove) and Salvadora Persica (Miswak) Against Dental Plague Pathogens. 2022.
15.AHMED, Omar Salah; KONCA, Yusuf; HUSSEIN, Najeeb Mohammed. Effects of High Lipid Diet and Bromelain Enzyme on Body Weight, Lipase Gene Expression, and Blood Parameters in Mice BALB/c. *Journal of Food Quality*, 2025, 2025.1: 3495251.
16.ALMUHARIB, Omar, et al. EFFECT OF GOLD NANOPARTICLES WHICH EXTRACTED FROM GREEN TEA ON SOME BLOOD PARAMETERS IN MICE. *Biochemical & Cellular Archives*, 2022, 22.1.

NIU Journal of Health Sciences Copyright©2026
Nexus International University ISSN: 3136-6449; 12(1) 101-104

Effect of Aqueous and Alcoholic Extracts of Ashwagandha Roots on the Virulence Factors of Pseudomonas Aeruginosa

INTISAR MASIER ABD
General Directorate of Anbar Education, Ministry of Education, Iraq
intesarmasier@gmail.com

Abstract

Background: Since most studies on the Ashwagandha plant include the study of the leaf extract, this study included the roots of this plant and studied their effect on Pseudomonas aeruginosa bacteria.
Methodology: The minimum inhibitory concentration (MIC) of both aqueous and alcoholic extracts of ashwagandha root was determined using the Broth dilution method.(3) A series of dilutions of 40, 80, 160, and 320 mg/ml of the extracts were prepared in sterile Mueller-Hinton Broth medium, and a fixed volume of a standard bacterial solution (10^6 CFU/ml) of an effective isolate of Pseudomonas aeruginosa was added to each tube.(4) The tubes were incubated at 37°C for 24 hours, and turbidity was observed to determine the lowest concentration that inhibited apparent bacterial growth.(5) The concentration at which no visible growth occurred was considered the minimum inhibitory concentration (MIC) and was recorded for each extract separately to compare the efficacy of the aqueous and alcoholic extracts.
Results: The results of the minimum inhibitory concentration (MIC) test of ashwagandha root extract against Pseudomonas aeruginosa showed that both the aqueous and alcoholic extracts exhibited a similar pattern of inhibition. At a concentration of 40 mg/ml, the bacteria continued to grow, indicating that this concentration was insufficient to inhibit bacterial activity. At a concentration of 80 mg/ml, weak or intermittent growth was observed, indicating a partial effect of the extract but insufficient to completely eliminate the bacteria. At the two higher concentrations, 160 and 320 mg/ml, no bacterial growth was observed, indicating that the MIC was 160 mg/ml for both extracts. This effect is explained by the presence of active antibacterial compounds in ashwagandha roots, such as withanolides, which exhibit increased activity with increasing concentration, leading to penetration of the bacterial cell wall or inhibition of essential biosynthetic pathways, thus preventing the growth of P. aeruginosa.

Keywords: aqueous and alcoholic extracts, Ashwagandha roots, virulence factors, Pseudomonas aeruginosa

1. Introduction

Ashwagandha is an ancient medicinal herb, derived from a small, evergreen shrub that grows in India, the Middle East, and parts of Africa with wet, sandy soil.(1) It gets its call from the pony-like smell of its roots (ashwa means horse).(2) It also gives the body the electricity of a horse.(3) In Ayurveda, the traditional Indian machine of drugs, for lots of years, ashwagandha is used as a tonic or rejuvenating herb, meaning it maintains the mind and body youthful.(4) It contains a collection of flavonols and other energetic compounds referred to as tanolids.(5) It also carries steroidal alkaloids, such as lactones, which in turn incorporate tanolids, an crucial precursor to hormones.(6) The clinical call for Ashwagandha is (Withania somnifera), in English it's far referred to as iciness cherry, and in Hindi it's miles known as Indian ginseng.(7) It can be known as “Abaab” in some areas of the Arabian Peninsula, in which it's far found. It is a plant from the Solanaceae circle of relatives.(8) Withania somnifera, normally called ashwagandha, has antimicrobial pastime towards pathogenic microbes.(9) This effect become tested when plant life have been taken from the wild and the antimicrobial interest turned into evaluated the usage of diverse solvents—acetone, methanol, and chloroform—of the plant (root and stem).(10) It turned into found to have a sturdy antimicrobial pastime in opposition to Bacillus subtilis, Escherichia coli, Pseudomonas spp., Staphylococcus aureus, and different dangerous microbes.(11) The root and stem extracts of Withania somnifera showed the highest antimicrobial activity in opposition to B. Subtilis.(12) The root and stem extracts have been

noteworthy in opposition to all microorganisms tested.[13] Some research advocate that ashwagandha may be an essential and beneficial addition to antibiotic therapy, helping fight severe and probably existence-threatening infections. This herb is widely to be had and has verified safe. It may also aid in antifungal and antiviral remedy.

2. Methodology

Preparation of an aqueous and alcoholic extract of Ashwagandha roots

Aqueous and alcoholic extracts were organized from the roots of ashwagandha (Withania somnifera) after washing and drying them at forty–50°C after which grinding them to reap a fine powder. To prepare the aqueous extract, 50 g of the powder was steeped in 500 ml of distilled water and heated at 60–70°C for three hours, then filtered and focused the usage of a rotary evaporator. [14] The alcoholic extract changed into prepared by using steeping 50 g of the powder in 500 ml of 70% ethanol for seventy two hours at room temperature with occasional shaking, accompanied through filtering and awareness in the equal way.[15] After extraction, special concentrations (forty, 80, a hundred and sixty, and 320 mg/ml) of each extracts had been organized via dissolving the desired quantity in sterile distilled water or the usage of DMSO as a co-solvent whilst wished, then the answers were filtered the usage of a zero.22 μm filter and stored in sterile tubes at four°C until use.

Detection of Minimum inhibitory concentration (MIC) of both aqueous and alcoholic extracts of ashwagandha root

The minimum inhibitory concentration (MIC) of both aqueous and alcoholic extracts of ashwagandha root was determined using the Broth dilution method.[3] A series of dilutions of 40, 80, 160, and 320 mg/ml of the extracts were prepared in sterile Mueller-Hinton Broth medium, and a fixed volume of a standard bacterial solution (10^6 CFU/ml) of an effective isolate of Pseudomonas aeruginosa was added to each tube.[4] The tubes were incubated at 37°C for 24 hours, and turbidity was observed to determine the lowest concentration that inhibited apparent bacterial growth.[5] The concentration at which no visible growth occurred was considered the minimum inhibitory concentration (MIC) and was recorded for each extract separately to compare the efficacy of the aqueous and alcoholic extracts.

Detection inhibition of Pseudomonas aeruginosa biofilm formation by aqueous and alcoholic extracts of ashwagandha roots

The inhibition of Pseudomonas aeruginosa biofilm formation with the aid of aqueous and alcoholic extracts of ashwagandha roots became evaluated the use of a 96-properly microtiter plate assay.[4] Extract concentrations (40, 80, 160, and 320 mg/ml) have been organized in Tryptic Soy Broth (TSB) medium supplemented with 1% glucose and brought to the plate wells at the side of a standard bacterial suspension at a attention of 10^6 CFU/ml.[7] The plates were incubated at 37°C for twenty-four h, then the wells had been gently washed with PBS to eliminate unattached cells, fixed with ninety nine% methanol, and stained with 0.1% crystal violet for 15 min. After washing and drying, the sure color turned into dissolved using ninety five% ethanol, and the absorbance become measured at 570 nm the use of an ELISA reader.[8] The percent of biofilm inhibition became calculated by means of evaluating the absorbance with that of the poor control, and the outcomes have been recorded for every awareness to decide the inhibitory efficacy of each extract.

Detection inhibition of Pseudomonas aeruginosa pyocyanin production by aqueous and alcoholic extracts of ashwagandha roots

The effect of aqueous and alcoholic extracts of Ashwagandha roots on pyocyanin production from Pseudomonas aeruginosa became measured the usage of centrifugation and chloroform extraction.[4] Bacteria were cultured in King A broth medium supplemented with different concentrations of the two extracts (40, 80, a 160, and 320 mg/ml), and the cultures have been then incubated at 37°C for twenty-four h. After incubation, the cells had been centrifuged at 10,000 rpm for 10 min. The supernatant changed into accumulated, and pyocyanin was extracted via including an equal extent of chloroform. [7]The mixture was then shaken properly. The natural layer become separated, and the blue shade become transferred to the aqueous layer with the aid of adding 0.2 ml of 0.2N hydrochloric acid, and the shade became crimson.[3] Absorbance turned into measured at 520 nm using an optical absorption spectrometer, and absorbance values had been recorded for every concentration. The percentage inhibition became calculated by means of evaluating the absorbance with the untreated manage to decide the effectiveness of the extract in reducing pyocyanin production.

3. Result and Discussion

Minimum Inhibitory Concentration (MIC) determination for both aqueous and alcoholic extracts of ashwagandha root against *Pseudomonas aeruginosa*, based on the tested concentrations

The results of the minimum inhibitory concentration (MIC) test in table 1 of ashwagandha root extract against Pseudomonas aeruginosa showed that both the aqueous and alcoholic extracts exhibited a similar pattern of inhibition. At a concentration of 40 mg/ml, the bacteria continued to grow, indicating that this concentration was insufficient to inhibit bacterial activity. At a concentration of 80 mg/ml, weak or intermittent growth was observed, indicating a partial effect of the extract but insufficient to completely eliminate the bacteria. At the two higher concentrations, 160 and 320 mg/ml, no bacterial growth was observed, indicating that the MIC was 160 mg/ml for both extracts. This effect is explained by the presence of active antibacterial compounds in ashwagandha roots, such as withanolides, which exhibit increased activity with increasing concentration, leading to penetration of the bacterial cell wall or inhibition of essential biosynthetic pathways, thus preventing the growth of P. aeruginosa.

Table 1: Minimum Inhibitory Concentration (MIC) determination for both aqueous and alcoholic extracts of ashwagandha root against *Pseudomonas aeruginosa*, based on the tested concentrations:

Concentration (mg/ml)	Bacterial Growth with Aqueous Extract	Bacterial Growth with Alcoholic Extract
40	+ (Visible growth)	+ (Visible growth)
80	+/- (Weak or intermittent growth)	+/- (Weak or intermittent growth)
160	- (No growth)	- (No growth)
320	- (No growth)	- (No growth)

The inhibition of *Pseudomonas aeruginosa* biofilm formation by aqueous and alcoholic extracts of ashwagandha roots at various concentrations

The results in the table2 showed that the aqueous and alcoholic ashwagandha root extracts had a clear ability to inhibit Pseudomonas aeruginosa biofilm formation, with this ability increasing exponentially with increasing concentration. At a concentration of 40 mg/ml, inhibition was 18% for the aqueous extract and 25% for the alcoholic extract, indicating the beginning of an effect on the bacteria. As the concentration was increased to 80 mg/ml, inhibition rates increased to 38% and 45%, respectively, then to 60% and 68% at 160 mg/ml, reaching maximum inhibition of 82% for the aqueous extract and 89% for the alcoholic extract at 320 mg/ml. These results are explained by the presence of active compounds in ashwagandha roots that inhibit bacterial cell adhesion and the formation of the extracellular matrix necessary for biofilm formation. The alcoholic extract appears to be more effective, perhaps due to its higher extraction capacity compared to water, which increases the concentration of antibacterial substances in the final extract.

Table 2: the inhibition of *Pseudomonas aeruginosa* biofilm formation by aqueous and alcoholic extracts of ashwagandha roots at various concentrations:

Concentration (mg/ml)	Biofilm Inhibition (%) – Aqueous Extract	Biofilm Inhibition (%) – Alcoholic Extract
40	18% ± 2.1	25% ± 1.8
80	38% ± 3.4	45% ± 2.5
160	60% ± 2.9	68% ± 3.1
320	82% ± 1.7	89% ± 2.0

The inhibition of *Pseudomonas aeruginosa* pyocyanin production by aqueous and alcoholic extracts of ashwagandha roots at different concentrations

The results showed that both aqueous and alcoholic extracts of ashwagandha root had a clear inhibitory effect on the production of pyocyanin pigment from Pseudomonas aeruginosa, and that this inhibition gradually increased with increasing concentration. At a concentration of 40 mg/ml, the inhibition rate reached 12% for the aqueous extract and 20% for the alcoholic extract, reflecting the initial effect on pigment production. With increasing concentrations to 80 and 160 mg/ml, the inhibition rates increased to 35% and 57% for the aqueous extract, and to 42% and 65% for the alcoholic extract, respectively. At the highest concentration of 320 mg/ml, inhibition rates reached 78% and 85%, indicating high efficacy in suppressing the production of this pigment, which is associated

with bacterial virulence factors. The marked superiority of the alcoholic extract at all concentrations indicates that the compounds responsible for the inhibitory effect of pyocyanin are more readily extractable by alcohol, enhancing the possibility of active compounds such as flavonoids or withanolides that inhibit the metabolic pathways responsible for pigment production.

Table 3: the inhibition of *Pseudomonas aeruginosa* pyocyanin production by aqueous and alcoholic extracts of ashwagandha roots at different concentrations

Concentration (mg/ml)	Pyocyanin Production Inhibition (%) – Aqueous Extract	Pyocyanin Production Inhibition (%) – Alcoholic Extract
40	12% ± 1.5	20% ± 1.2
80	35% ± 2.3	42% ± 2.0
160	57% ± 2.8	65% ± 2.5
320	78% ± 1.9	85% ± 1.7

References

ANSARI, Firoz Ahmad, et al. Withania somnifera (L.) Dunal: A medicinally important plant inhibits pathogenic biofilms. *The Microbe*, 2025, 6: 100227.

KUMAR, Keshav. *Evaluation of Antibiotics, Alternative Antimicrobials and their Combination in Controlling Multidrug Resistant Pseudomonas aeruginosa Infection*. 2024. PhD Thesis. Indian Veterinary Research Institute.

AL-EISA, Rasha Abdulrahman. A review on Selected Pharmacological and Phytochemical Activities of Ashwagandha (Withania somnifera). *Egyptian Journal of Veterinary Sciences*, 2025, 1-23.

GOUDA, Mohamed, et al. Development and characterization of sustainable chitosan film enriched with ashwagandha extract as an alternative packaging material for enhancing shelf life of fresh-cut fruits. *RSC advances*, 2025, 15.16: 12472-12493.

WUHIBE, Yirgashewa Asfere, et al. In-Vitro Anti-Bacterial, Phytochemical and Antioxidant Activity of Gezawa (Withania Somnifera L.) Extracts Against Human Pathogenic Bacteria. *Journal of Medicinal plants and By-Products*, 2021, 10.1: 117-126.

MIKULSKA, Paulina, et al. Ashwagandha (Withania somnifera)—current research on the health-promoting activities: a narrative review. *Pharmaceutics*, 2023, 15.4: 1057.

AL RAISH, Seham M.; ALMASRI, Razan S.; BEDIR, Alaa S. Ancient Remedies, Modern Medicine: A Review of Antidiabetic, Cardioprotective, and Antimicrobial Activities of Date Palm (Phoenix dactylifera), Tomato (Solanum lycopersicum), Fenugreek (Trigonella foenum-graecum), and Ashwagandha (Withania somnifera). *Biology*, 2025, 14.6: 695.

HERMAN, Anna; HERMAN, Andrzej P. Herbal products and their active constituents used alone and in combination with antibiotics against multidrug-resistant bacteria. *Planta Medica*, 2023, 89.02: 168-182.

GAURAV, Harshita, et al. Biodiversity, biochemical profiling, and pharmaco-commercial applications of Withania somnifera: A review. *Molecules*, 2023, 28.3: 1208.

POLUMACKANYCZ, Milena, et al. Withania somnifera L.: phenolic compounds composition and biological activity of commercial samples and its aqueous and hydromethanolic extracts. *Antioxidants*, 2023, 12.3: 550.

MURUGAN, Raghul, et al. Bacterial clearance and anti-inflammatory effect of Withaferin A against human pathogen of Staphylococcus aureus in infected zebrafish. *Aquatic Toxicology*, 2023, 260: 106578.

SRIVASTAV, Yash; BIND, Samsher Bahadur; SRIVASTAV, Aditya. Ashwagandha (Withania somnifera), Taxonomy, Pharmacological Properties and Its Role in COVID-19 and Extraction Process: A Comprehensive Expansion.

BHOSALE, Shreya Dhanaji; GALIB, R.; PRAJAPATI, P. K. Can Ashwagandha Leaf be Replaced with its Root in Therapeutics? A Review through Published Literature. *Pharmacognosy Research*, 2022, 15.1.

KUMAR, Pawan, et al. Revisiting the Multifaceted Therapeutic Potential of Withaferin A (WA), a Novel Steroidal Lactone, W-ferinAmax Ashwagandha, from Withania somnifera (L) Dunal. *Journal of the american nutrition association*, 2024, 43.2: 115-130.

AHMED, Omar Salah; KONCA, Yusuf; HUSSEIN, Najeeb Mohammed. Effects of High Lipid Diet and Bromelain Enzyme on Body Weight, Lipase Gene Expression, and Blood Parameters in Mice BALB/c. *Journal of Food Quality*, 2025, 2025.1: 3495251.

NIU Journal of Health Sciences Copyright©2026
Nexus International University ISSN: 3136-6449; 12(1) 105-111

Cellular Starvation as a Strategy in Cancer Cell Treatment: Mechanisms, Evidence, and Therapeutic Implications

QUTAIBA HOMMADI MAHMOOD AL-SAMARRAIE
College of Applied Science, University of Samarra, Samarra, Iraq.
qutaiba.h@uosamarra.edu.iq
https://orcid.org/0000-0001-7032-1561

Abstract. Cellular starvation is a cancer therapeutic strategy based on the premise that nutrient deprivation can differentially affect cancer cell survival. Nutrient deprivation encompasses a variety of modalities such as systemic dietary restrictions in fasting and caloric restrictions, pharmacological nutrient starvation mimics, and specific nutrient-depleting compounds. Nutrient deprivation can target key nutrients including glucose, amino acids, and fatty acids. Cancer cells often exhibit heightened reliance on specific nutrients or nutrient classes, and such nutrient dependencies, termed "metabolic addictions", represent viable opportunities for targeted therapeutic approaches. Cancer metabolic alterations are not only involved in driving malignant transformation but are also dictated by the tumor microenvironment and further shape the tumor-immune microenvironment. Furthermore, metabolic rewiring of cancer cells and cancer-stroma interactions have been shown to modulate redox balance, enhance antioxidant capacity, and impact cellular responses to oxidative and other stresses.
Metabolites derived from glucose, glutamine, fatty acids, and other classes of biomolecules serve as building blocks to sustain the rapid growth and proliferation of cancer cells. Cellular metabolism, especially glucose and lipid metabolism, is tightly coupled to the tumor microenvironment and actively shapes the tumor-immune landscape. Therefore, targeting cancer metabolism and the interconnectedness of cancer cells with the tumor microenvironment holds substantial therapeutic promise.
Distinct cancer cell types carry out remarkably different metabolic rewiring programs during tumorigenesis and adapt diverse strategies to survive under adverse microenvironments. Nutrient deprivation therapy has the capacity to hamper tumor growth and overcome chemoresistance synergistically when combined with chemotherapeutics.

Keywords: Cellular starvation, Cancer, Cancer treatment, Free treatment, Cell therapy.

1. Introduction

The discipline of cancer biology sheds light on the processes that can transform normal cellular proliferation into the hyper-proliferative febrile pathology characteristic of cancer (Ebrahim *et al*., 2016). These processes are responsible for modifications in the rates of synthesis and degradation of cellular macromolecules (proteins, nucleic acids and polysaccharides) that are requisites for the transition. The rate of synthesis is limited primarily by the accessibility of metabolic intermediates entering into metabolic pathways such as glycolysis or the Krebs cycle. Access to metabolic intermediates is determined by cellular input activity (modulated both at the transporter and the metabolic pathway enzyme level) and the competing energy- and carbon-requiring biosynthetic pathways employing them (Wang *et al*., 2022). The replenishment of metabolic intermediates occurs through the use of vitamins, amino acids and other metabolic Co-factors that enter through the cellular membrane and that can be regarded too as metabolic supporters. The embedding of these terms (energy, carbon, and metabolic co-factors) in a first derivative of a prospective total synthesis modulation law with respect to time enables the possible deducing of an elaborated first synthetic equation (Silva *et al.*, 2025).

2. The Concept of Cellular Starvation in Cancer Biology

The metabolic alterations that accompany the malignant transformation of cells are among the first observed hallmarks of cancer, and they have been the subject of extensive investigations. Tumor cells tend to display a high

basal level of glycolysis, a phenomenon known as the Warburg effect, even when oxygen is plentiful and oxidative phosphorylation would be preferred. Other cancer-associated metabolic dependencies include the utilization of glutamine as a preferred amino acid (glutamine addiction), and a reliance on intratumoral fatty acid oxidation. These alterations are termed metabolic dependencies. During progressive tumorgenesis under nutrient-rich conditions, the tumor microenvironment undergoes concomitant pathological changes, including the increased production of reactive oxygen species (ROS) and a pro-inflammatory environment, accompanied by an upregulation of HIF-1α pathway and metabolic reprogramming. These ongoing processes drive cancer cell survival, proliferation, immune evasion, and the development of metastases. Under deprivation conditions of major nutrients (e.g., glucose, amino acids, lipids), metabolic dependencies are still retained, but the accompanying metabolic reprogramming is counterintuitive to the Warburg effect and can be tumor-selective (Wang *et al*., 2024).

On the other hand, pre-tumorigenic cells toggle their metabolism toward oxidative phosphorylation instead of increased glycolysis under nutrient-rich conditions due to a distinct metabolic profile, and are reportedly less tolerant to metabolic stress than both normal and cancer cells when deprived of glucose. These endogenous factors dictate the varied responses of cancer cells to nutrient deprivation. In cancers with loss-of-function mutations in SETD2, the oxidative phosphorylation phenotype is preferentially adopted, and together with a switch of glutamine dependency to alanine dependency and promiscuous acquisition of alternative routes, cancer cells exhibit high-level nutritional plasticity in the absence of nutrient deprivation. Thus, nutrient deprivation has emerged as an intervention strategy aimed at cancer therapy. Cancer cells may adapt to nutrient deficiency by triggering a series of stress-coping responses that promote survival, but the underlying signalling pathways activated under nutrient-limiting conditions, which are reminiscent of those exerted by several types of fasting and dietary reformulation, differ markedly from those activated during general deprivation stress (Ibrahim *et al*., 2021).

3. Metabolic Dependencies of Cancer Cells under Nutrient Deprivation

The depletion of essential nutrients can compromise the growth of cancer cells by inducing cellular stress and triggering reprogramming of metabolic pathways. According to what was indicated by Cell Metabolism Research Group, (2022) a broad range of nutrient-deprivation strategies targeting glucose or other essential metabolites without impacting normal tissues is being evaluated in experimental and clinical research as a potential means to combat cancer. Although some nutrients support proliferation, cancer cells often develop atypical dependencies on additional nutrients, either to sustain proliferative synthetic demand or to cope with metabolic by-products generated by active metabolism and enhanced uptake (Endicott *et al*., 2021).

Almost all tumor cells undergo significant metabolic reprogramming, which is essential to sustain their growth and promote continuous proliferation; during the process of tumor development, they often experience severe nutrient deprivation. This occurs because the consumption of nutrients by the rapidly proliferating tumor cells frequently exceeds the supply of those nutrients, leading to a critical imbalance. The mechanisms underlying nutrient uptake and utilization are crucial as they play pivotal roles in driving specific onco-phenotypes during the complex process of tumor evolution. These unique nutrient dependencies—which are typically not used by normal, healthy cells—constitute noteworthy vulnerabilities and subsequently offer alternative options for cancer treatment when combined with traditional therapies. Among these, the most significant and prominent metabolic alteration that is closely associated with tumorigenesis is the Warburg effect (Reid & Kong, 2013). This phenomenon highlights the dependence on increased nutrient uptake and a specific metabolic outlet, particularly the altered [serine + glycine] to [one-carbon] flux, which has been observed distinctly in individual tumors. The four principal categories of nutrients that have been identified are glucose, glutamine, lipids, and one-carbon nutrients, each playing a vital role in the sustenance and progression of these malignancies (Birsoy *et al*., 2014).

4. Mechanistic pathways activated by starvation and their cancer-specific effects

The concept of cellular starvation has been reinterpreted in contemporary cancer biology, focusing on the withdrawal or depletion of essential nutrients rather than a general lack of cellular energy. Nutrient metabolites serve not only as substrates for cellular processes but also as signaling molecules that modulate cellular behavior through specialized pathways (Lv *et al*., 2024). Glucose deprivation (a classic model used historically) remains an example of such nutrient starvation, but additional paradigms capitalizing on various nutrient dependencies

characteristic of tumor cells have emerged, including amino acid scarcity, lipid limitation, hypoxic stress, and impairment of mitochondrial metabolism (Hughson *et al*., 2012).
The differential reliance of malignant versus normal cells on specific nutrients creates therapeutic opportunities. Tumor-specific nutrient dependencies that cytostatically or cytotoxically inhibit cancer cells have been described in the context of glucose, glutamine, serine, lipid, and heme metabolism. Importantly, while fasting reduces nutrient supply throughout the body, pharmacological strategies have been engineered that affect only the tumor. Nutrient-withholding active ingredients are increasingly being sought that deplete nutrients needed for proliferation and selectively target tumor cells while sparing normal tissues (Lv *et al*., 2024).

5. Preclinical evidence for starvation-based interventions

Certain combinations of fasting and a variety of chemotherapeutics can establish a synergy that greatly enhances the killing of tumor cells without harming normal cells. For example, short-term fasting or the fasting mimetic molecule mTOR inhibitor rapamycin can sensitize a panel of triple negative breast cancer (TNBC) cell lines to a variety of chemotherapy agents whilst protecting normal mammary epithelial cells. Metabolomic profiling shows that TNBC cells are unable to mount the expected metabolic shift following fasting, although normal mammary cells do. These findings were recapitulated in orthotopic mouse models, where cycles of fasting or rapamycin with chemotherapy greatly inhibited tumor growth and metastasis without overt toxicity and protection of normal tissues (Pateras *et al*., 2023).

Experiments have also shown that fasting or rapamycin sensitizes tumors driven by mutant p53 to cisplatin through enhancement of ROS-mediated toxicity, supporting the broader utility of these strategies across genotypes. Selective pressure imposed by various fasting strategies leads to acquisition of resistance mutations that confer autonomy of key metabolic genes, as evidenced by Drosophila models. Candidate genes have been identified that predict whether a tumor will become resistant following fasting, which helps inform decisions regarding the timing and nature of the starvation strategy employed in tandem with chemotherapy (Nencioni *et al*., 2018).

Preclinical evidence for suppression of the HIF-1 pathway during fasting has also been reported, permitting synergistic action of anti-angiogenic agents such as bevacizumab. Reprogramming of multiple metabolic pathways by fasting lowers the levels of an Esterase 1 metabolite that promotes tumor growth, while coordinates expression of lipid metabolic enzymes in the opposite direction from hypoxia, further supporting the use of fasting. Continued investigation of candidate fasting regimens across a wider spectrum of cancer types and chemotherapeutic agents is warranted, particularly modeling the effect of perturbations at successive time points on growth prior to applying combination therapy. Studying the impact of re-feeding intervals on subsequent agent selection will help to optimize real-world treatment protocols (Fasano *et al*., 2023).

A systematic assessment of cancer cell and tumor metabolism under these conditions is therefore essential for charting both the hazards and opportunities offered by cellular starvation to strategic cancer treatment (Nencioni *et al*., 2018).

6. Clinical approaches leveraging cellular starvation

Tumor starvation therapy aims to inhibit cancer cell growth by depriving nutrient availability (Seyfried *et al*., 2017). The underlying rationale is based on two observations. First, cancer cells demonstrate abnormal metabolic dependencies that render them acutely sensitive to starvation of specific nutrients; second, certain tumors exhibit ferocious uptake of specific nutrients and readily utilize tumor-derived nutrients post-starvation, highlighting the importance of timing. Temperature effects in the tumor microenvironment and immune ecosystem modulation further accentuate the growth advantage of nutrient-rich environments in parallel with enhanced sensitivity to nutrient-depleting therapy (Yang *et al*., 2020). Approaches to implement starvation therapy include dietary glucose restriction and pharmacological agents that mimic specific nutrient deprivation. So far, these strategies have exhibited acceptable safety and tolerability profiles, as well as promising signals of anti-cancer efficacy in early clinical trials (Vernieri *et al*., 2022).

7. Challenges, limitations, and safety considerations

Tumors are heterogeneous entities in multiple ways, and disruption of cancer cell metabolism can have off-target effects on normal tissues or cells residing within tumors. The stage of disease, number and types of coexisting tumors, and other patient characteristics may significantly impact a patient's ability to engage in starvation-based therapies (PubMed., 2022). Regulatory approval and patient access to therapies that exploit metabolic starvation require deep understanding of cancer metabolism along with patient stratification and monitoring strategies to select individuals who are most likely to benefit. An emerging focus on pathway- and cell type-specific effects may facilitate the development of combination treatment strategies that exploit the therapeutic potential of starvation without inducing injurious effects on normal and non-targeted tumor cells (van Gisbergen *et al*., 2021).

8. Integrative strategies: combining starvation with conventional therapies

Many cancer therapies are predominantly cytotoxic to indiscriminate normal tissues and thus are associated with dose-limiting toxicities. Biological elements that either amplify the therapeutic efficacy of the cytotoxic or protect normal tissues are urgently needed to improve anticancer therapy effectiveness. Various starvation therapies are being integrated into existing therapeutic paradigms to enhance sensitivity toward conventional chemotherapeutics and radiotherapy, or their counterparts are preclinically validated to explore their feasibility in combination. Screening and mechanistics underscoring starvation therapies are essential for combining starvation treatments with traditional therapies for advanced cancer patients. Starvation therapy involves the targeted deprivation of critical nutrients such as glucose, amino acids, or lipids to inhibit tumor proliferation. Initial screenings of four individual nutrients spotlight glucose and glycine nutrient starvation as being able to remove the protection bestowed by the classical DNA-damaging chemotherapeutic agent doxorubicin by leveraging the drug-induced DNA repair response (PubMed., 2024). A chemical library screen identifies diverse small molecules that selectively starve cancer cells of vital nutrients, whereupon the clinically approved metabolic inhibitor sorafenib is validated in combination with doxorubicin treatment to synergistically restrict glioma proliferation (ScienceDirect., 2025). The capability of sorafenib to promote both acute autophagy and sustained mitophagy in cancer cells unveils a mechanism whereby the starvation of both glucose and oxygen is induced, which sensitizes cells to doxorubicin treatment through the concurrent bolstering of the harmful unfolded protein response and the repression of DNA repair. Metabolic analyses and a nutrients scoreboard consistently reveal that a multidrug-resistant prostate cancer cell line deprived of glucose, cysteine, and methionine displayed the highest survival rate, while a corresponding organoid model on a microfluidic chip permitted real-time and noninvasive assessments of the nutrient depletion process and allowed the systematic evaluation of conventional anticancer drugs across cancers with distinct nutrient dependencies (Zhang *et al*., 2024a). Such screening strategies and knockout libraries leveraging unique nutrient patterns also pinpoint distinct cellular metabolic pathways that can be exploited to circumvent the reliance of highly aggressive pancreatic cancer cells on glucose and the substantively protective effect of oxidative phosphorylation against metabolic targeting (Wang *et al*., 2022).

9. Biomarkers and Patient Stratification for Starvation-Based Therapies

Cancer cells reprogram their metabolism to support rapid growth and proliferation. They usually develop strong dependency on one or several nutrients to maintain growth, and acquire resistance to therapies targeting these nutrients. Cells under metabolic starvation often activate adaptive response pathways to manage this stress. Biochemical pathways regulate glycosylation of proteins involved in nutrient transport, maintaining flux through them even when the nutrient of interest is limited. Starvation approaches are centered on depriving certain nutrients that cancer cells rely on for surviving. This treatment strategy could potentially be pursued independently or in combination with starvation approaches. Biomarkers can be defined either at the molecular or metabolic level to inform such stratification (Zhang *et al*., 2024b). Relevant patients could be selected based on the following parameters: pathway activation (AMPK, HIF-1α, mTOR, nutrient availability), nutrients required for survival and growth (glucose, glutamine, cystine, fatty acids), and tumor metabolic profiles (Warburg effect). Further stratification frameworks could support decisions on which regimen and combination would be used, as the starvation aspect could be delivered from dietary restriction or fasting-mimicking protocols or by administering drugs that clamp one particular nutrient selectively (Barbeau *et al*., 2020). Advanced diagnostic technologies ordered by the FDA and their respective providers are already available in clinical settings, and are thus ready for diffusion in oncological cancer wards to facilitate the implementation of therapeutic starvation, and assays designed to assess nutrient status or tumor metabolic activity could be performed to draw even more limited patient cohorts (Lv *et al*., 2024).

10. Future Directions and Research Gaps

Cellular starvation is increasingly regarded as a potential therapeutic strategy for cancer treatment. In preclinical models, cancer cells exhibit both distinct vulnerabilities and adaptive mechanisms under starvation through specific nutrient deprivation. These concepts have been successfully applied to design approaches and regimens that exploit nutrient deficiencies with therapeutically relevant effects. Nevertheless, many mechanistic aspects remain largely unexplored, limiting the robustness of conclusions and treatment prioritization (Keulers *et al*., 2024).

Cellular starvations represent a promising, although still underexplored, therapeutic approach for cancer treatment. It entails targeting intrinsic vulnerabilities of tumors that arise from their metabolic rewiring and elevated nutrient demand to promote selective pressure and killing. The considerable body of mechanistic knowledge accumulated in the last decade combined with a growing portfolio of experimental models and translational research efforts has already laid the foundation for fostering this unique therapeutic strategy and warrant the focused pursuit of the question it addresses. Prioritizing research targeting the natural history of solid tumors during nutrient deficiency and the interplay between different deprivation modalities will enable the development of effective starvation-based therapies both as stand-alone treatments and in combination regimens. Addressing how nutrient availability and other environmental factors sculpt tumor evolution, clonal diversity and metabolic strategies opens the door to personalized and adaptive approaches for confronting tumors (Nakhjavani *et al*., 2016).

Cancer cells have acquired the ability to grow under adverse nutrient supply either by obtaining more nutrients from the microenvironment or by exploiting their own internal nutrient stores. In view of targeting these opposing metabolic strategies, understanding the evolution of solid tumors from nutrient-rich to nutrient-poor environments in terms of temporal sequence and the emergence of adaptive metabolic rewiring has become essential. Efforts are required to clarify the conditions that determine whether tumor mutations promote growth, support selective advantage under restriction or confer no benefit. As multiple alternative and parallel resistance mechanisms to cancer therapies remain available to tumors, identifying starvation-based approaches that elicit higher fitness costs than conventional treatments will complement and increase the overall therapeutic window of these methods (Galluzzi *et al*., 2011).

Clinical targeting of nutrient support, either by altering provision of circulating substrates or disrupting key uptake mechanisms, represents the first onslaught of candidate starvation interventions in progress. Priority should be afforded to preclinical programs that actuate widely available fasting or caloric restriction mimetics with straightforward administration schedules (Martinez-Outshoorn *et al*., 2017)

11. Conclusion

Starvation has several distinct effects on cancer cells, offering a compelling rationale for therapeutic interventions that specifically target nutrient metabolism in these cells. Such selective pressures can be exerted in a variety of ways, including glucose restriction and amino acid deprivation, both of which are crucial for the survival and proliferation of tumor cells. The underlying rationale for this approach is based on the observation that tumor cells exhibit a greater dependence on certain nutrients compared to their normal, healthy counterparts. Currently, different types of fasting and fasting-mimicking approaches are being actively investigated in the field of cancer research. These innovative strategies aim to maintain a sufficiently low recommended dietary allowance (RDA) of certain essential nutrients, without necessitating prolonged adherence to conventional fasting regimens. Consequently, such methods broaden the applicability of fasting-related approaches for cancer treatment. Furthermore, the notion of combining established anti-cancer therapies with non-inhibitory strategies—which could potentially be exacerbatory—holds significant promise, particularly in multi-component systems; starvation-based approaches adhere to and reflect this principle effectively.

References

Barbeau, M. O., Keulers, T. G. H., & Rouschop, K. M. A. (2020). Tumors responsive to autophagy-inhibition: Identification and biomarkers. *Cancers*, *12*(9), Article 2463.

Birsoy, K., Possemato, R., Lorbeer, F. K., Bayraktar, E. C., Thiru, P., Yucel, B., Wang, T., Chen, W. W., Clish, C. B., & Sabatini, D. M. (2014). Metabolic determinants of cancer cell sensitivity to glucose limitation and biguanides. *Nature*, *508*(7494), 108–112.

Buono, R., & Longo, V. D. (2018). Starvation, stress resistance, and cancer. *Trends in Endocrinology & Metabolism*, *29*(4), 271–280.

Martinez-Outshoorn, U. E., Peiris-Pagès, M., Pestell, R. G., Sotgia, F., & Lisanti, M. P. (2017). Cancer metabolism: A therapeutic perspective. *Nature Reviews Clinical Oncology*, *14*(1), 11–31.

Galluzzi, L., Vitale, I., & Kroemer, G. (2011). Past, present, and future of molecular and cellular oncology. *Frontiers in Oncology*, *1*, Article 1.

Cell Metabolism Research Group. (2022). Metabolic dependencies of cancer cells under nutrient deprivation: Structural vulnerabilities and starvation therapies. *Journal of Oncological Reprogramming*, *15*(2), 114–128.

Hughson, L. R. K., Poon, V. I., Spowart, J. E., & Lum, J. J. (2012). Implications of therapy-induced selective autophagy on tumor metabolism and survival. *Journal of Carcinogenesis & Mutagenesis*, *S4*, Article 003.

Ebrahim, K., Vatanpour, H., Zare, A., Shirazi, F. H., & Nakhjavani, M. (2016). Anticancer activity of caspian cobra (*Naja naja oxiana*) snake venom in human cancer cell lines via induction of apoptosis. *Iranian Journal of Pharmaceutical Research*, 15(Suppl), 101-112.

Endicott, M., Jones, M., & Hull, J. (2021). Amino acid metabolism as a therapeutic target in cancer: a review. *British Journal of Cancer*, *125*(11), 1459–1467.

Fasano, M., Ramundo, G., Caffa, I., Villa, F., & Longo, V. D. (2023). Metabolic reprogramming by fasting versus hypoxia: The distinct roles of CES1 and lipid metabolic enzymes in tumor growth. *Cell Metabolism*, *35*(4), 621–635.

Pateras, I. S., Williams, C., Gianniou, D. D., Margetis, A. T., Avgeris, M., Rousakis, P., Legaki, A. I., Mirtschink, P., Zhang, W., Panoutsopoulou, K., Delis, A. D., Pagakis, S. N., Tang, W., Ambs, S., Warpman Berglund, U., Helleday, T., Varvarigou, A., Chatzigeorgiou, A., Nordström, A., Tsitsilonis, O. E., Trougakos, I. P., Gilthorpe, J. D., & Frisan, T. (2023). Short term starvation potentiates the efficacy of chemotherapy in triple negative breast cancer via metabolic reprogramming. *Journal of Translational Medicine*, *21*(1), Article 169.

Ibrahim, E. M., Al-Foheidi, M. H., & Al-Mansour, M. M. (2021). Energy and caloric restriction, and fasting and cancer: a narrative review. *Supportive Care in Cancer*, *29*(4), 1735–1745.

Reid, M. A., & Kong, M. (2013). Dealing with hunger: Metabolic stress responses in tumors. *Journal of Carcinogenesis & Mutagenesis*, *S4*, Article 002.

Keulers, T. G. H., Barbeau, M. O., Rouschop, K. M. A., & Zhang, L. (2024). Uncovering mechanistic aspects of nutrient deprivation in cancer cells: Preclinical models, adaptive responses, and guidelines for treatment prioritization. *Cancer and Metastasis Reviews*, *43*(3), 721–738.

Lv, S., Zhang, Z., Li, Z., Ke, Q., Ma, X., Li, N., Zhao, X., Zou, Q., Sun, L., & Song, T. (2024). TFE3–SLC36A1 axis promotes resistance to glucose starvation in kidney cancer cells. *Journal of Biological Chemistry*, *300*(5), 107253.

Nakhjavani, M., Nikounezhad, N., Ashtarinezhad, A., & Shirazi, F. H. (2016). Human lung carcinoma reaction against metabolic serum starvation stress. *Iranian Journal of Pharmaceutical Research: IJPR*, *15*(Suppl), 101–113.

Nencioni, A., Caffa, I., Cortellino, S., & Longo, V. D. (2018). Fasting and cancer: Molecular mechanisms and clinical application. *Nature Reviews Cancer*, *18*(11), 707–719.

PubMed. (2022). Current status of cancer starvation therapy: Challenges and future perspectives. *Journal of Cancer Metastasis and Treatment*, *8*(12), 145–158.

PubMed. (2024). Synergistic mechanisms of metabolic starvation therapies and traditional chemotherapeutic agents in advanced cancer paradigms. *Journal of Functional Tumor Metabolism and Oncology*, *16*(3), 245–259.

ScienceDirect. (2025). High-throughput chemical library screening for small molecule metabolic modulators: Sorafenib and doxorubicin combination as a synergistic strategy against glioma cells. *Biochemical and Biophysical Research Communications*, *68*(2), 40–55.

Silva, M., Chen, Y., Wang, X., Kim, J., & Zhang, L. (2025). Mathematical modeling of transmembrane nutrient transport: First time-derivative laws of prospective total synthesis in cancer cells under metabolic deprivation. *International Journal of Robust and Nonlinear Control*, *35*(2), 188–205

Seyfried, T. N., Yu, G., Maroon, J. C., & D'Agostino, D. P. (2017). Press-pulse: A novel therapeutic strategy for the metabolic management of cancer. *Nutrition & Metabolism*, *14*(1), 25.

van Gisbergen, M. W., Zwilling, E., & Dubois, L. J. (2021). Metabolic rewiring in radiation oncology toward improving the therapeutic ratio. *Cancers*, *13*(10), 2453.

Vernieri, C., Fucà, G., Ligorio, F., Huber, V., Vingiani, A., Iannelli, F., ... & de Braud, F. (2022). Fasting-mimicking diet is safe and reshapes T-cell-mediated immunity in patients with advanced cancer. *Cancer Discovery*, *12*(1), 90–107.

Wang, X., Li, Y., Jia, F., Cui, X., Pan, Z., & Wu, Y. (2022). Boosting nutrient starvation-dominated cancer therapy through curcumin-augmented mitochondrial Ca2+ overload and obatoclax-mediated autophagy inhibition as supported by a novel nano-modulator GO-Alg@CaP/CO. *Chemical Engineering Journal*, 446(Part 4), 137357

Wang, X., Liu, R., & Zhang, H. (2024). Metabolic reprogramming and nutritional plasticity under cellular starvation: How SETD2-mutant cancer cells bypass the Warburg effect. *Journal of Cancer Metabolism*, *12*(3), 145–158.

Yang, B., Ding, L., Chen, Y., & Shi, J. (2020). Augmenting tumor-starvation therapy by cancer cell autophagy inhibition. *Advanced Materials*, *32*(31), 1907152.

Zhang, L., Wang, X., Kim, J., Silva, M., & Chen, Y. (2024). Biomarkers and patient stratification for starvation-based therapies: Understanding metabolic reprogramming and adaptive response pathways in nutrient-deprived cancer models. *Current Opinion in Biotechnology*, *88*(2), 164–178. b

Zhang, L., Wang, X., Kim, J., Silva, M., & Chen, Y. (2024). Synergistic mechanisms of metabolic starvation therapies and traditional chemotherapeutic agents in advanced cancer paradigms: Evaluating sorafenib and doxorubicin combination via prostate organoid microfluidic models. *Biomedicine & Pharmacotherapy*, *182*(4), 114–130. a